JOINT RESEARCH CENTRE
EUROPEAN COMMISSION

OECD OCDE PARIS

AEN NEA

EUR 18708 EN

NEA/CSNI/R(99)4

International Standard Problem 40

Aerosol Deposition and Resuspension

Final Comparison Report

February 1999

Alfredo de los Reyes Castelo
Joaquim Areia Capitão
Giovanni De Santi

AEN AGENCE DE L'OCDE POUR L'ÉNERGIE NUCLÉAIRE

NEA OECD NUCLEAR ENERGY AGENCY

Paris, 1 February 1999

The International Standard Problem No. 40 exercise was devoted to deposition and resuspension of aerosols in pipes. It was based on the results of STORM test SD-11/SR-11, made available to the CSNI by JRC Ispra.

The exercise was divided in two parts : the deposition phase and the resuspension phase. Fifteen organisations, submitting twenty-one sets of calculations using nine computer codes, participated in the deposition part; they represented eight OECD Member countries, the EC, and the Russian Federation. Eleven organisations, submitting ten sets of calculations using six codes, participated in the resuspension part; they represented eight OECD Member countries and the EC.

Three meetings were organised. A Preparatory Workshop was held on 17-18 March 1997. It was followed by a Preliminary Comparison & Interpretation Workshop on 23-24 March 1998 and a Final Comparison & Interpretation Workshop on 25-26 June 1998. All these meetings were hosted by JRC Ispra.

The Co-ordinator of the ISP-40 exercise was Mr. Joaquim Areia Capitão (JRC Ispra). He was assisted by Dr. Alfredo de los Reyes Castelo (CSN, Spain). Both of them, and other members of the STORM team, devoted considerable time and effort to the preparation of the exercise and its specifications, the collection and the comparison of the calculations performed by the participants, and the interpretation of the results. On behalf of the CSNI and the NEA, we express to all of them our sincere gratitude for their fine spirit of co-operation, the high quality of their work, and their ability to meet stringent deadlines.

We also thank very much JRC Ispra for their hospitality and their strong support in favour of the exercise, and first of all for making the results of the STORM test available for an ISP. Collaboration with the JRC has been most effective. Ispra staff has constantly demonstrated high standards of competence and professionalism, and a very fine spirit of international co-operation.

Jacques Royen

Deputy Head

Nuclear Safety Division

PARTICIPANTS IN ISP-40

This report is based on the ISP-40 calculations performed by:

CEA/IPSN/DPEA
Institut de Protection et de Sûreté Nucléaire – Département de Prévention et d'Etude des Accidents –France

A. Fallot

CEA/IPSN/DRS
Institut de Protection et de Sûreté Nucléaire – Département de Recherches en Sécurité –France

M. Missirlian

CIEMAT
Centro de Investigaciones Energéticas Medioambientales y Tecnológicas –Spain

R. Arias, E. Hontañón

CSN
Consejo de Seguridad Nuclear - Spain

A. de los Reyes

ENEA
Ente per le Nuove Tecnologie, l'Energia e l'Ambiente – Italy

F. De Rosa, R. Mari

ENEL
Ente per l'Energia Elettrica S.p.A. – Italy

F. Parozzi, L. Tagliaferri

ETH
Eidgenössische Technische Hochschule –Switzerland

H. Friess

GRS
Gesellschaft für Anlagen- und Reaktorsicherheit – Germany

H.-G. Friederichs, B. M. Schmitz

JAERI
Japan Atomic Energy Research Institute –Japan

A. Hidaka, J. Sugimoto

JRC
Joint Research Center – European Union

J. Areia Capitão, C. Kröger, R. Monti

KINS
Korea Institute of Nuclear Safety – Korea

J.-S. Choi, H.-C. Kim

KURCHATOV
Russian Research Centre "Kurchatov Institute" - Russian Federation

P. Slavyagin

TAC
Toshiba Advanced System Corporation – Japan

T. Yoshino

TRACTEBEL
Tractebel Energy Engineering – Belgium

M. Auglaire, D. Magnus

U-Bochum
Ruhr-Universität Bochum – Germany

T. Steinrötter, N. Pohl, H. Unger

U-Karlsruhe
Universität Karlsruhe –Germany

H.-J. Schmid

U-Pisa
Universitá degli Studi di Pisa - Italy

S. Paci

VEIKI
Institut for Electric Power Research Co. – Hungary

G. Lajtha, L. G. Horváth

ISP-40 Secretary (OECD)

J. Royen

STORM SR11 STAFF

Project Management

G. De Santi

Plant Operation

A. Krasenbrink, J. Bachler, U. Jung, E. Malgarini,

H. Pfitzner

Electrical Devices

H. Hülser, G. Barberi, G. Lanappe

Instrumentation

R. Hummel, R. Colombo, N. Röhrig, R. Männle, M. Sculati

Data Acquisition System

F. Bossi

Control System

G. Lanappe

Post-Test Analysis

P. Dilara, A. Bopp

Data Analysis

J. Areia Capitão, A. de los Reyes, R. Monti

Design Office

F. Peters, A Renoldi

Administrative Support

H. Petruccioli, E. Occhetta

Table of contents

1. Introduction

The Committee on the Safety of Nuclear Installations of the OECD/NEA, in its meeting of November 1996, endorsed the adoption, as International Standard Problem number 40 (ISP-40) [52], of an experiment on aerosol deposition and resuspension to be run in the STORM facility of the Joint Research Centre of the European Commission (JRC). The problem was run as two consecutive blind exercises.

A preparatory workshop took place at the JRC in March 1997 [53] and approved the test specifications, the experimental data to be supplied to the ISP participants and the results to be submitted to them. It was also decided that the CPU times needed for the different calculations should not be compared in absolute terms but "normalised" by the CPU time needed for the same computers to run a reference number-crunching code, *linpackd*, supplied by GRS and already used for another International Standard Problem.

The test, STORM test SR11, took place in April 1997 [13] and included two distinct phases, the first concentrating on aerosol deposition mostly by thermophoresis and eddy impaction and the second on aerosol resuspension under a stepwise increasing gas flow.

The International Standard Problem was also divided into two phases, each one concerning one of the phases of the experiment. Each organisation could participate in only one or both phases of the exercise. The decision whether or not to model resuspension also during the deposition phase of the exercise was left to the participants.

The experimental data for the deposition phase of the exercise - thermal-hydraulics and aerosol feed rate and physical characteristics at the inlet of the test section - were distributed in mid-June 1997 and the deadline for submission of the results for the deposition phase was the end of September 1997. The experimental data for the resuspension phase - thermal-hydraulics, initial deposited mass and size distribution of the resuspended particles - was distributed to the participants in mid-October 1997 and the deadline for submission of the results of this second phase was the end of January 1998.

A first draft of this comparison report was produced in March 1998, followed by a workshop in Ispra in mid-March [54]. Two errors in the supplied data had been detected and were communicated to the participants in this workshop, one concerning the steam flow rate in the deposition phase of the exercise and the other the size distribution of the resuspended aerosols in the resuspension phase. The decision whether or not to re-do their calculations was left to the each ISP participant and the deadline for the submission of new results, with these or other modifications relative to the previous ones, was the end of May 1998. These new calculations, having been performed in open conditions, are presented separately in this report.

The final draft of the comparison report was distribute in June 1998, followed by a final workshop in Ispra the same month.

This report is divided into six main sections, one concerning the experimental set-up and results, two each for the deposition and resuspension phases of the International Standard Problem (blind and open calculations), and one on general conclusions and recommendations. According to the opinion of the ISP participants, the results in the

two sections on the deposition and resuspension exercises are listed by computer code and, for each code, by organisation. The calculations submitted by the Joint Research Centre are included together with the others. Although the JRC staff who performed the calculations did not have access to the experimental results before submitting their results, their knowledge of the facility puts their calculations in a separate class.

2. STORM test SR11 - Experimental results

2.1. Introduction

The full experimental results are the object of the STORM SR11 quick-look report that is published as a JRC technical note [13]. The data reported here are extracted from that technical note and concern only the data that is considered by the authors to be relevant for the purpose of the International Standard Problem.

The experimental conditions in the STORM tests were selected following a detailed examination of a number of severe accident calculations for full plants. In particular, the conditions selected correspond broadly to those that can be expected in the relief lines of a PWR in a station blackout sequence. Given the experimental constraints and the uncertainties of the thermal-hydraulic calculations in those lines after a core slump, a wide range of carrier gas velocities is used in the resuspension phase of the different STORM tests.

The STORM test facility is shown in Fig. 1 and the test section is a 5.0055 meter long straight pipe with 63 mm internal diameter [8]. In the deposition phase, the carrier gas and aerosols pass through the mixing vessel a first straight pipe into the test section and then straight to the wash and filtering system. In the resuspension phase, the clean gas is injected through the resuspension line directly into the test section and the resuspended aerosols are collected in the main filter before the gas goes through the wash and filtering system.

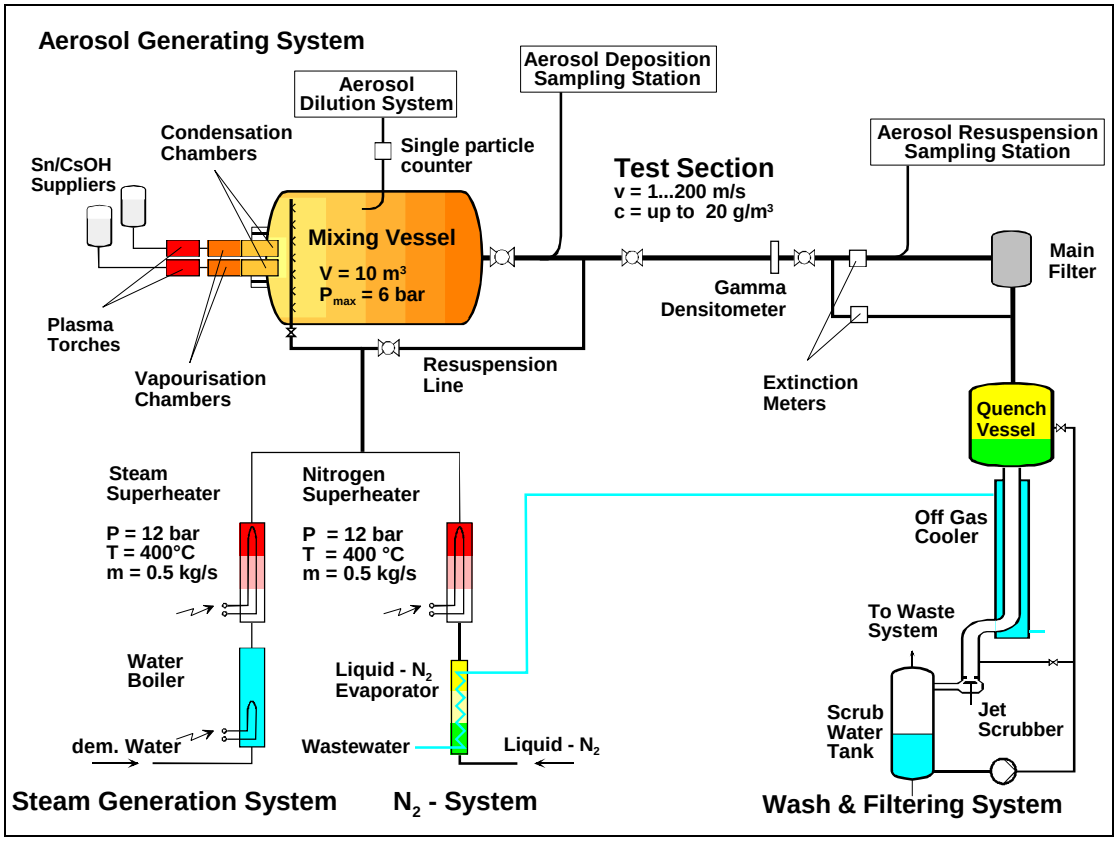

Fig. 1 - The STORM experimental facility

The aerosol concentration and size distribution is measured upstream of the test section in the deposition phase of the experiment and downstream of the test section in the resuspension phase.

The STORM test SR11 was performed in two consecutive days, with the deposition phase in the first day and the resuspension phase in the second day. The test section is enclosed in an oven, which was kept open during the deposition phase to maximise thermophoretic deposition and was closed and heated immediately after the deposition phase, to ensure a constant temperature between the two phases and avoid thermophoretic re-deposition during the resuspension phase.

The aerosols used were of tin oxide (SnO_2) and the carrier gas was a mixture of nitrogen and steam, plus the argon, helium and air needed for the operation of the aerosol generation system, during the deposition phase. In the resuspension phase, pure nitrogen was used as carrier gas.

2.2. Thermal-hydraulics of the deposition phase

The deposition phase of the STORM test SR11 was preceded by a long preparation in terms of pre-heating of the facility and stabilisation of the thermal-hydraulic conditions.

The deposition phase of the test was done using a steam/nitrogen mixture as carrier gas, in addition to the argon and helium that are fed through the plasma torch and that are needed for the particle generation, and to the air injected to cool the aerosol generation system and oxidise the vaporised tin. The flow rates for the different components of the carrier gas were therefore those given in Tab. 1.

Tab. 1 - Carrier gas mass flow rates in the deposition phase

Gas	Mass flow rate (kg/s)
Steam	$1.7467*10^{-2}$ (*)
Nitrogen	$0.5467*10^{-2}$
Air	$0.5728*10^{-2}$
Argon	$0.7194*10^{-2}$
Helium	$0.0119*10^{-2}$

(*) An error in the conversion from measured voltage to mass flow rates was detected just before the second ISP-40 workshop, and the correct steam mass flow rate was actually $1.1060*10^{-2}$ kg/s.

The temperature evolution shown in Fig. 2 illustrates the fact that during the deposition phase of the test, which lasted from 12:00 to 14:30, the thermal-hydraulic conditions can be assumed to have remained practically constant. The thermal-hydraulic data supplied to the ISP participants therefore assumed steady-state conditions during the whole deposition phase (Fig. 3).

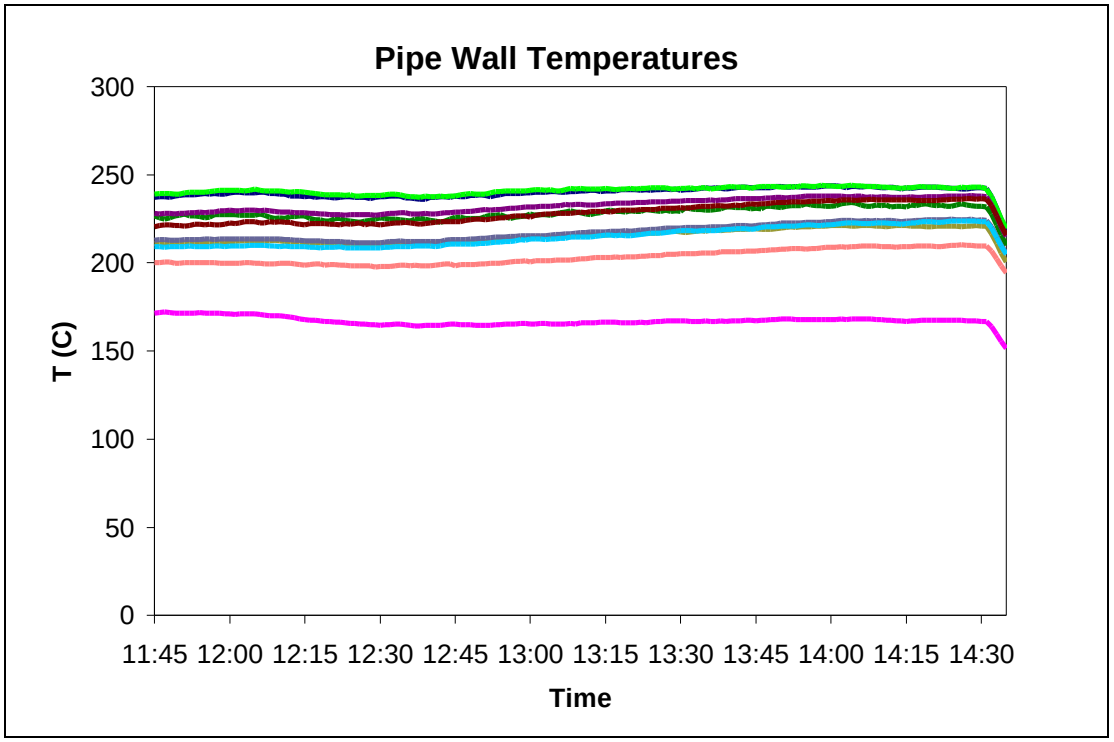

Fig. 2 - Wall temperatures in the deposition phase

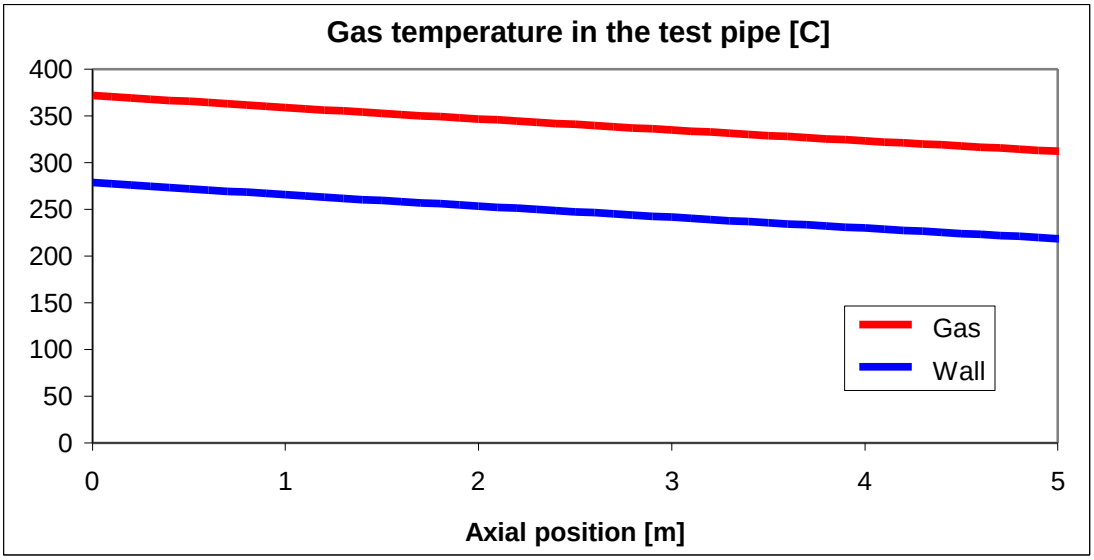

Fig. 3 - Estimated gas and wall temperatures in the deposition phase

The gas and wall temperatures and the pressure supplied to the participants were obtained with a thermal-hydraulic calculation that used the measured wall temperatures and the gas temperature at the inlet as boundary conditions and the gas temperature at the outlet to verify the goodness of the results. The results can only be verified qualitatively, because the insulation characteristics of the pipe change considerably at the end of the test pipe and before the outlet gas temperature is measured.

Following the correction of the steam mass flow rate mentioned above, the thermal-hydraulic calculation was repeated, reaching a better agreement with the experimental measurements. A new set of thermal-hydraulic conditions was therefore distributed to the participants, to be used by those who wished to repeat the deposition calculations with the correct steam flow rate. The gas to wall temperature difference, which is determinant for thermophoretic deposition, is therefore estimated to be higher than the value previously distributed (Fig. 4).

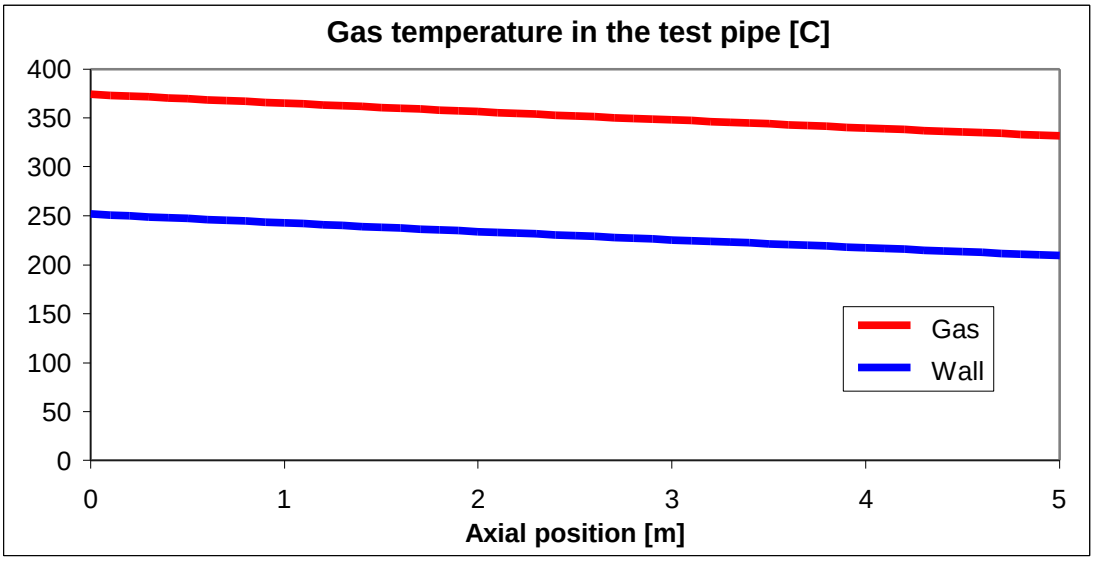

Fig. 4 - Estimated gas and wall temperatures in the deposition phase with the correct steam flow rate

2.3. Aerosol deposition

The aerosol flow at the entrance of the test pipe was practically constant during the whole deposition phase of the experiment. The average mass flow rate was calculated by deducting the total mass of aerosols deposited up to the entrance of the test pipe from the total mass of aerosols generated and dividing the result by the duration of the deposition phase. The constant mass flow rate was therefore supplied as $3.83*10^{-4}$ kg/s of SnO_2. The effective aerosol density was estimated from weighing of samples from the deposit and the comparison of the aerodynamic size measurements obtained with the impactors with the geometric size measurements obtained with the optical instruments. The value supplied to the ISP participants was 4000 kg/m^3, which corresponds to particles with a relatively small void fraction. Finally, the aerosol heat conductivity was estimated to be 11 W/m/K, the heat conductivity of SnO_2 at 400 °C.

The parameters of the particle size distribution - 0.43 µm geometric mean diameter and 1.7 geometric standard deviation - were estimated from the measurements obtained with impactors upstream of the test pipe. Due to the small fraction of aerosols that deposit in the test pipe, this distribution can be considered to remain practically constant along the pipe. This was verified in a previous test without resuspension phase, in which the two sampling stations, upstream and downstream of the test pipe, were used almost simultaneously, yielding similar results.

In the experiment, the two phases, deposition and resuspension are done consecutively, and the test pipe is not examined between them. That means that there is no actual measurement of the deposited aerosols in the deposition phase. After the resuspension phase, all the material that remains in the test pipe is weighed and the mass is added to the mass of aerosols collected in the sampling station and in the total filter downstream of the test pipe. That way, there is a precise measurement of the total mass of aerosols that was in the test pipe plus two valves and two short connecting pipes before the resuspension phase. This is the same as the total mass of aerosols deposited in the test pipe, valves and connecting pipes during the deposition phase. The distribution of the deposit along the pipes was estimated from previous tests with only deposition done under similar conditions.

The mass of the aerosols deposited in the test pipe alone during the deposition phase can therefore be estimated to be 162 grams, and the estimated spatial distribution of deposition is shown in Fig. 5.

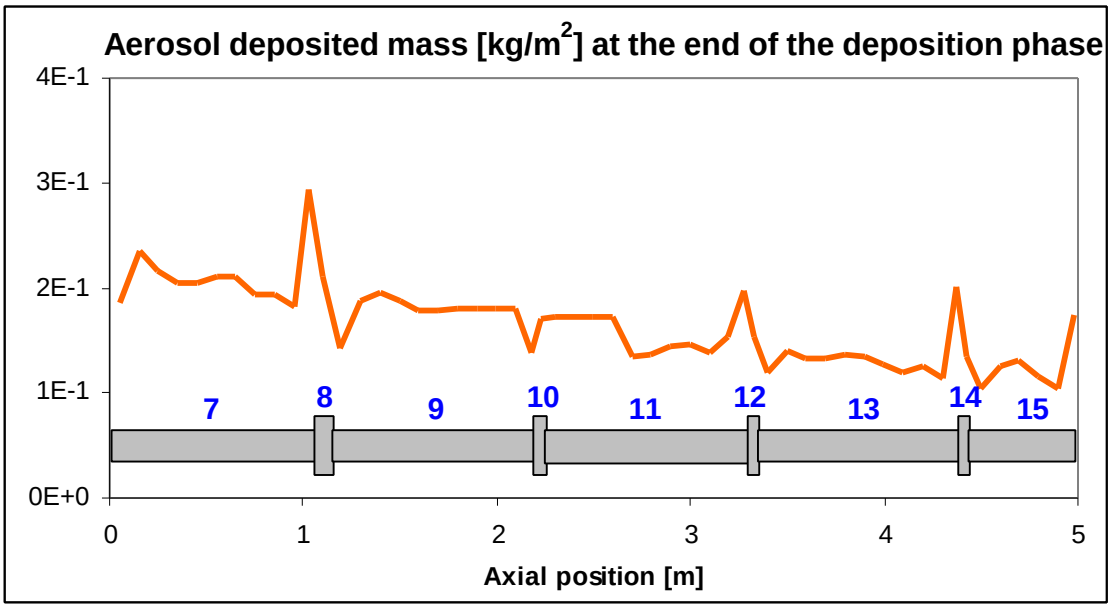

Fig. 5 - Estimated aerosol deposition along the test pipe

2.4. Thermal-hydraulics of the resuspension phase

In the resuspension phase, which was divided into six steps of increasing gas velocity, the carrier gas was pure nitrogen, with the flow rates given in Tab. 2.

Tab. 2- Carrier gas mass flow rates in the resuspension phase

Step	Mass flow rate (kg/s)
1	0.102
2	0.126
3	0.152
4	0.175
5	0.199
6	0.224

As shown in Fig. 6, the thermal-hydraulic conditions were practically unchanged during the whole resuspension phase. The temperature difference between the carrier gas and the wall was always less than 10 °C, to avoid any significant re-deposition. As for the deposition phase, the supplied thermal-hydraulic conditions were calculated using the measured wall temperatures and the gas temperature at the inlet as boundary conditions and the gas temperature at the outlet to verify the goodness of the results. Also, as in the deposition phase, the results can only be verified qualitatively, because the insulation characteristics of the pipe change considerably at the end of the test pipe and before the outlet gas temperature is measured.

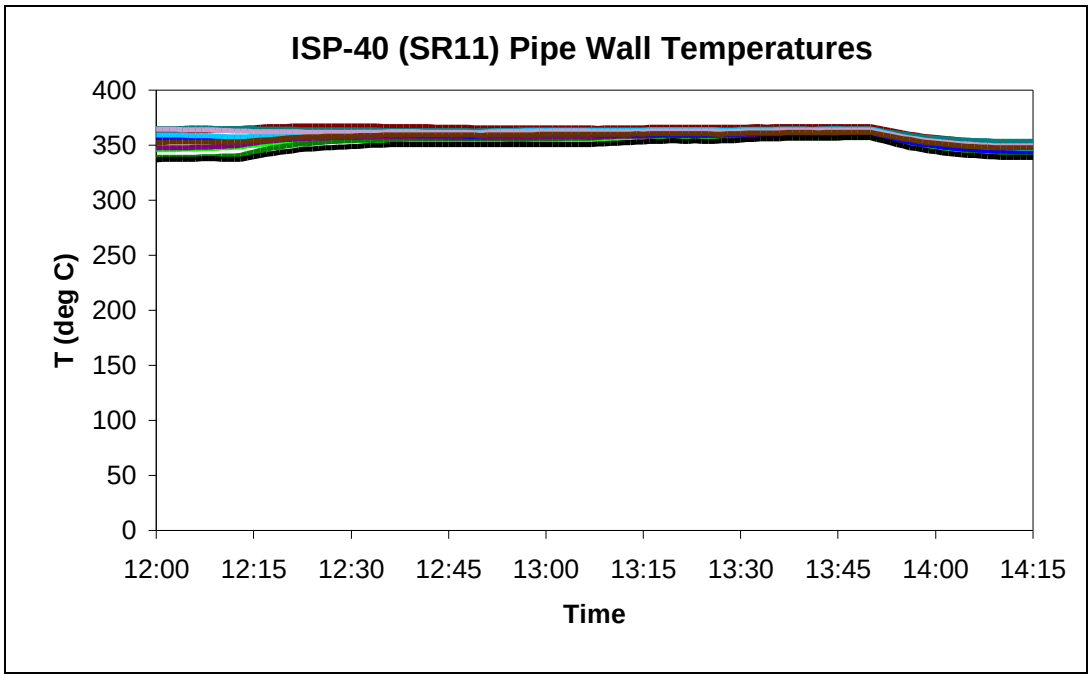

Fig. 6 - Wall temperatures in the resuspension phase

2.5. Aerosol resuspension

The initial deposited mass was estimated as described above when discussing the results of the deposition phase. The total mass of aerosols deposited in the test pipe

was estimated to be 162 grams and its estimated spatial distribution is shown in Fig. 5.

The distribution of the particles remaining deposited in the test pipe at the end of the resuspension phase was measured by collecting and weighing all the remaining material in the pipe in sections of a few centimetres. It is shown in Fig. 7. The total mass collected from the test pipe at the end of the test was 42 grams. The filter and impactor measurements were used to estimate the amount of material resuspended in each velocity step. The calculated masses remaining in the test pipe at the end of each step were 156 g, 151 g, 124 g, 96 g and 70 g at the end of steps 1 through 5, respectively.

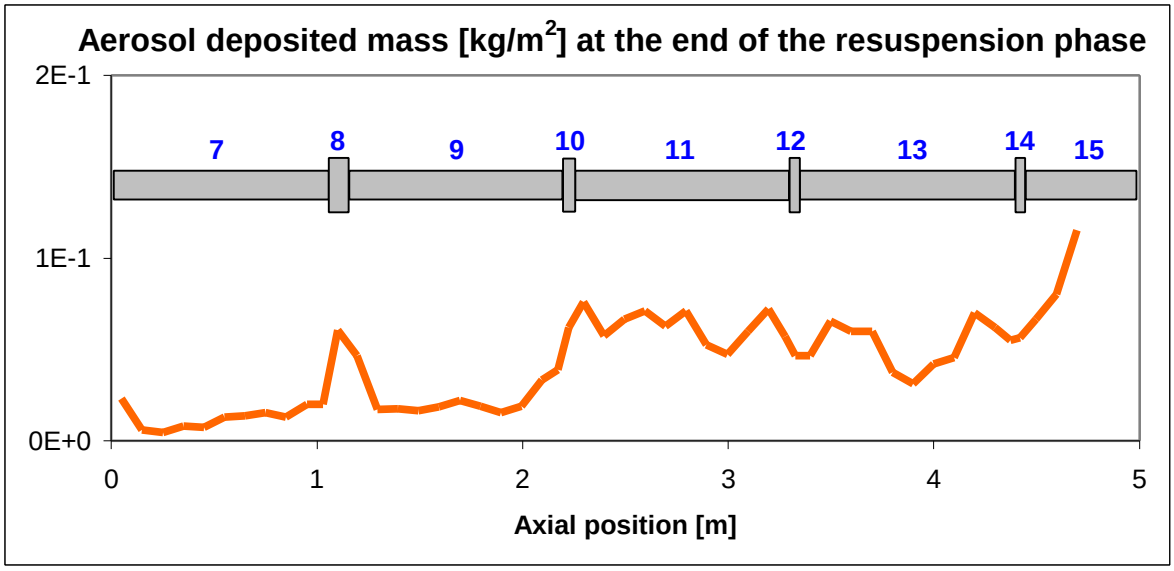

Fig. 7 - Aerosol remaining deposited along the test pipe

The aerosol particles resuspended from the walls were measured by an extinction meter and a sampling station with impactors and filters located downstream from the test pipe. While the extinction meter had an integration time of 5 seconds and measured continuously, the impactors and filters had integration times of approximately 2 minutes and were used one impactor and one or two filters in each velocity step. Each impactor was opened just before the velocity increase to capture the particles resuspended in the first seconds of each step. The aerosol concentrations shown in Fig. 8, measured with the extinction meter, the impactors and the filters, show that the effective duration of resuspension in each velocity step was of the order of seconds or, at most, a few minutes, after which very little resuspension occurred until the gas velocity was raised again. The particle size distributions measured with the impactors should therefore be representative of the aerosols resuspended in each step, since each impactor collected material for the first two minutes of each step. One thing that needs to be taken into consideration, however, is that the filters and impactors collect samples from the centre of the pipe and therefore cannot pick up any larger particles that might be rolling along the bottom.

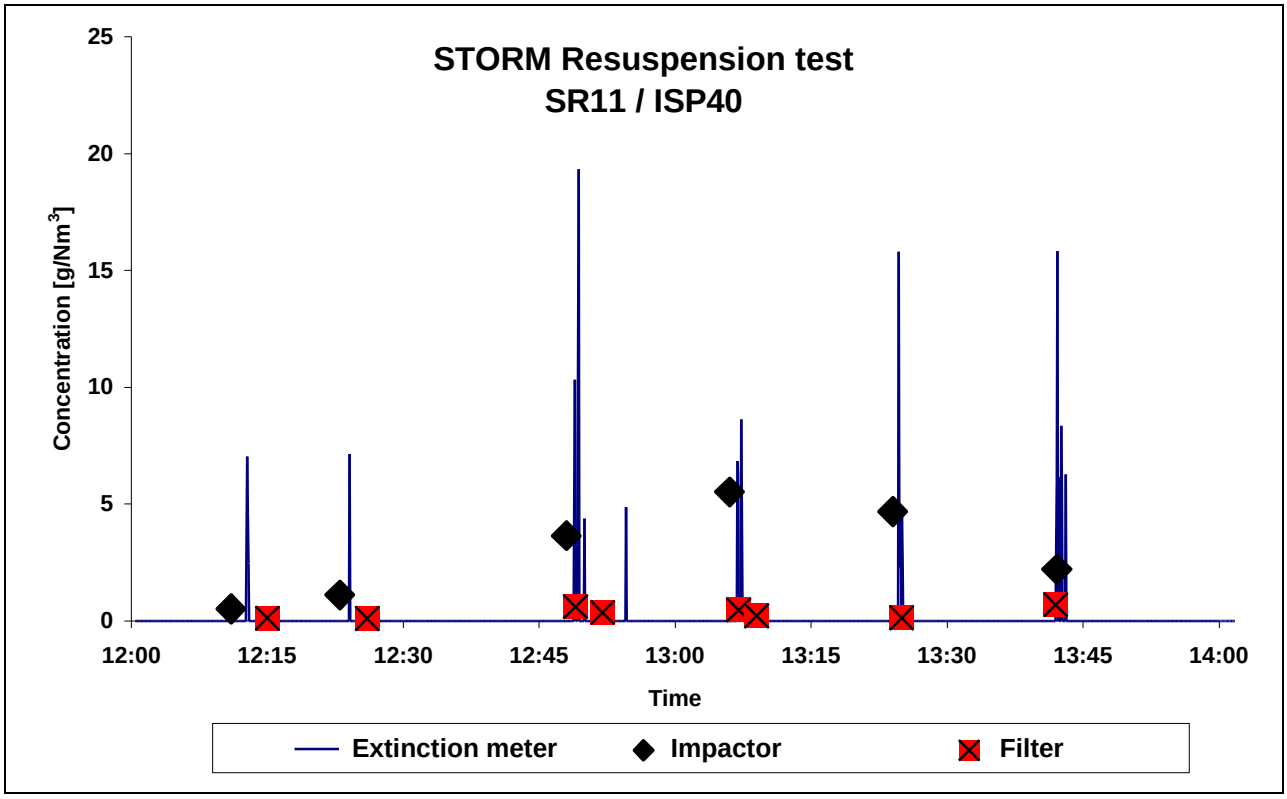

Fig. 8- Aerosol concentration in the resuspension phase

The sizes of the particles collected in each of the six impactors can generally be reproduced by a bi-modal log-normal distribution. Only in the third and sixth velocity steps can they be assimilated to a uni-modal distribution.

The parameters of the log-normal distributions, geometric mean diameters and geometric standard deviations, that were distributed to the ISP participants are given in Tab. 3. The error that was announced in the intermediate workshop, in the evaluation of the geometric mean diameters, led to an over-estimation by a factor of 2. The correct values are shown in Tab. 4.

Tab. 3 - Particle size distributions in the resuspension phase as distributed

Step	Mass fraction in dist. 1	dg_1 (µm)	s_1	dg_2 (µm)	s_2
1	0.921	5.94	2.28	0.68	1.68
2	0.804	4.20	1.98	0.64	1.43
3	1.000	5.83	2.77		
4	0.980	4.00	2.39	1.17	1.11
5	0.878	3.82	2.47	1.29	1.38
6	1.000	3.87	3.10		

Tab. 4 - Correct particle size distributions in the resuspension phase

Step	Mass fraction in dist. 1	dg_1 (µm)	s_1	dg_2 (µm)	s_2
1	0.921	2.97	2.28	0.34	1.68
2	0.804	2.10	1.98	0.32	1.43
3	1.000	2.92	2.77		
4	0.980	2.00	2.39	0.59	1.11
5	0.878	1.91	2.47	0.65	1.38
6	1.000	1.94	3.10		

3. ISP-40 calculations - Deposition

3.1. Aerosols-B2

3.1.1. Introduction

Aerosols-B2 is a code developed by IPSN to predict the behaviour of an aerosol population injected into a containment vessel or a circuit with known thermal-hydraulic conditions [22].

Aerosols-B2 is a purely aerosol physics code, and does not include aerosol formation or chemical interactions. It models aerosol agglomeration due to gravity, Brownian motion and turbulence, and aerosol deposition by gravitational settling, thermophoresis, diffusiophoresis, Brownian diffusion, turbulent diffusion, eddy impaction and centrifugal impaction on bends.

The thermophoretic deposition model uses Talbot's equation [75] and the eddy impaction deposition is calculated with the Liu-Agarwal model [42].

3.1.2. CEA/IPSN/DPEA

The results submitted by CEA/IPSN/DPEA were calculated with Aerosols-B2 (Circuit) mod 1.0 [15]. No specific changes were made to the code to run this particular problem.

3.1.2.1. ISP calculation

The ISP calculation was performed in a Sun SparcStation 5 and took almost 116 minutes of CPU, which is $4.2*10^4$ times more than the reference *linpackd* code.

Ten identical computational cells were used, and the code uses a variable time step calculated internally, with a minimum of $4.0*10^{-15}$ seconds and a maximum of 800 seconds.

The heat transfer between the carrier gas and the walls was derived from the Trapmelt formulation.

The total deposited mass in the test pipe was calculated to be 243 grams, distributed almost uniformly along the test pipe (Fig. 9), and the rate of deposition was constant in time (Fig. 10).

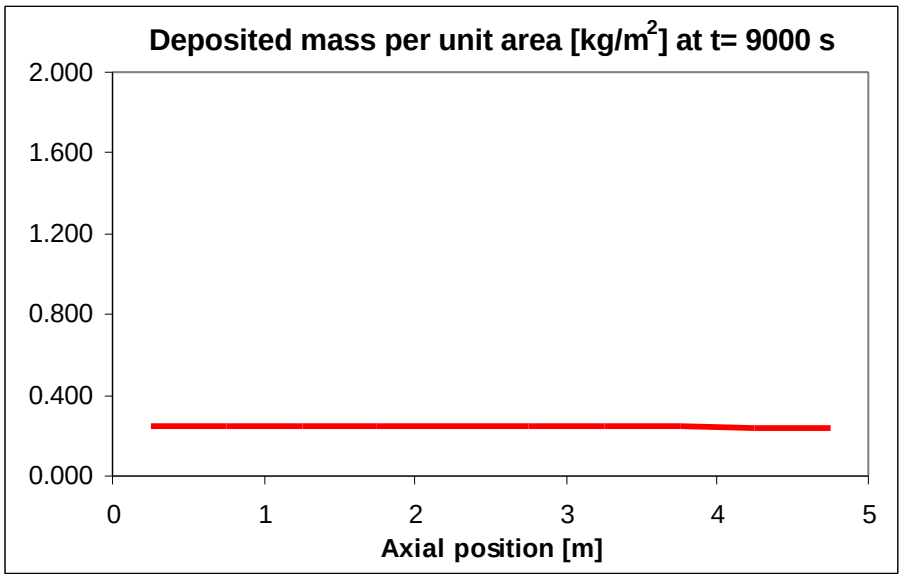

Fig. 9 - Spatial distribution of deposition (CEA/IPSN/DPEA)

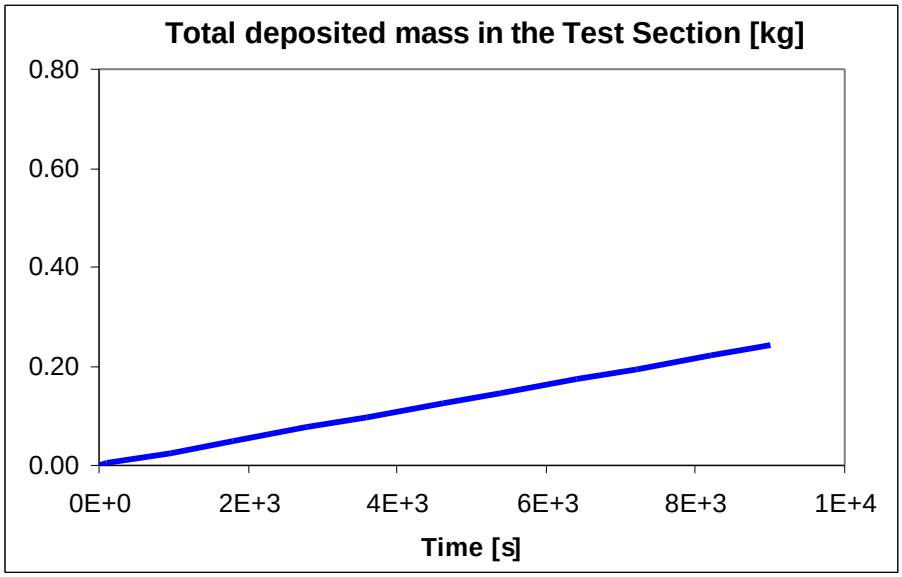

Fig. 10 - Time evolution of deposition (CEA/IPSN/DPEA)

The Aerosols-B2 calculation predicted thermophoresis to be the dominant deposition mechanism, with 87% of the total deposition. Eddy impaction was responsible for practically all of the remaining deposition. This distribution among deposition mechanisms was practically constant in time and the dominance of thermophoresis increased very slightly along the test pipe, due to the larger radial temperature gradient towards the exit of the pipe (Fig. 11).

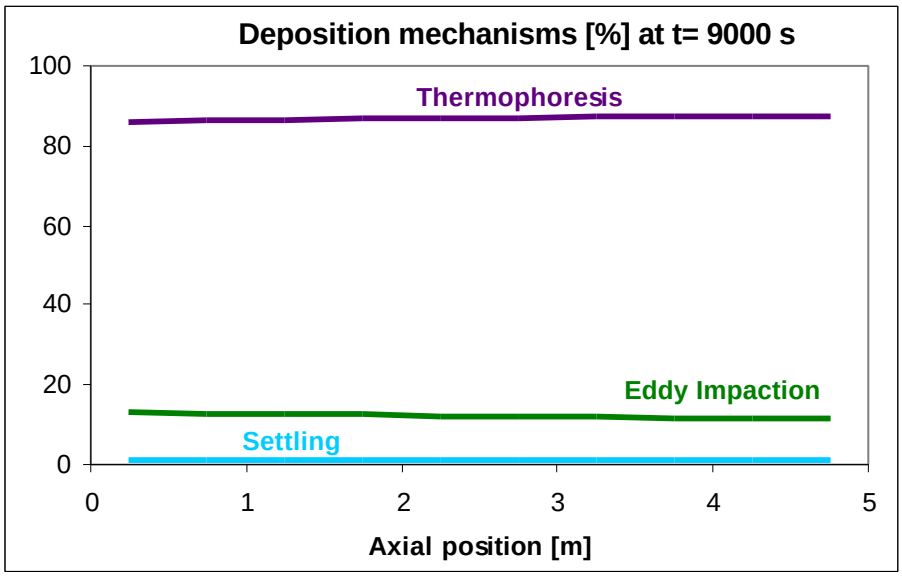

Fig. 11 - Deposition mechanisms along the test pipe (CEA/IPSN/DPEA)

The particles that exited the test pipe had a constant geometric mean diameter of 0.44 µm and a geometric standard deviation of 1.7.

3.2. Art

3.2.1. Introduction

Art is a code developed by JAERI for the calculation of fission product transport in the coolant circuit and containment of an LWR under severe accident conditions [32].

The Art code models aerosol growth by agglomeration and vapour condensation on the particle surface, aerosol deposition, resuspension and revaporisation.

Models for aerosol deposition include thermophoresis, diffusiophoresis, turbulent diffusion, Brownian diffusion, eddy impaction and gravitational settling. The thermophoretic deposition velocity is calculated using Brock's equation [3] for Knudsen numbers smaller than 0.2 and Waldman's equation [21] for higher Knudsen numbers. Deposition due to turbulence is calculated using the Friedlander-Johnstone model for eddy impaction [17] and the Davies model [7] for turbulent diffusion.

3.2.2. JAERI

The ISP-40 calculation submitted by JAERI was performed using Art mod. 2, and no specific changes were needed for this particular problem [24].

3.2.2.1. ISP calculation - without resuspension

Two calculations were submitted by JAERI, the first one excluding the resuspension module, and the second allowing for simultaneous deposition and resuspension.

The calculations were performed on a SparcStation 10 compatible workstation (AS5080) and took about 40 hours each, which is about $7.2*10^4$ times more than the reference *linpackd* code.

The full length of the test pipe was discretised into 10 identical computational cells, and the time step used was 0.01 seconds. No indication was given about the discretisation of the aerosol size distribution.

The total deposited mass calculated for the test pipe was 241 grams, slightly decreasing along the test pipe (Fig. 12). The time evolution of the deposit was calculated to be linear (Fig. 13).

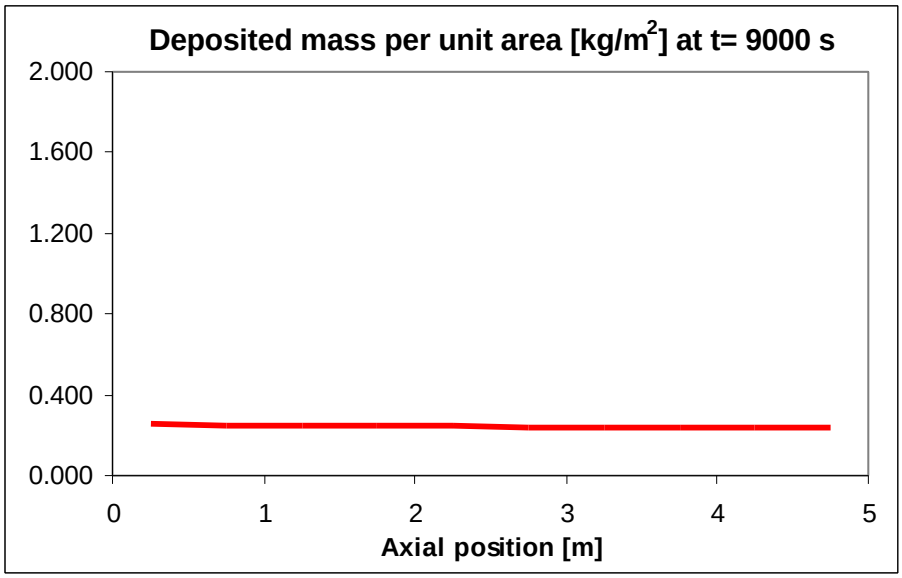

Fig. 12 - Spatial distribution of deposition (JAERI-1)

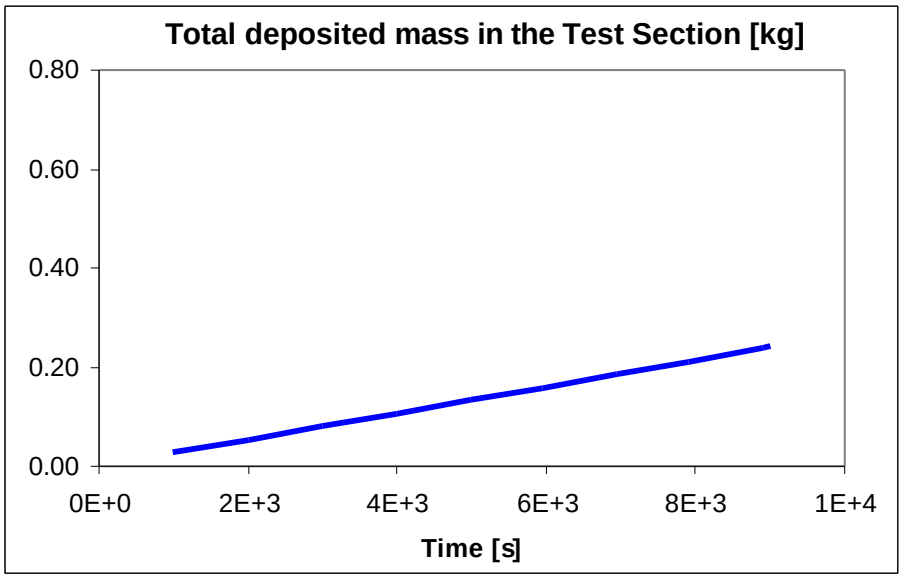

Fig. 13 - Time evolution of deposition (JAERI-1)

The dominant deposition mechanisms were thermophoresis, responsible for 70.5 % of the total deposition, and eddy impaction, with 28.3 % of the deposition. A smaller percentage (1.2 %) is due to gravitational settling. The fraction of deposition due to thermophoresis increases along the test pipe (Fig. 14).

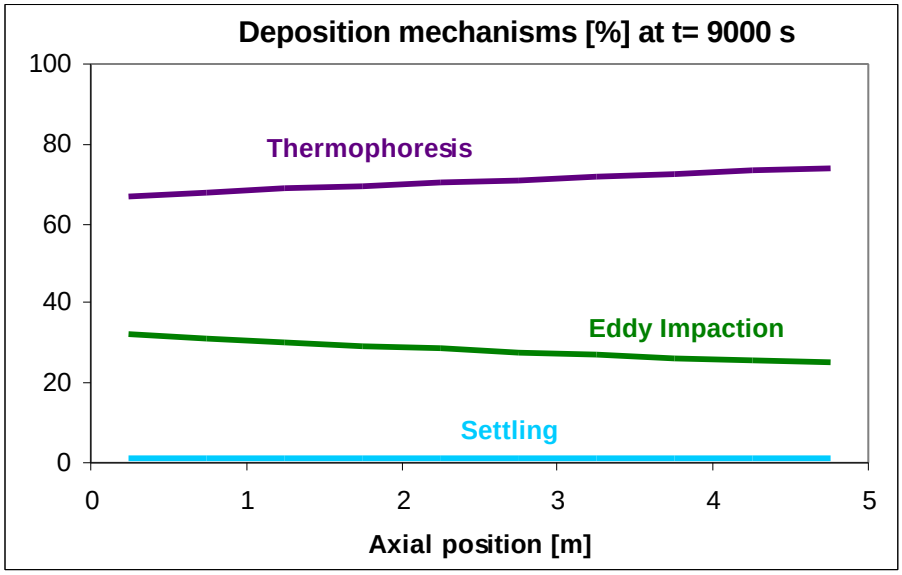

Fig. 14 - Deposition mechanisms along the test pipe (JAERI-1)

The particles that did not deposit in the test pipe left it with a geometric mean diameter of 0.44 µm and a geometric standard deviation of 1.7.

3.2.2.2. ISP calculation - with resuspension

If the resuspension module of Art is used, the total deposited mass calculated for the test pipe becomes 195 grams, increasing very slightly along the test pipe (Fig. 15). The time evolution of the deposit was still practically linear (Fig. 16)

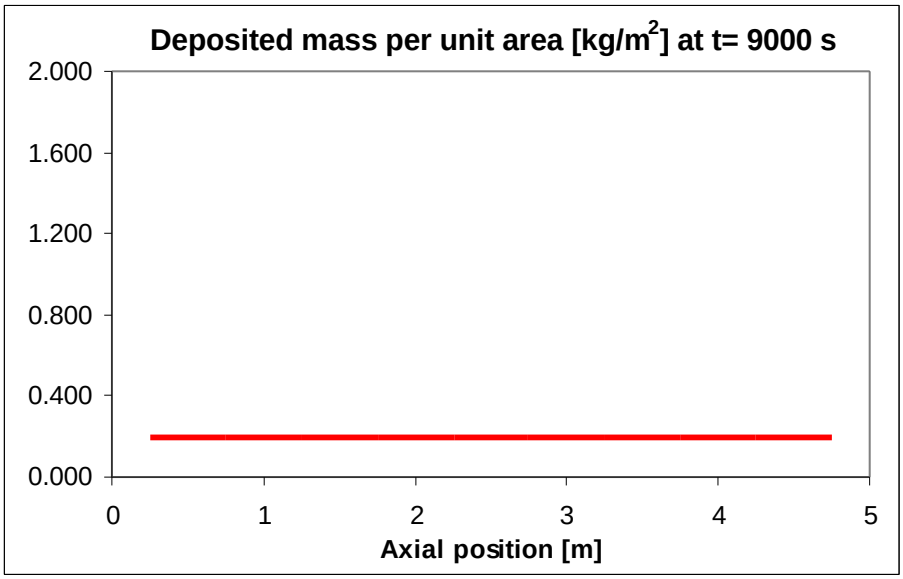

Fig. 15 - Spatial distribution of deposition (JAERI-2)

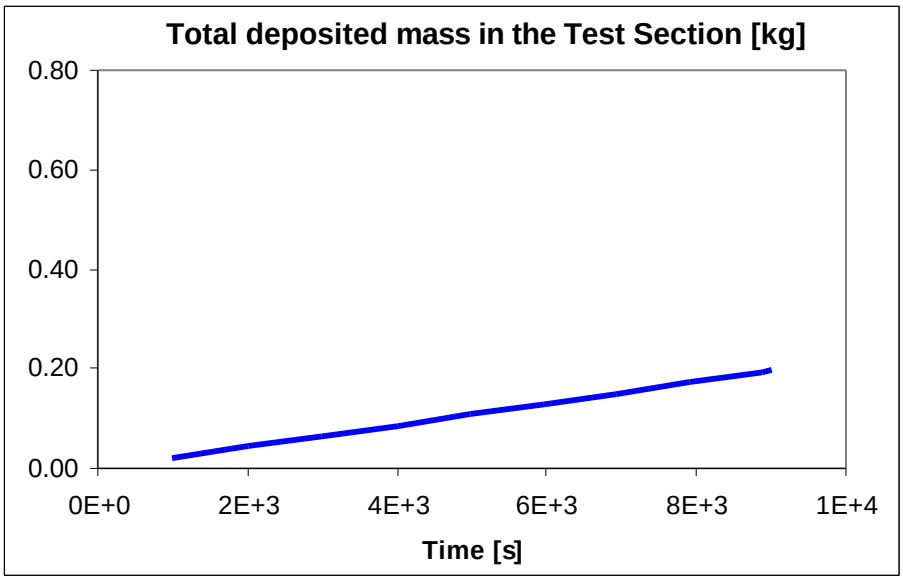

Fig. 16 - Time evolution of deposition (JAERI-2)

Even if thermophoresis is still the dominant deposition mechanism, its importance decreases to 66.0 % of the total deposition, while eddy impaction becomes more important, with 32.8 % of the deposition. Gravitational settling remains a minor deposition mechanism, with the same 1.2 % as in the case without resuspension. The distribution among deposition mechanisms remains practically constant along the test pipe (Fig. 17).

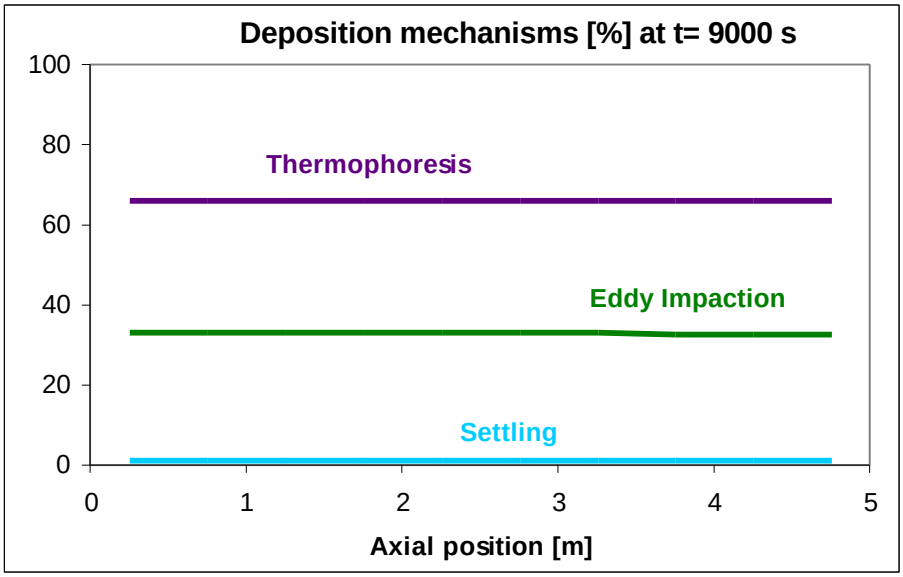

Fig. 17 - Deposition mechanisms along the test pipe (JAERI-2)

The size distribution of the particles exiting the test pipe remains practically identical to the one calculated without resuspension.

3.3. Athlet-CD

3.3.1. Introduction

Athlet-CD is a severe accident analysis code that includes thermal-hydraulics and aerosol transport [6], [41], [76]. The aerosol transport module used in the ISP calculations was version 1.1 GRS of the Sophaeros code, for which a brief description is given below. In particular, the thermophoretic deposition velocity is calculated using Talbot's formulation [75], eddy impaction is given by the Liu-Agarwal model [42] and turbulent diffusion is calculated using Davies' formulation [7].

3.3.2. University of Bochum-1

The University of Bochum submitted two sets of results for ISP-40, calculated with two different codes. For the first submission, the computer code used was version 1.1D/0.2E of Athlet-CD, and the code was not modified specifically for solving this problem [72].

3.3.2.1. ISP calculation

The ISP calculation was performed on a Sun SparcStation 10 workstation and took just over 40 minutes to run, which is about 300 times more than the reference *linpackd* code.

The test pipe was divided into 25 control volumes and additional volumes were added upstream and downstream of the test pipe to establish the appropriate flow conditions. No information was given about the time step used in the calculation.

The particle size distribution was discretised into 10 bins, covering the range of particle diameters between 0.1304 µm and 0.739 µm.

The total deposition in the test pipe was calculated to be 200 grams, decreasing slightly along the test pipe, with the exception of the four flanges, where the deposition per unit area was calculated to be about 60% higher than in the pipes themselves (Fig. 18).

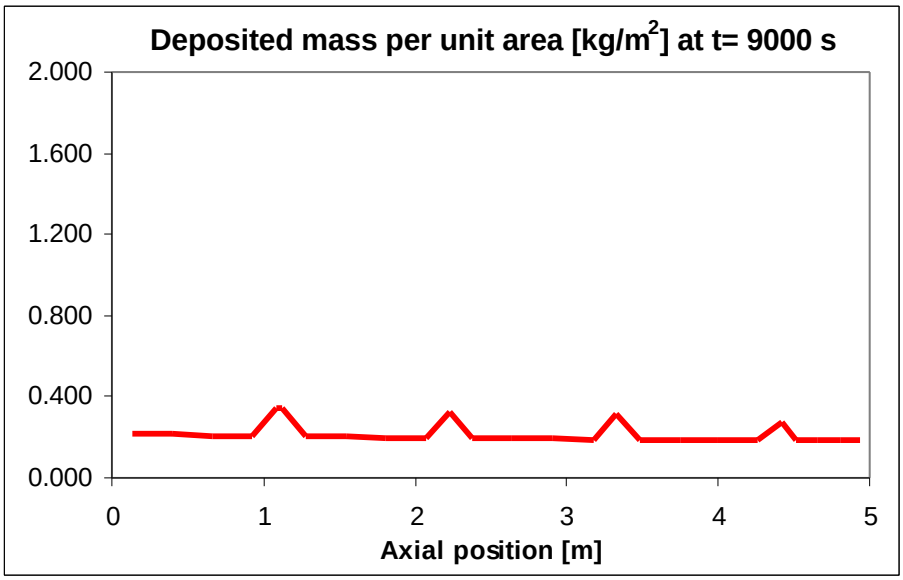

Fig. 18 - Spatial distribution of deposition (U. Bochum-1)

This is due exclusively to a sharp increase of the thermophoretic deposition in the corresponding control volumes, due to the higher mass of metal in those volumes and to the consequent different thermal properties of the wall. The time evolution of the deposited is calculated to be linear, as expected (Fig. 19).

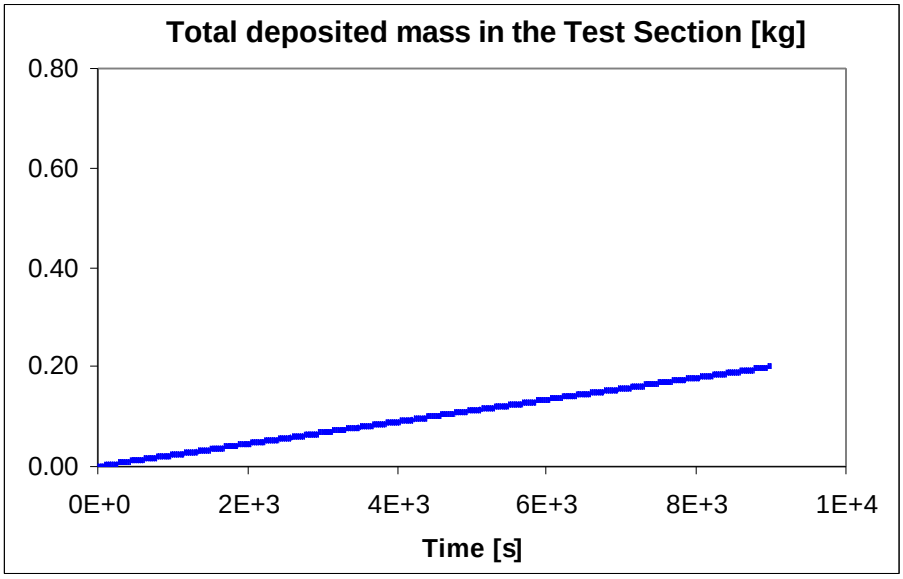

Fig. 19 - Time evolution of deposition (U. Bochum-1)

Thermophoresis was calculated to be responsible for 98.6 % of the total deposition, practically constant along the test pipe except for the flanges, where, as mentioned before, it is even more dominant, with more than 99% of the deposition. The remaining aerosol deposition is due, in almost equal parts, to gravitational settling and eddy impaction (Fig. 20).

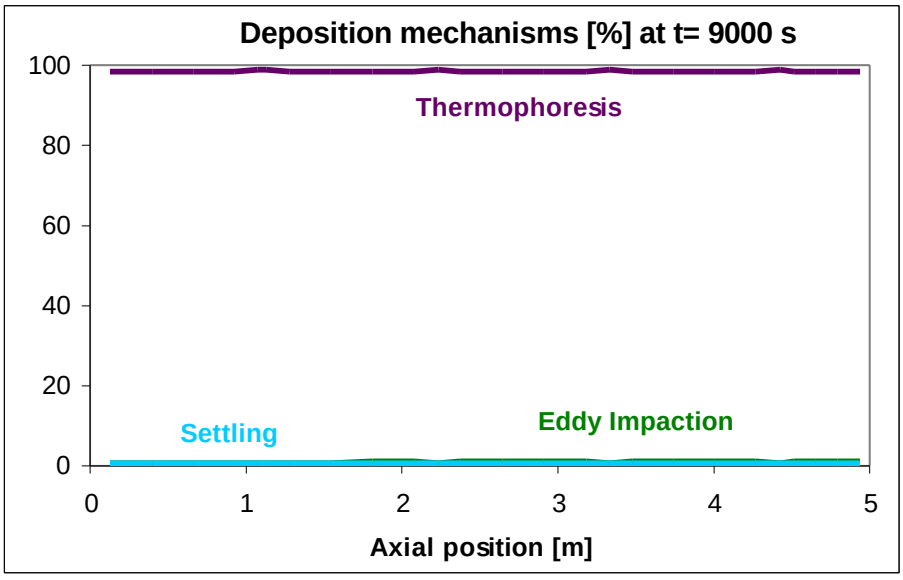

Fig. 20 - Deposition mechanisms along the test pipe (U. Bochum-1)

The particles that do not deposit exit the test pipe with a geometric mean diameter of 0.38 μm and a geometric standard deviation of 1.5.

3.4. DeNiro

3.4.1. Introduction

The DeNiro code is a particle tracking code for calculating aerosol deposition that is currently under development at the JRC [37], [38]. It calculates the movement of single particles under the effect of drag and lift forces due to the velocity difference between the particle and the carrier gas, and thermophoretic forces due to the spatial variation of temperature in the gas.

The drag force is calculated with the Stokes equation [21] and corrections for gas-particle slip (Cunningham) and for bounded flows (Dahneke, Happel and Brenner). The lift force model uses the Saffman equation [61] and thermophoresis is calculated with the Talbot formulation [75].

3.4.2. JRC-1

Three different calculations were done by the JRC for ISP-40, with three different codes. The first calculation was done with the DeNiro code, without any specific changes for this problem [36].

3.4.2.1. ISP calculation

The DeNiro calculation was done on a Sun SparcStation 10 workstation. No information on the CPU time needed to run the calculation is available.

Since this is a particle tracking calculation, there is no spatial discretisation. For the presentation of the results, the test pipe was divided into 6 cells, with the total deposition calculated for each cell. The maximum time step used in the calculation was set to be equal to the particle relaxation time. The actual time step is adjusted by the code to obtain the desired precision in the numerical solution.

The particle size distribution was discretised into 100 bins, covering the range up to 5 μm. Particles with a diameter of less than 0.16 μm were not tracked and assumed not to deposit, since similar calculations had shown that to be the case, and to save computational time.

The total deposited mass was calculated to be 188 grams decreasing along the test pipe (Fig. 21). Since the particle trajectories are calculated sequentially, and independent of each other, the time dependence is given only in the boundary conditions at the inlet. Since these were given as steady state, the temporal evolution of deposition was assumed to be linear.

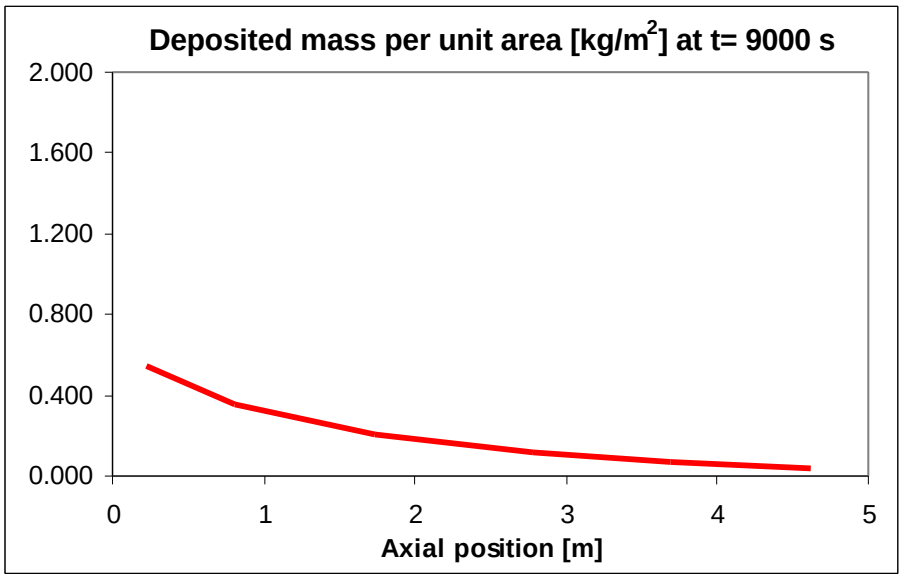

Fig. 21 - Spatial distribution of deposition (JRC-1)

The calculation was done assuming that thermophoresis was the only mechanism responsible for aerosol deposition in the test pipe. Transport of particles across the boundary layer upper limit was not considered and only particles that were in the boundary layer at the inlet were tracked.

The particles that do not deposit in the test pipe exit with a geometric mean diameter of 0.47 μm and a geometric standard deviation of 2.0.

3.5. Ecart

3.5.1. Introduction

The Ecart code is a joint ENEL/EDF code for severe accident simulation that fully couples aerosol and vapour transport with thermal-hydraulics and chemical equilibrium [58], [59]. It includes models for particle agglomeration by gravity, Brownian motion and turbulence, and for particle deposition by thermophoresis, diffusiophoresis, gravitational settling, Brownian diffusion, turbulent diffusion, eddy impaction and impaction in bends.

The model for thermophoretic deposition uses Talbot's equation [75], while for eddy impaction the Liu-Agarwal model [42] is used. The Davies model [7] is used for turbulent diffusion.

The Ecart code also includes a semi-empirical resuspension model which inhibits particle deposition when the aerodynamic forces acting on the particle are stronger than the adhesive forces that tend to attach the particle to the surface.

3.5.2. ENEL

The ISP-40 calculation submitted by ENEL was performed with version 97.2 of Ecart [57]. The resuspension module was activated, and only the dry aerosol models were used.

3.5.2.1. ISP calculation

The ISP calculation was performed on an IBM 486 personal computer and took 32.9 hours, which is 10^4 times longer than the reference *linpackd* code.

Five identical control volumes were used, and the time step was 0.05 seconds, which is slightly above the Courant limit. The particle size distribution was discretised in 20 bins.

The wall roughness was set to 5.0 µm, which is typical of clean commercial steel. The aerodynamic and collision shape factors were taken equal to 1, assuming that the particles were spherical and lightly porous.

To model the carrier gas, the air used in the experiment was decomposed into nitrogen (added to the pure nitrogen injected in the experiment) and oxygen.

The total deposited mass in the test pipe was calculated to be 31.6 grams, with considerably higher deposition towards the end of the test section (Fig. 22). The temporal evolution of deposition is constant (Fig. 23).

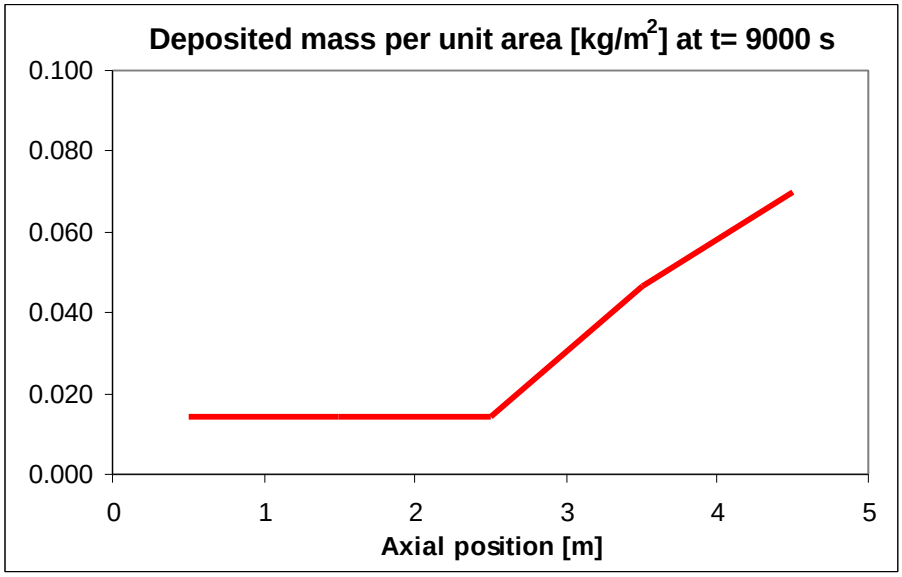

Fig. 22 - Spatial distribution of deposition (ENEL)

Thermophoresis was calculated to be responsible for 99.2% of the total deposition, with that percentage decreasing very slightly towards the exit of the test pipe, while the rest of the deposition is due to eddy impaction (0.5%) and sedimentation (Fig. 24).

The particles exiting the test pipe had a constant geometric mean diameter of 0.44 µm with a geometric standard deviation of 1.7.

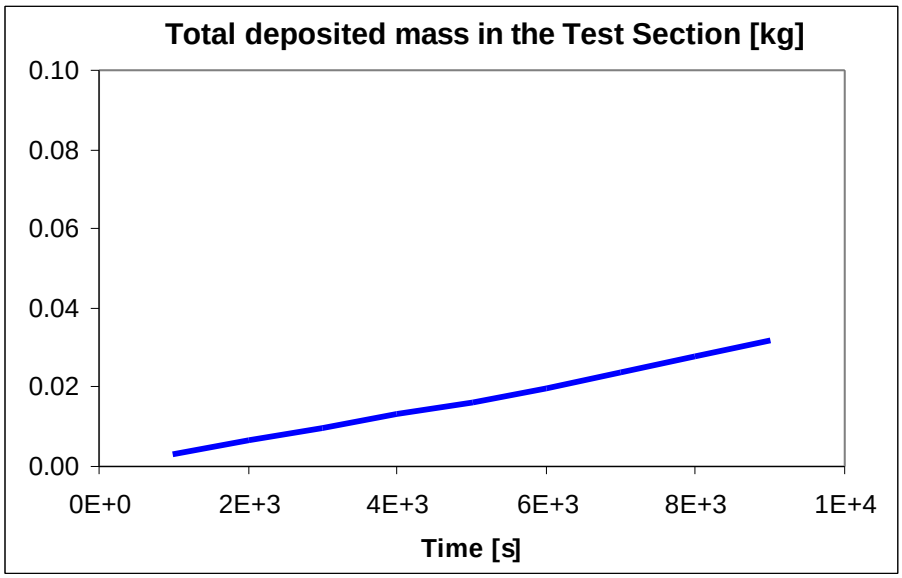

Fig. 23 - Time evolution of deposition (ENEL)

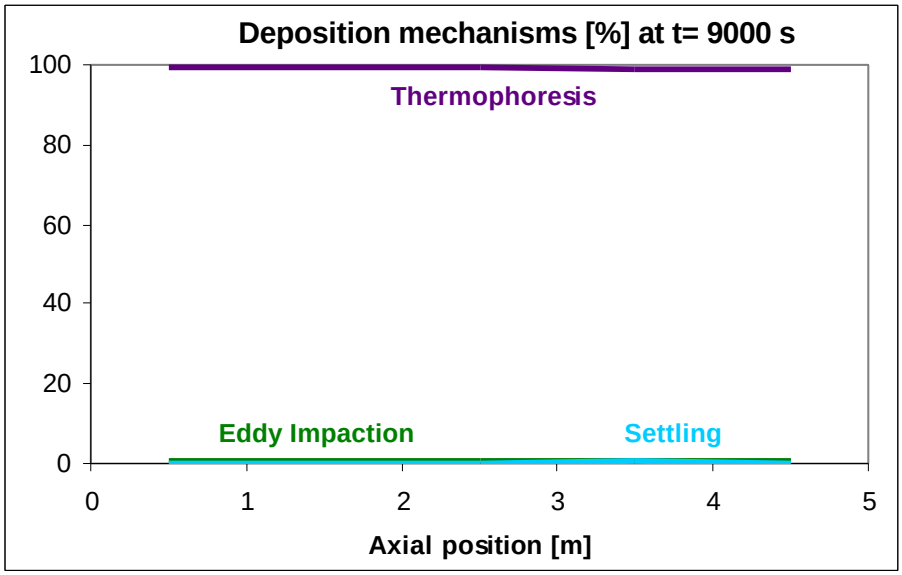

Fig. 24 - Deposition mechanisms along the test pipe (ENEL)

3.5.2.2. Sensitivity calculations

The activation of the resuspension module in Ecart effectively inhibits inertial deposition of larger particles by either gravitational settling or eddy impaction. If the resuspension module is excluded, total deposition in the test pipe is increased to 283.4 grams.

3.5.3. University of Pisa

The calculations submitted by the University of Pisa were performed with version 97.2 of Ecart [55]. No specific changes were needed to solve this problem.

3.5.3.1. ISP calculation - without resuspension

The University of Pisa submitted two sets of results for the deposition phase of ISP-40. In the first one the resuspension module in Ecart was not activated, while it was used in the second submission.

The calculations were performed on an IBM Risc 6000/250 workstation, and took just over 60 minutes to run, which is 2180 times more than the reference *linpackd* code.

The test pipe was divided into five control volumes of different lengths, chosen to accommodate the physical units (pipes and flanges) in the experimental set-up. To obtain the desired flow conditions, two additional control volumes were added, one upstream and the other one downstream of the test pipe.

The time step used in the calculation was 0.1 second, which is up to four times higher than the Courant limits in some control volumes. Additional runs with smaller time steps confirmed that this violation of the Courant limit did not create numerical problems, though considerably reducing the run time.

The particle size distribution was discretised into 20 size bins.

The wall roughness was set initially to 10.0 μm. The roughness in each cell and in each time step is determined by the code, depending on the amount of deposit present in the cell and on the size distribution of the deposited particles. The initial value, however, can be important in determining the initial location of deposition and hence the time evolution of the deposition in each control volume.

The carrier gas was modelled splitting the air mass flow rate used in the test into nitrogen, oxygen, carbon dioxide and argon.

The total deposited mass in the test pipe is calculated to be 284 grams, decreasing very slightly along the test pipe (Fig. 25). Deposition is also practically uniform in time (Fig. 26).

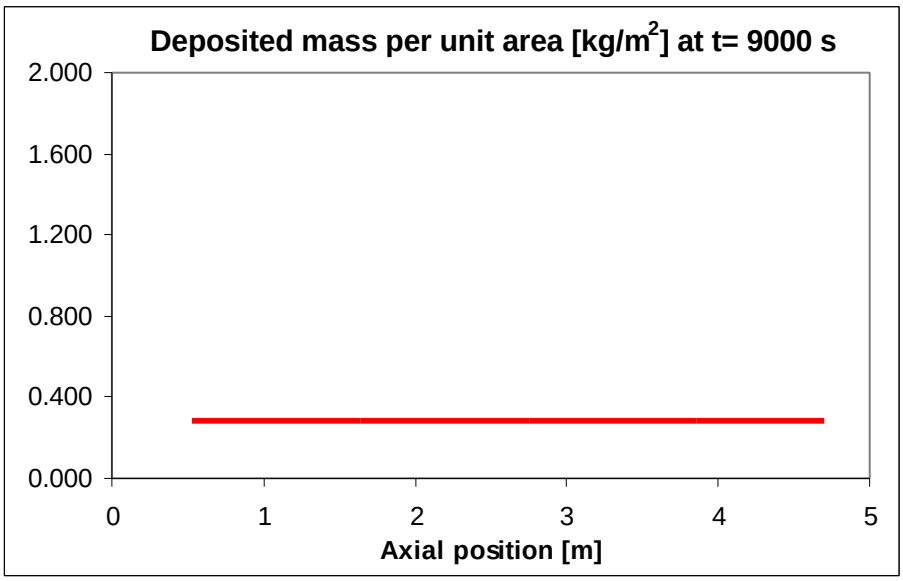

Fig. 25 - Spatial distribution of deposition (U. Pisa-1)

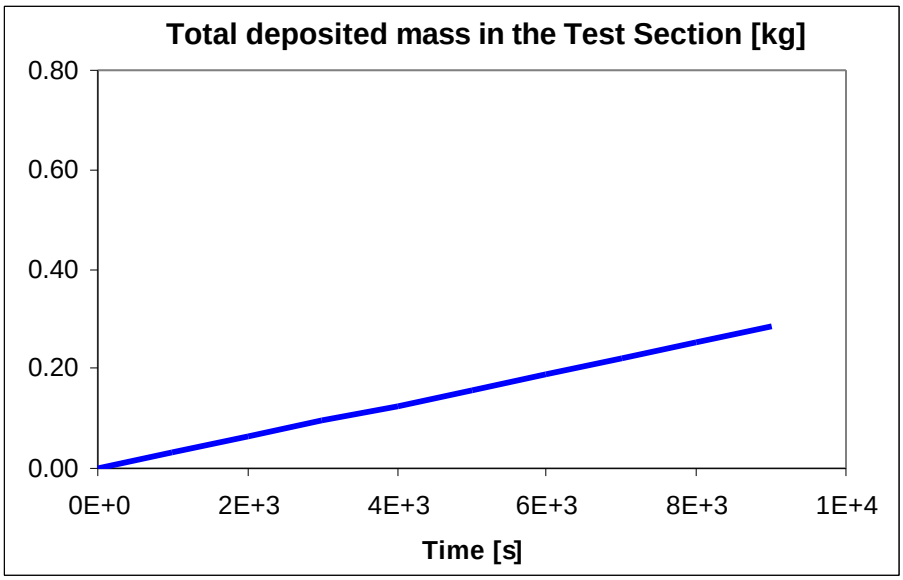

Fig. 26 - Time evolution of deposition (U. Pisa-1)

Thermophoresis is the main deposition mechanism, accounting for 87.4 % of the total deposition. The remaining 12.6 % are caused mostly by eddy impaction (11.7 %) and gravitational settling (0.9 %). This distribution remains almost constant along the test pipe, with the relative importance of thermophoresis increasing slightly towards the end of the pipe (Fig. 27).

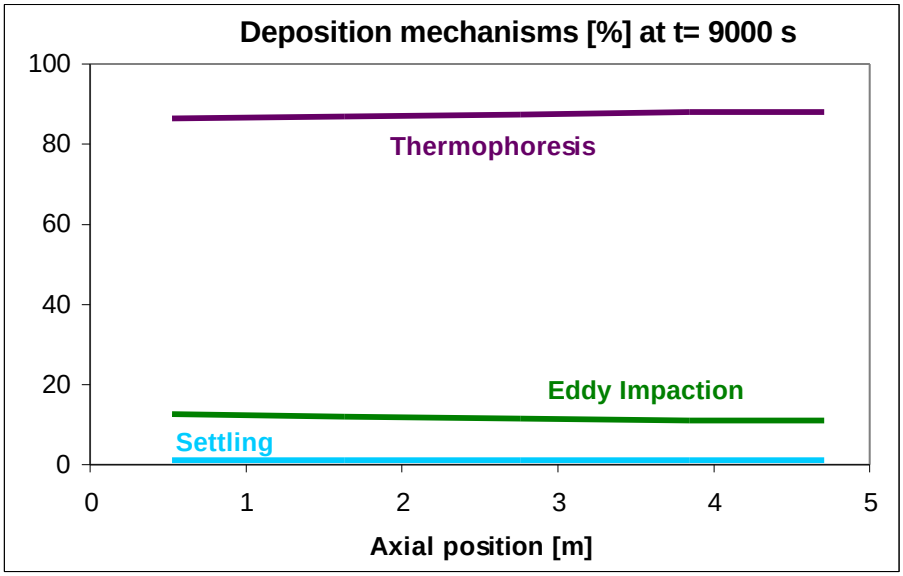

Fig. 27 - Deposition mechanisms along the test pipe (U. Pisa-1)

The particles that do not deposit in the test pipe exit with a geometric mean diameter of 0.44 μm and a geometric standard deviation of 1.7. Except for a slightly lower mean diameter at the beginning, this particle size distribution remains constant during the test.

3.5.3.2. ISP calculation - with resuspension

The second calculation submitted by the University of Pisa was performed using the same aerosol deposition models as in the first calculation, but enabling also the aerosol resuspension module.

The calculation was performed in the same IBM Risc 6000/250 workstation and took a bit more than 62 minutes to run, which is 2240 times more than the reference *linpackd* code.

The nodalisation, time step and discretisation of the particle size distribution were the same as before, and the same is true for the initial wall roughness and the way in which the carrier gas was modelled.

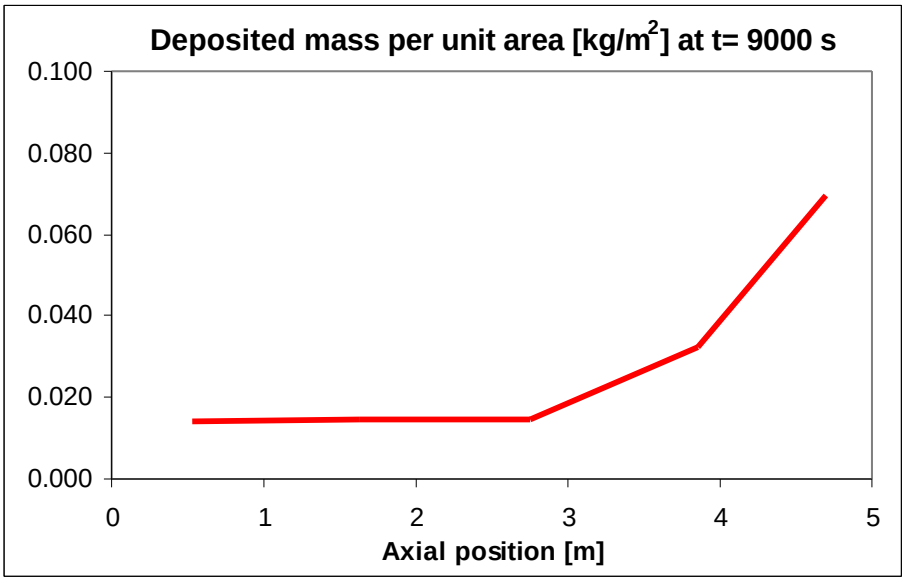

Fig. 28 - Spatial distribution of deposition (U. Pisa-2)

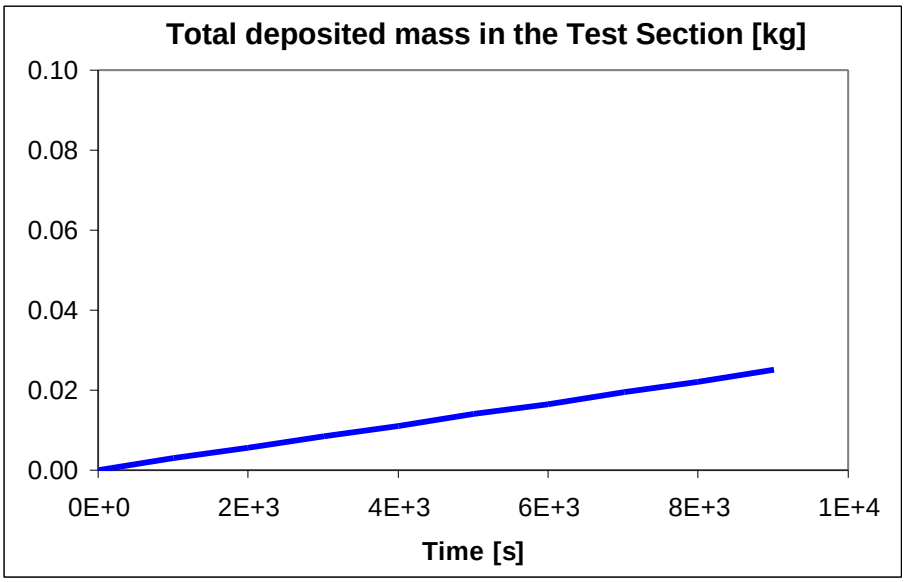

Fig. 29 - Time evolution of deposition (U. Pisa-2)

The total deposited mass in the test pipe was, in this case, calculated to be 25 grams, increasing very slightly in the first 3 meters of the test pipe and then sharply towards the outlet (Fig. 28). Time evolution was still practically constant (Fig. 29).

The dominance of thermophoresis as the main deposition mechanism is even clearer than in the first case, with 99.2 % of the total deposition. The contribution of eddy impaction decreased to only 0.5 % and that of gravitational settling to only 0.3 % (Fig. 30).

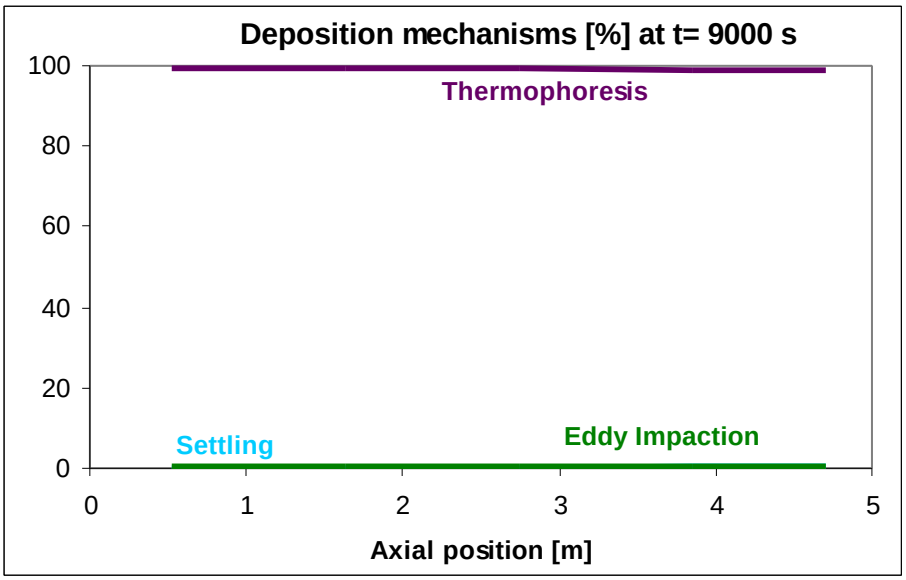

Fig. 30 - Deposition mechanisms along the test pipe (U. Pisa-2)

The particle size distribution of the aerosols exiting the test pipe is still characterised by a geometric mean diameter of 0.44 µm and a geometric standard deviation of 1.7, practically constant in time with the exception of slightly smaller sizes at the beginning of the test.

3.5.3.3. Sensitivity analysis

Since the aerodynamic forces acting on the deposited particles depend on the wall roughness, the calculation with resuspension was repeated for different initial values of the wall roughness, from 5 to 100 µm. It was found that if the initial wall roughness was in the low range (5 or 10 µm), a certain mass of aerosols would accumulate on the walls, lowering the effective roughness even more and therefore reducing resuspension (or, more adequately, inhibition of deposition) and increasing the effective deposition. This is particularly true in the last two meters of the test pipe, where the initial conditions are favourable for the deposition of particles in the range of 0.2 to 0.3 µm.

If the initial wall roughness is set to 50 or 100 µm, the amount of deposition calculated by Ecart is not enough to change this roughness, and the increased deposition at the end of the test pipe disappears.

3.6. Marie

3.6.1. Introduction

Marie is a particle tracking code in development at the University of Karlsruhe. The particle movement is calculated from the interaction between a fluid field and individual particles.

The forces considered in the model are the drag and lift forces generated by the different velocities of the particle and the carrier gas, and the thermophoretic force due to the spatial variation of the gas temperature. The drag force is modelled with the Stokes formulation [21] and corrections for gas-particle slip (Cunningham) and for inertial effects (Hinds). The lift force is calculated using Saffman's formulation [61] and the thermophoretic force is calculated with Talbot's equation [75].

3.6.2. University of Karlsruhe

The calculations submitted by the University of Karlsruhe were performed with the Marie computer code [62].

3.6.2.1. ISP calculation

No information was made available on the computer used and the time needed to perform the calculation.

Being a particle tracking calculation, there is no spatial nodalisation. To evaluate the spatial distribution of deposition, the pipe was divided into 50 sections. On the other hand, no information was supplied about the time step used in the calculations.

To make sure that the flow field was correctly established and that the radial distribution of particles at the inlet section was correct, two fictitious pieces of pipe were added in the calculation, before and after the test pipe.

The log-normal particle size distribution was discretised into 10 bins of equal mass. The mean diameter of the smallest size bin is 0.1816 µm, and the one of the largest bin is 1.0410 µm.

The total deposition in the test pipe was calculated to be 638 grams, decreasing from the inlet to the outlet of the test pipe, mainly in the first metre (Fig. 31).

Although it is not clear how the contribution of different mechanisms was calculated, the results submitted indicate that eddy impaction is responsible for about 2/3 of the total deposition, with the other 1/3 due to thermophoresis. The proportion between the two mechanisms oscillates along the test pipe, but always stays near these values (Fig. 32).

According to the submitted results, the particles that do not deposit leave the test pipe with a geometric mean diameter of 0.43 µm and a geometric standard deviation of 1.75. It is very likely, however, that 0.43 µm is the mass median diameter and not the geometric mean diameter, as mentioned later in the discussion of the results.

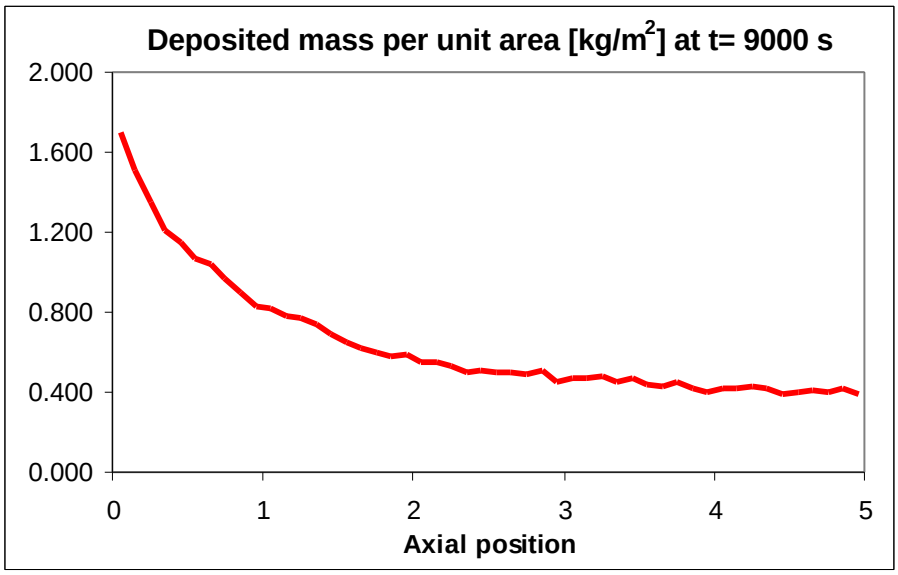

Fig. 31 - Spatial distribution of deposition (U. Karlsruhe)

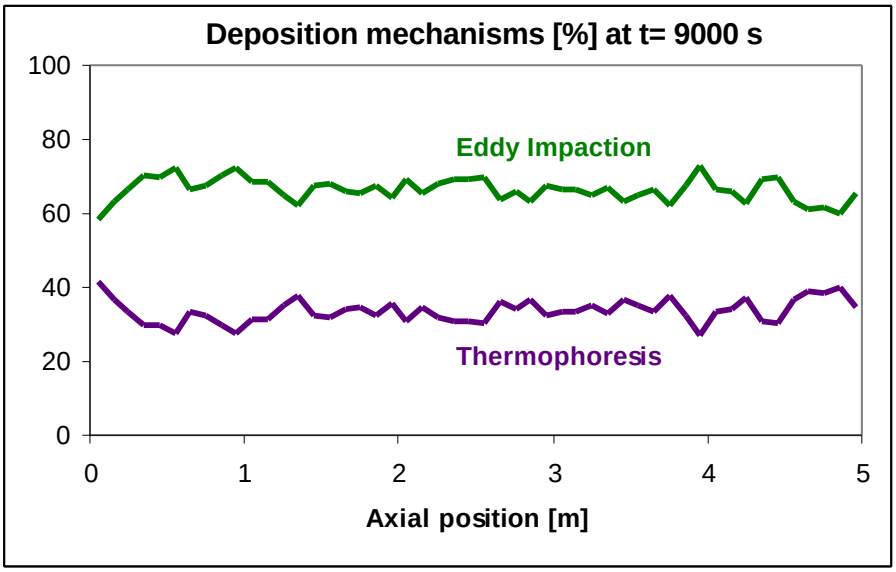

Fig. 32 - Deposition mechanisms along the test pipe (U. Karlsruhe)

3.7. Melcor

3.7.1. Introduction

The Melcor code was developed at Sandia National Labs. for the USNRC, and it is an integrated computer code that models the progression of severe accidents in LWR nuclear plants [73], [74].

The aerosol dynamics module of the code is based on Maeros, and was developed specifically to deal with containment conditions. It includes aerosol agglomeration due to gravity, turbulence and Brownian motion, and aerosol deposition by gravitational settling, Brownian diffusion, thermophoresis and diffusiophoresis.

Deposition mechanisms that are typical of circuit conditions, including eddy impaction, are not modelled. To reduce the stiffness of the set of differential equations that is solved by the code, condensation/evaporation is handled separately, using the Mason equation.

The thermophoretic deposition is calculated in Melcor using Brock's equation [3], which is the same applied in the Talbot formulation used in other codes. The user can specify the slip factor and the thermal accommodation coefficient, which, by default, have values within the range recommended by Brock.

3.7.2. ENEA

For the aerosol deposition calculation ENEA used version 1.8.3 of Melcor [12], with the default values for the slip factor and thermal accommodation coefficient. No specific modifications were necessary to solve this problem.

3.7.2.1. ISP calculation

The ISP calculation was performed on an IBM RISC 6000/375 workstation, and took 118.5 hours to run, which is $6.3*10^4$ times more than the reference *linpackd* code.

After a number of preliminary runs showed no effect of the nodalisation, a total of 5 practically identical computational cells were used. The time step was automatically set by the code and was 10^{-2} seconds.

Since preliminary calculations showed thermophoresis to be the main deposition mechanism, the temperature difference between gas and wall temperatures was particularly important, but the experimental values could not be reached if the supplied gas temperature at the inlet was used in Melcor. The supplied gas and wall temperatures were therefore modified to obtain the correct temperature difference between gas and wall, without deviating too much from the measured temperatures.

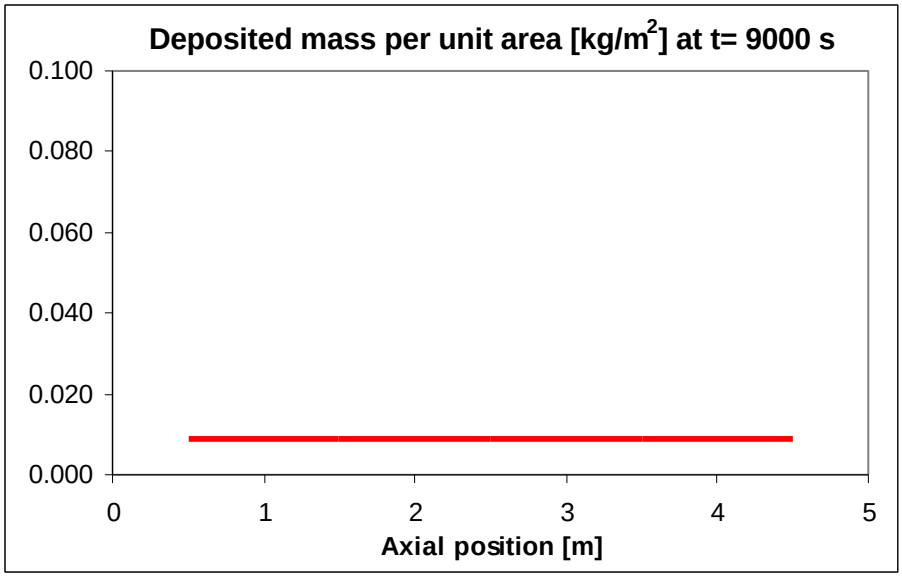

Fig. 33 - Spatial distribution of deposition (ENEA)

The total deposited mass in the test pipe was calculated to be 8.85 grams, with a slightly lower deposition in the first computational cell, attributed by ENEA to inlet effects and an almost uniform deposition in the rest of the pipe (Fig. 33). Variation of deposition with time is linear in all computational cells (Fig. 34).

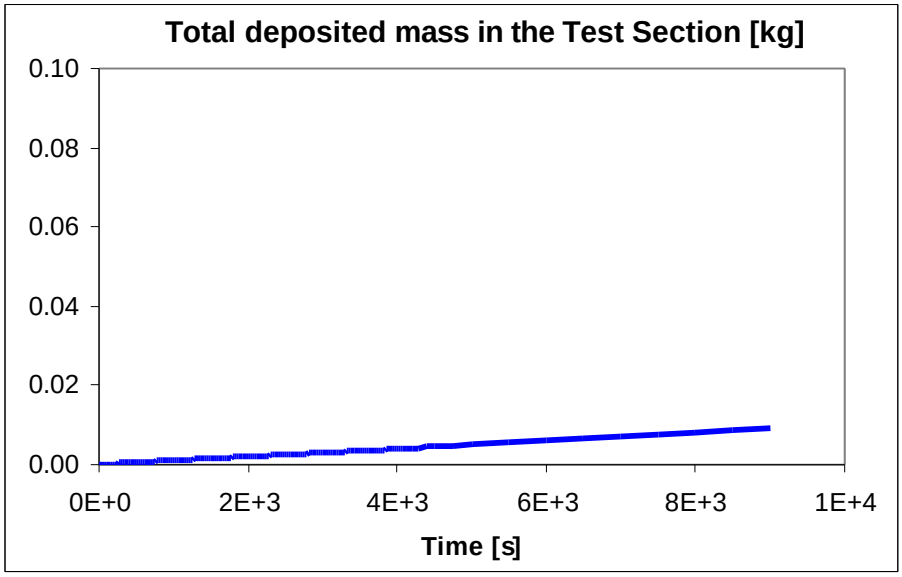

Fig. 34 - Time evolution of deposition (ENEA)

Although thermophoresis is expected to be the dominant deposition mechanism, due to the temperature difference between gas and wall and to the small size of the aerosol particles, the Melcor code does not produce a break-up of deposition by mechanisms and hence the relevance of the different mechanisms considered cannot be quantified.

The particles exiting the test pipe had a geometric mean diameter of 0.42 µm, with a geometric standard deviation of 1.7. The slight reduction of the mean particle size with respect to the one at the pipe inlet is due to deposition of particles at the high end of the size distribution.

3.7.3. KINS

The results submitted by KINS were calculated with version 1.8.3 of Melcor [35]. The code was modified so that it would write in the output files the percentage of deposition due to each mechanism.

3.7.3.1. ISP calculation

The ISP calculation was performed on a Sun Center 2000 workstation, and it took almost 70 hours to run, which is about $3.6*10^4$ times more than the reference *linpackd* code.

A total of 12 computational cells were used, of which 10 represented the test pipe itself and the other two represented a sink for vapours and aerosols and the environment. The maximum time step was fixed at 0.1 second. The particle size distribution was discretised into 8 bins, covering the range between 0.4 and 10 µm. An error in the interpretation of the parameters given for the specified particle size distribution versus the ones required by the code led to an incorrect specification of

the initial particle size distribution. The supplied value of the geometric mean diameter was used instead of the required mass median diameter.

The default options in Melcor were used except that thermodynamic equilibrium in each computational cell was not assumed. Air was decomposed into nitrogen plus oxygen.

Total deposition in the test pipe was calculated to be 55 grams, distributed almost uniformly, except for the first cell, where deposition was slightly lower (Fig. 35). The growth of the deposit with time is calculated to be practically linear (Fig. 36).

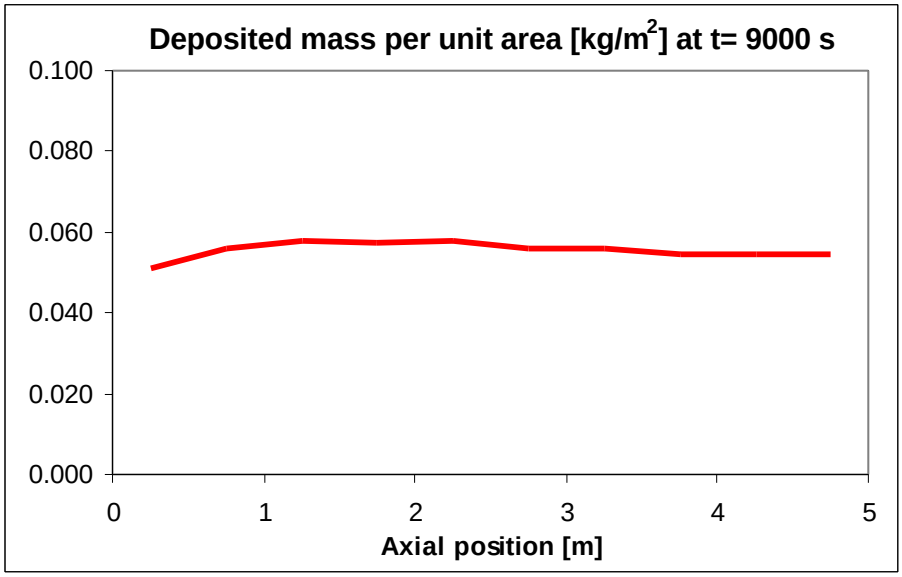

Fig. 35 - Spatial distribution of deposition (KINS)

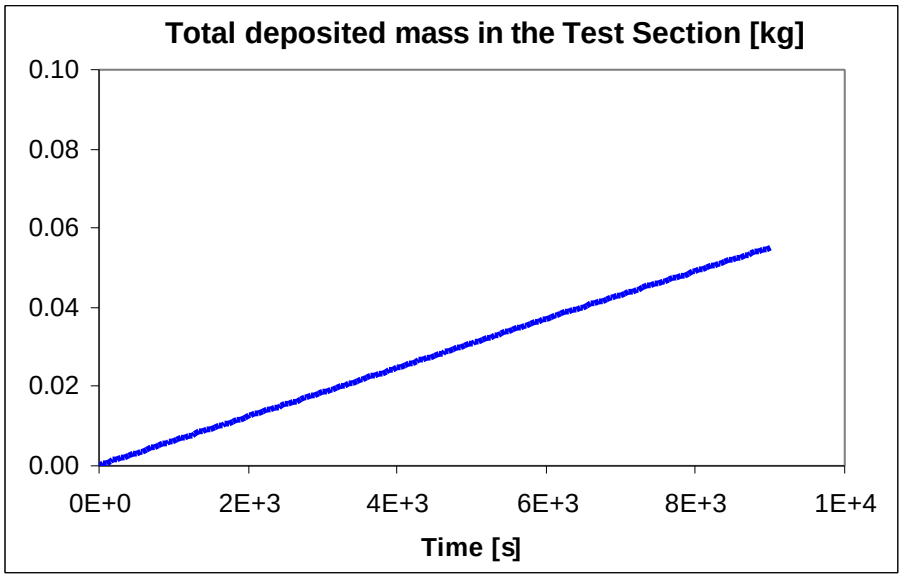

Fig. 36 - Time evolution of deposition (KINS)

Thermophoresis is largely dominant as a deposition mechanism, being responsible for 93 % of the total deposition. That percentage is slightly lower in the first cell and

almost constant (decreasing very slightly) from there till the end of the test pipe (Fig. 37). Practically all the remaining deposit is calculated to be due to gravitational settling, but it should be noted that eddy impaction is not modelled in the code.

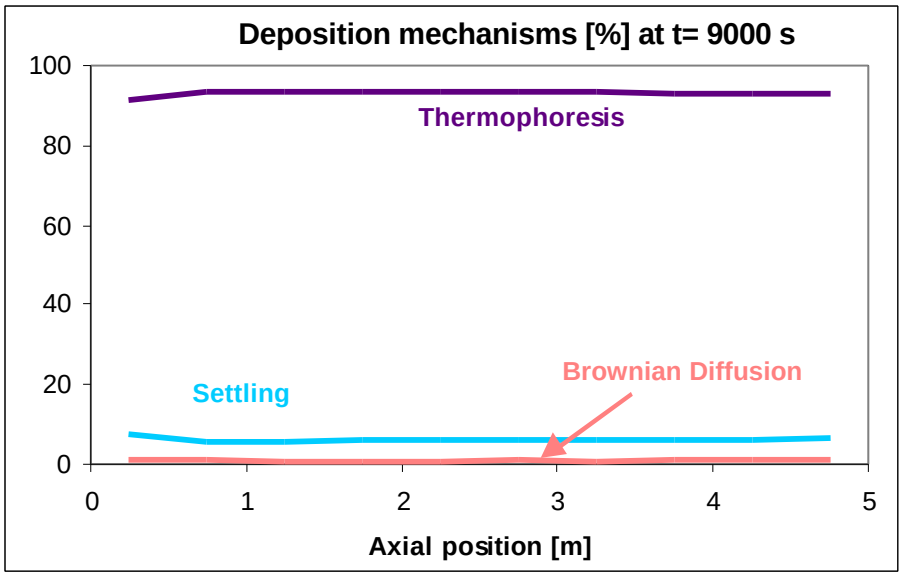

Fig. 37 - Deposition mechanisms along the test pipe (KINS)

The size distribution of the particles exiting the test pipe changes quickly in the first time steps and then stabilises and remains constant until the end of the calculation, with a geometric mean diameter of 2.9 µm and a geometric standard deviation of 2.2. These large particles are due to the incorrect specification of the size distribution at the inlet, as described above.

3.7.4. Kurchatov Institute

The ISP submission from Kurchatov Institute was calculated with version 1.8.2 of Melcor and no modifications were done to the code specifically for this problem [69].

3.7.4.1. ISP calculation

The calculation was performed on a Peacock Pentium-90 personal computer and took about 11.5 hours to run, which is 10^4 times more than the reference *linpackd* code.

The test pipe was discretised into ten identical computational cells, and the time step was 0.2 seconds for the first second and 20 seconds for the rest of the calculation. The aerosol size distribution was discretised into 10 size bins, covering the range between 0.1 and 10 µm. For the calculation of the flow velocity, the "time-dependent flow path" option was used.

The list of aerosol materials in Melcor 1.8.2 does not include SnO_2, and it was modelled using the less volatile class in Melcor, class N12.

The total mass deposited in the test pipe was calculated to be 13.7 grams, decreasing significantly in the first metre of the pipe and only slightly in the rest of the test pipe

(Fig. 38). The time variation of the deposit is calculated to be practically linear (Fig. 39).

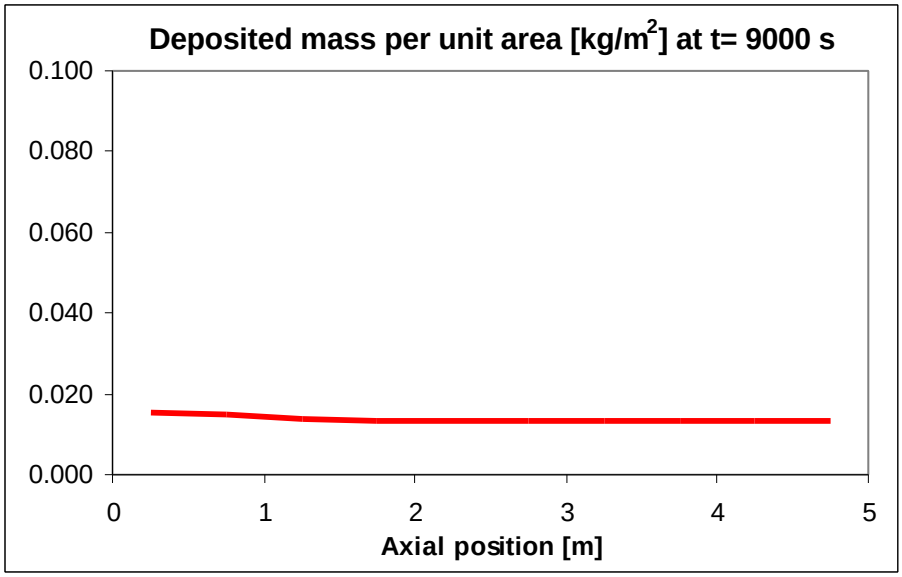

Fig. 38 - Spatial distribution of deposition (Kurchatov)

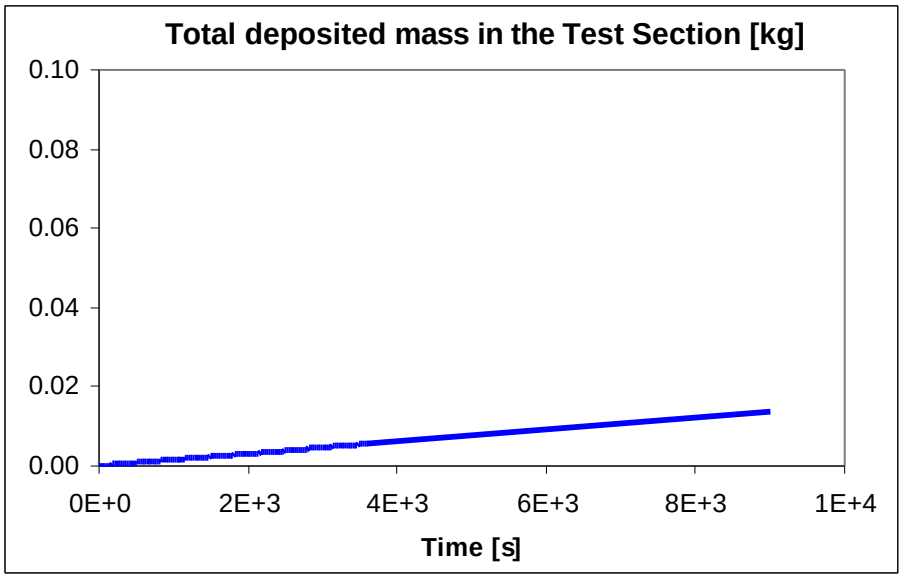

Fig. 39 - Time evolution of deposition (Kurchatov)

Since Melcor does not calculate the contribution of each mechanism to the total deposition, the distribution among mechanisms is unknown.

The particles that do not deposit in the test pipe exit with a geometric mean diameter of 0.41 μm and a geometric standard deviation of 1.7, constant during the whole period of the calculation.

3.7.5. Tractebel

Tractebel submitted two different calculations, both performed with version 1.8.3 of Melcor, using different coefficients in the calculation of the thermophoretic deposition velocity [43]. In the first calculation, the default coefficients were used, while the second one tested the sensitivity to the use of different coefficients within the range recommended by Brock. A modification was needed in the calculation of the Nusselt number (ratio between total heat transfer and convective heat transfer) to obtain the right temperatures for the carrier gas, as explained in the next section.

3.7.5.1. ISP calculation - Default coefficients

The results submitted were calculated on a HP workstation and took about 15 hours to run, which is 5600 times more than the reference *linpackd* code.

The test pipe was divided into 5 control volumes of different lengths, from a minimum of 0.61 m to a maximum of 1.146 m. The number of nodes was chosen as a good compromise between accuracy of the imposed boundary conditions and computational efficiency. Six additional volumes are used, five upstream of the test pipe and one downstream, to control the carrier gases mass flow rates through the system. The time step is calculated by the code and was 0.012 s.

The particle size distribution was discretised into 5 bins, covering the range of 0.13 µm to 3.80 µm. With these values, the actual distribution at the inlet was characterised by a mass median diameter of 1.014 µm and a geometric standard deviation of 1.738 (instead of the specified values of 1.013 and 1.700) [27].

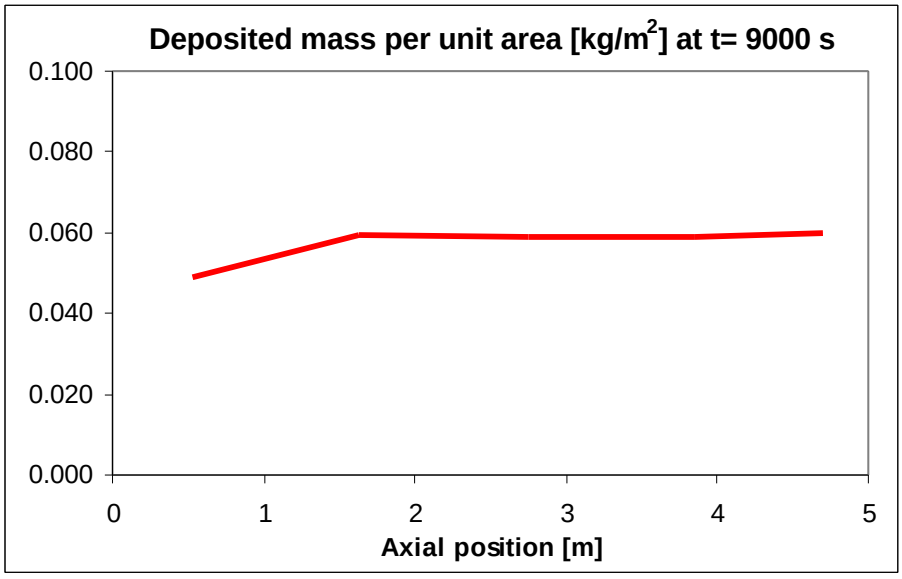

Fig. 40 - Spatial distribution of deposition (Tractebel-1)

The gas and wall temperatures were specified in terms of a mean gas temperature at different points along the test pipe and an inner wall temperature at the same points. However, in Melcor, imposing inner wall temperatures implies excluding those surfaces as deposition surfaces, which is not acceptable in this case. Imposing outer wall temperatures, Melcor indicates a temperature drop across the walls that is much smaller than measured. This could be due to extra insulation provided by the aerosol

deposit itself or, more likely, to some influence of the outside air on the measured outer wall temperatures. The measured outer wall temperatures were therefore corrected to reach the specified inner wall temperatures. The gas temperatures calculated by Melcor, however, were still quite different from the measured ones, and the only way to solve this was modifying the coefficient used to calculate the Nusselt number, which was changed from 0.023 to 0.0135.

The friction length of the junctions also had to be modified to obtain the correct pressure drop along the test pipe.

The total deposited mass in the test pipe was calculated to be 57 grams, practically uniform along the test pipe with the exception of the first cell, where deposition was slightly lower (Fig. 40). The time evolution of deposition was calculated to be linear (Fig. 41).

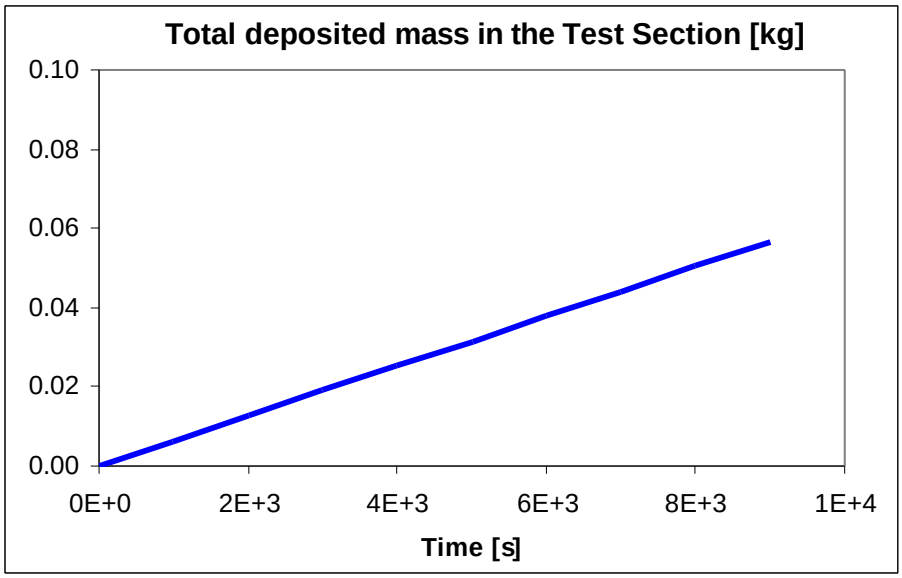

Fig. 41 - Time evolution of deposition (Tractebel-1)

Although Melcor does not give any indication of the distribution of deposition among the different mechanisms, a careful examination of the conditions in each control volume and for each size bin allowed Tractebel to draw the conclusion that thermophoresis is the most relevant mechanism, gravitational settling is relevant only for the bin that contains the largest particles, and Brownian diffusion is practically irrelevant in this case. Weighing the contributions of the different mechanisms, the global distribution is 68% thermophoresis and 32% gravitational settling.

The particles exiting the test pipe have a geometric mean diameter of 1.27 µm and a geometric standard deviation of 1.54. This seemed to indicate the existence of considerable agglomeration in the test pipe, which was not predicted by any other code or even by the other Melcor submissions. The particle size distribution at the outlet calculated by Tractebel was narrower but with a much higher (by a factor of almost 3) geometric mean diameter (Fig. 42). The reason for this behaviour was investigated and the effect was tracked to the fact that the submitted particle size distribution at the outlet is extracted from the code output for the extra computational cell after the test section. Since this cell is time-independent, all the aerosols that arrive there are kept in the cell for the whole duration of the test. The aerosol

concentration in this time-independent cell is therefore much higher than in the flow-through cells in the test section itself, favouring agglomeration. This is not, therefore, a physical effect, and the actual agglomeration in the test section is negligible also in this calculation.

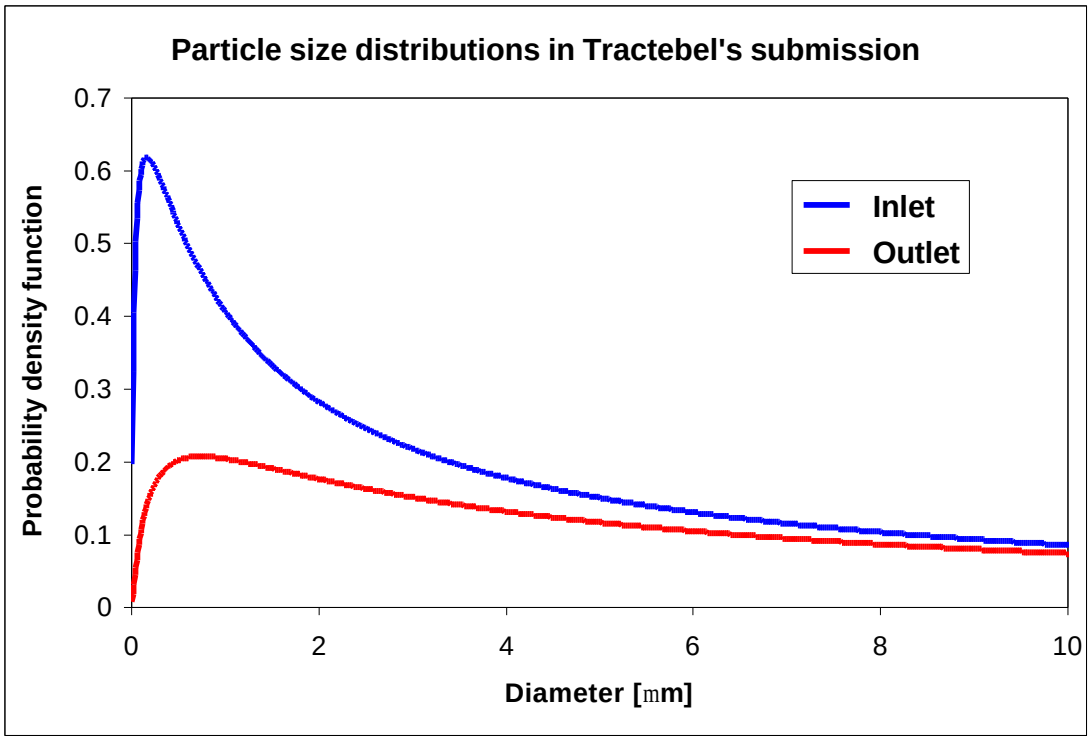

Fig. 42 - Particle size distributions in Tractebel's submission

3.7.5.2. ISP calculation – Sensitivity analysis

Since thermophoresis is expected to be the major deposition mechanism in this case, particular attention was devoted to the thermophoretic deposition model in Melcor, comparing it to other published models. While replacing the Brock-type formulation with different formulations like the one suggested by Springer would require major changes in the code, replacing the slip factor and the thermal accommodation coefficient used in Melcor with others can be done through the input file.

Different authors have proposed different values for the coefficients in the Brock equation. The most commonly used are the ones suggested by Brock himself and those suggested by Talbot [75]. Using the Talbot coefficients in the Melcor calculation also affected significantly the deposition by gravitational settling, and so Tractebel decided to perform a second calculation replacing the default coefficients with other within the range suggested by Brock.

The results submitted were calculated on a HP workstation and took about 15 hours to run, which is 5600 times more than the reference *linpackd* code.

The nodalisation, time step and discretisation of the particle size distribution were the same as in the first calculation. The same thing applies for the specification of the thermal-hydraulic boundary conditions.

The total deposited mass in the test pipe was calculated to be 130 grams, practically uniform along the test (Fig. 43). The time evolution of deposition was calculated to be linear (Fig. 44).

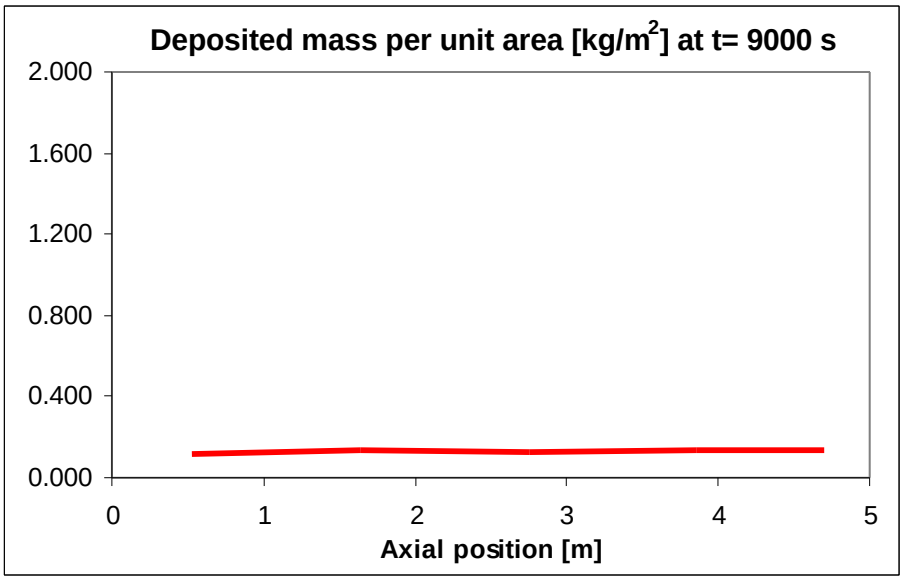

Fig. 43 - Spatial distribution of deposition (Tractebel-2)

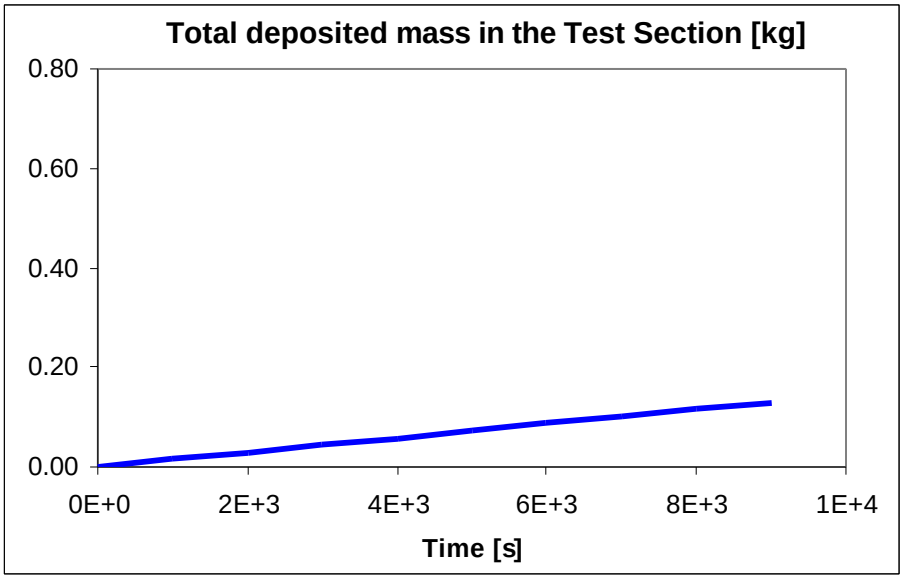

Fig. 44 - Time evolution of deposition (Tractebel-2)

The mechanisms that are responsible for the aerosol deposition are, in this case, thermophoresis (87%) and gravitational settling (13%).

The particles exiting the test pipe have a geometric mean diameter of 1.22 µm and a geometric standard deviation of 1.6. This apparent indication of agglomeration in the test pipe is due, as seen for the previous calculation, to a numerical artefact, and the actual particle size distribution at the outlet is similar to the one specified at the inlet.

3.7.6. University of Bochum-2

The second set of results submitted by the Univ. of Bochum was calculated with version 1.8.3 of Melcor [60]. The coefficients used in the Brock-type equation that calculates thermophoretic deposition are the ones indicated by Talbot [75]. The code was not modified specifically for solving this problem.

3.7.6.1. ISP calculation

The ISP calculation was performed on a Sun SparcStation 10 workstation and took just over 32 hours to run, which is about $1.5*10^4$ times more than the reference *linpackd* code.

The test pipe was divided into 9 identical control volumes and additional volumes were added upstream and downstream of the test pipe to establish the appropriate flow conditions. No information was given about the time step used in the calculation.

The particle size distribution was discretised into 10 bins, covering the range of particle diameters between 0.0783 µm and 0.791 µm.

The total deposition in the test pipe was calculated to be 139 grams, decreasing slightly along the test pipe (Fig. 45). The time evolution of the deposited is calculated to be linear, as expected (Fig. 46).

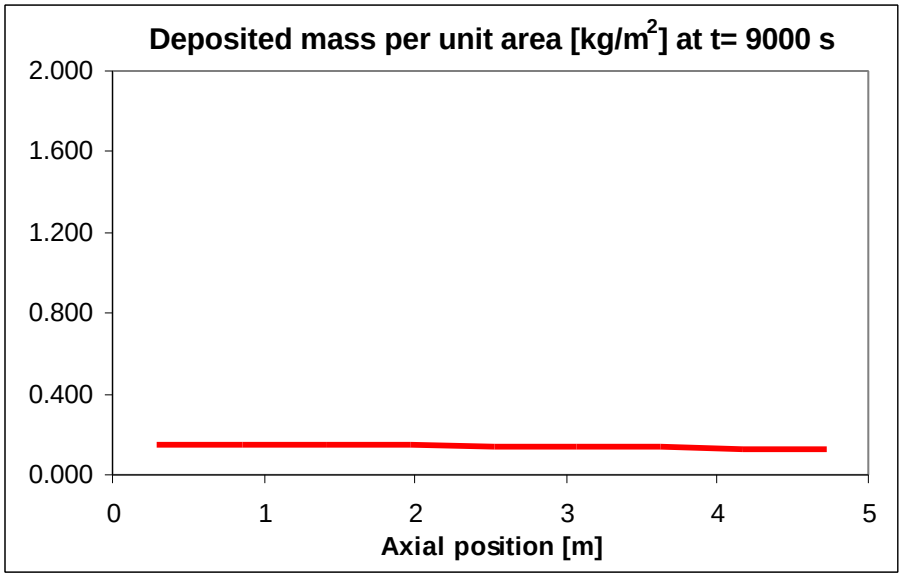

Fig. 45 - Spatial distribution of deposition (U. Bochum-2)

Since Melcor does not give a distribution of deposition among mechanisms, this distribution was not quantified. Nevertheless, the fact that only thermophoresis and diffusiophoresis were modelled and the comparison with the results obtained by the same organisation with another code (see the other University of Bochum submission) indicates that more than 99% of the deposition is probably due to thermophoresis.

The particles that do not deposit exit the test pipe with a geometric mean diameter of 0.49 µm and a geometric standard deviation of 1.3.

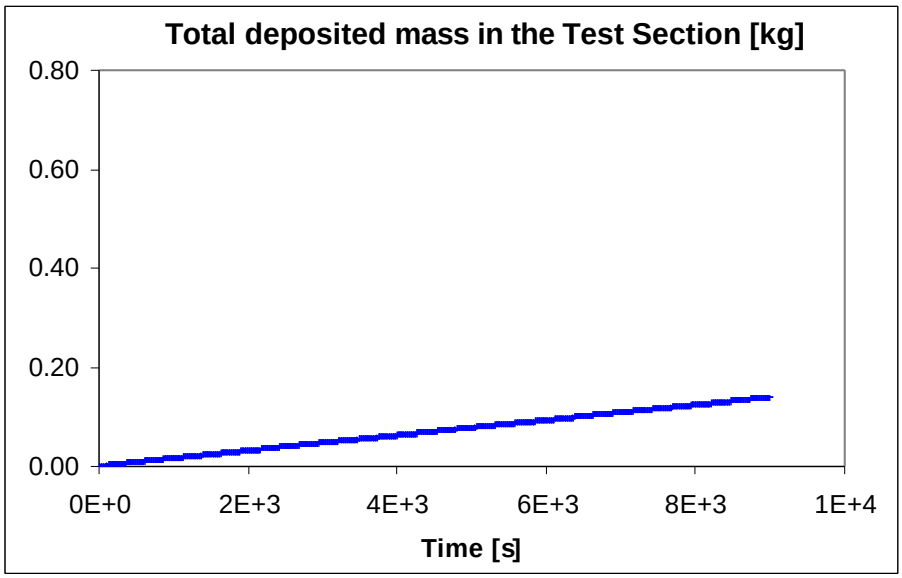

Fig. 46 - Time evolution of deposition (U. Bochum-2)

3.7.7. VEIKI-1

Two ISP-40 calculations were submitted by VEIKI, done with two different codes [40]. The first submission was done with version 1.8.3 of Melcor, which was not modified specifically for this problem.

3.7.7.1. ISP calculation

The ISP calculation was performed on a 100 MHz Intel 80486 personal computer and took approximately 2.5 hours to calculate the whole experiment, which is about 1500 time more than the reference *linpackd* code.

The test pipe was simulated as just one control volume, and two additional volumes were added, one upstream and one downstream of the test pipe. The time step used was 0.126 seconds.

The particle size distribution was divided into 5 bins, covering the range between 0.1 and 50 µm.

The total mass deposited in the test pipe was calculated to be 53 grams. Since only one control volume was used, there is no indication of the spatial distribution of the deposition. Although the results were submitted at only two points in time, the temporal evolution of the deposition seems to be approximately constant, slightly higher in the early phase of the test (Fig. 47).

No indications are given about the deposition mechanisms, which are not discriminated in the Melcor output. The particles exiting the test pipe were characterised by a geometric mean diameter of 0.43 µm and a geometric standard deviation of 1.7.

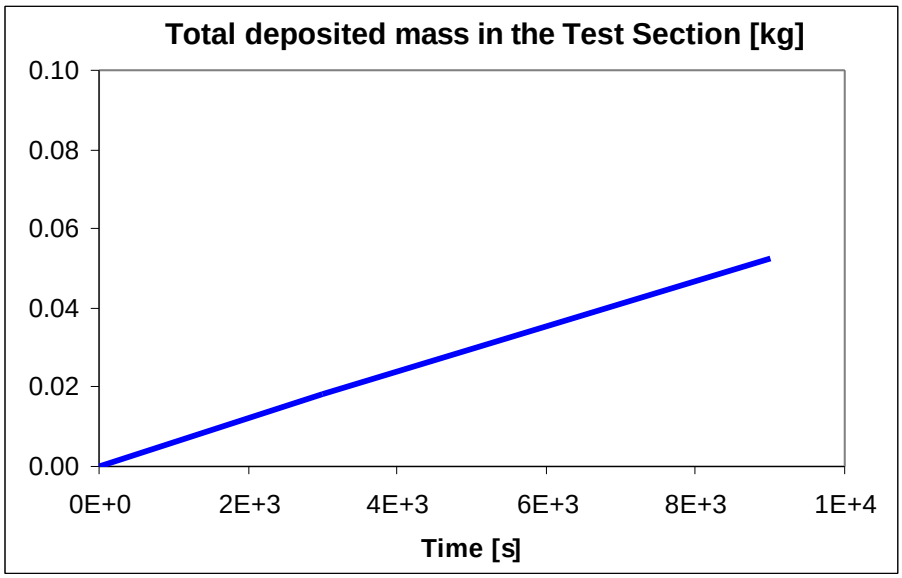

Fig. 47 - Time evolution of deposition (VEIKI-1)

3.8. Raft

3.8.1. Introduction

The Raft computer code was developed by EPRI to calculate the formation and transport of fission products through the primary circuit of a LWR, in case of a severe accident [31].

It includes models for homogeneous and heterogeneous nucleation, vapour condensation on the walls or on particles, aerosol agglomeration due to gravity, Brownian motion and turbulence, and aerosol deposition due to thermophoresis, eddy impaction, gravitational settling, Brownian diffusion and inertial impaction in bends.

The thermophoretic deposition velocity is calculated using Springer's model [71], and the eddy impaction model is based on the Friedlander-Johnstone correlation [17].

Raft uses a semi-lagrangian solution method, which means that for a given time step, the length of each computational cell is reduced iteratively until each of a number of specified parameters differs from the previous cell by less than a given fraction.

3.8.2. JRC-2

The second JRC calculation was done with version 1.1/JRC of Raft, without any specific changes for this problem [1].

3.8.2.1. ISP calculation

The Raft calculation was done on a Sun SparcStation 10 workstation and took 36.9 seconds to run, which is 4 times more than the reference *linpackd* code.

Given the semi-lagrangian method used in Raft, the number and dimension of the actual computational cells can change as is set internally by the code. For the output, a total of 10 practically identical "cells" was used. The time step used in these calculations is also irrelevant, since the calculation was performed as steady-state and therefore all time-dependent terms in the equations were automatically set to zero.

The particle size distribution was discretised into 40 bins, covering the range from 0.05 μm to 10 μm.

The total deposited mass was calculated to be 325 grams decreasing slightly along the test pipe (Fig. 48). The temporal evolution of deposition was implicitly assumed to be linear since the calculation was performed as steady state.

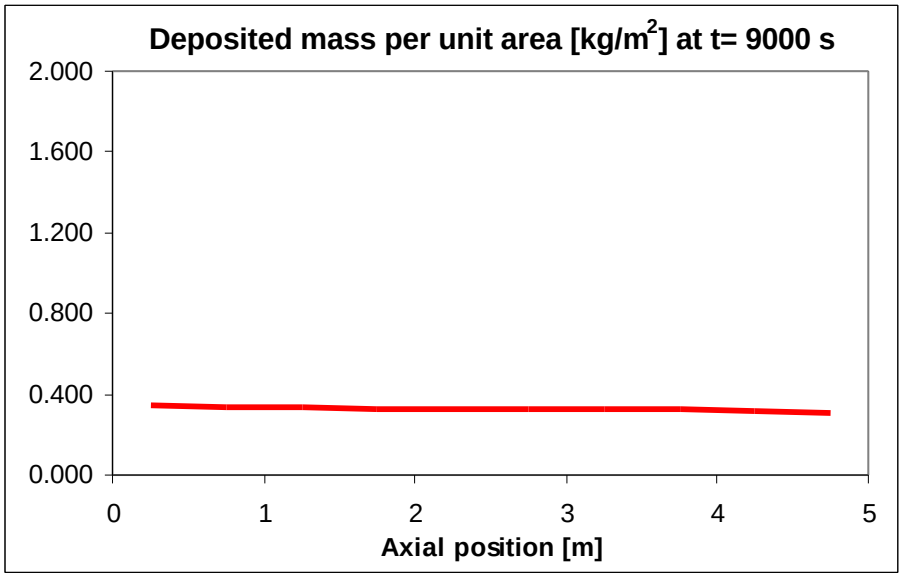

Fig. 48 - Spatial distribution of deposition (JRC-2)

Thermophoresis is the largely dominant deposition mechanism, with 90.4 % of the total deposition and eddy impaction is responsible for the remaining 9.6 %. The relative importance of thermophoresis increases very slightly along the test pipe (Fig. 49).

The size distribution of the particles exiting the test pipe is not given by RAFT. However, the mass mean radius of the suspended particles in the last cell is given as being 0.58 μm. Assuming that the geometric standard deviation remains approximately the same as at the inlet, which is not unreasonable given the small amount of deposition in the test pipe, the size distribution at the outlet would be characterised by a geometric mean diameter of 0.44 μm and a geometric standard deviation of 1.7.

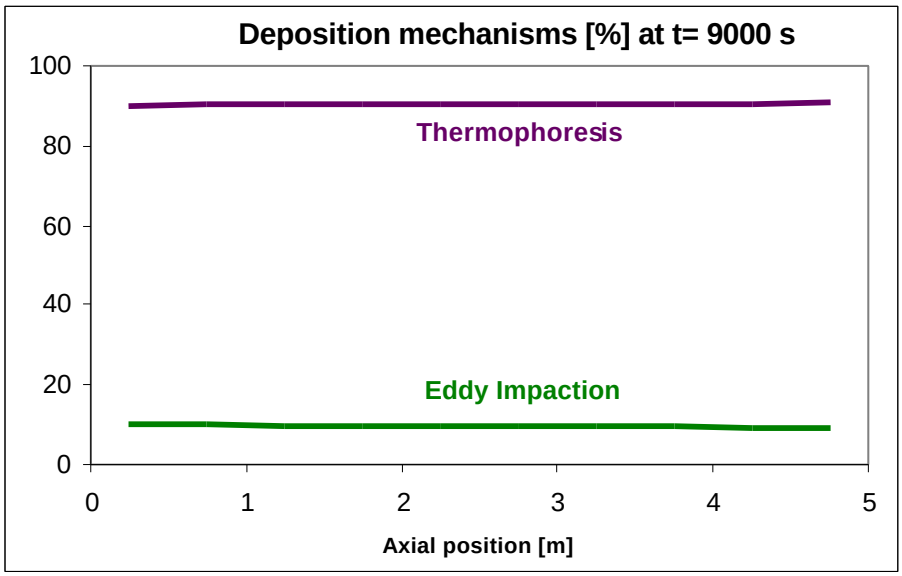

Fig. 49 - Deposition mechanisms along the test pipe (JRC-2)

3.9. Sophaeros

3.9.1. Introduction

The Sophaeros code was developed by IPSN to predict in a mechanistic way the fission product (f.p.) physical behaviour in LWR primary circuits during severe accidents [46], [47], [48]. The modular structure of the code allows a versatile choice of defining input thermal-hydraulic data, circuit geometry, and physical description of aerosol/vapour deposition, with possible switching on/off of all transport mechanisms.

The main phenomena modelled by the code are interaction of f.p. vapours with aerosols (condensation/evaporation), interaction of vapours with walls (condensation and sorption), aerosol fallback and coagulation, aerosol deposition on circuit walls.

The models for aerosol deposition include thermophoresis and eddy impaction as well as sedimentation, Brownian and turbulent diffusion, diffusiophoresis and centrifugal impaction in bends. The thermophoretic deposition model uses Talbot's equation [75] while for the eddy impaction mode the user has a choice between the Liu-Agarwal model [42] and the Friedlander-Johnstone model [17].

An agglomeration model is included in the code, considering Brownian, gravitational and turbulent coagulation. For coagulation kernels, the collision efficiency of larger particles (Pruppacher-Klett law) was also introduced. Particle growth can be due, besides agglomeration, to vapour condensation on aerosol particles.

The large number of mass balance equations with non-linear terms is solved using an implicit numerical method leading to short run times.

Version 1.3 of the Sophaeros code (used for the deposition exercise by IPSN/DRS) models also the vapour-phase chemistry. Version 1.4 GRS of the Sophaeros code (used for the deposition exercise by GRS) is identical to version 1.3 with the addition of a model for mechanical resuspension of aerosols. Version 2.0 of the Sophaeros

code (used for the resuspension exercise by IPSN/DRS) is identical to version 1.3 including the modeling of homogeneous nucleation and aerosol mechanical resuspension. The resuspension model is similar to the one included in the Ecart code [56].

3.9.2. CEA/IPSN/DRS

The results submitted by CEA/IPSN/DRS were calculated with version 1.3 of Sophaeros [45], [49]. The module that calculates vapour-phase chemistry was not activated, and small modifications had to be made to the code to simulate correctly the fluid composition in STORM test SR11.

3.9.2.1. ISP calculation

The ISP calculation was performed on a Sun SparcStation 10 workstation and took 13 seconds to run, which is 1.6 times more than for the reference *linpackd* code.

A total of 10 practically identical control volumes were used and the total time of 9,000 seconds was divided into 23 time steps, with one or two iterations per time step. The particle size distribution was discretised in 20 bins, covering the range from 10^{-2} µm to 10^{2} µm.

The heat transfer between the carrier gas and the walls and the physical properties of the carrier gas were derived from formulations consistent with the Cathare2 thermal-hydraulic models [44].

The total deposited mass in the test pipe was calculated to be 256 grams, slightly decreasing from the entrance to the exit of the test pipe (Fig. 50). Variation of deposition with time was linear in all control volumes, since the problem was specified as being in steady state (Fig. 51).

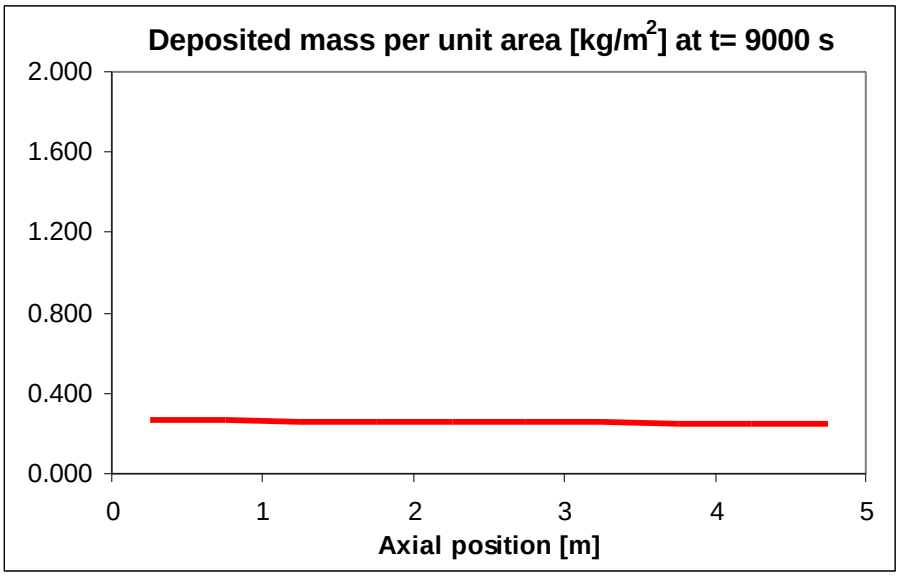

Fig. 50 - Spatial distribution of deposition (CEA/IPSN/DRS)

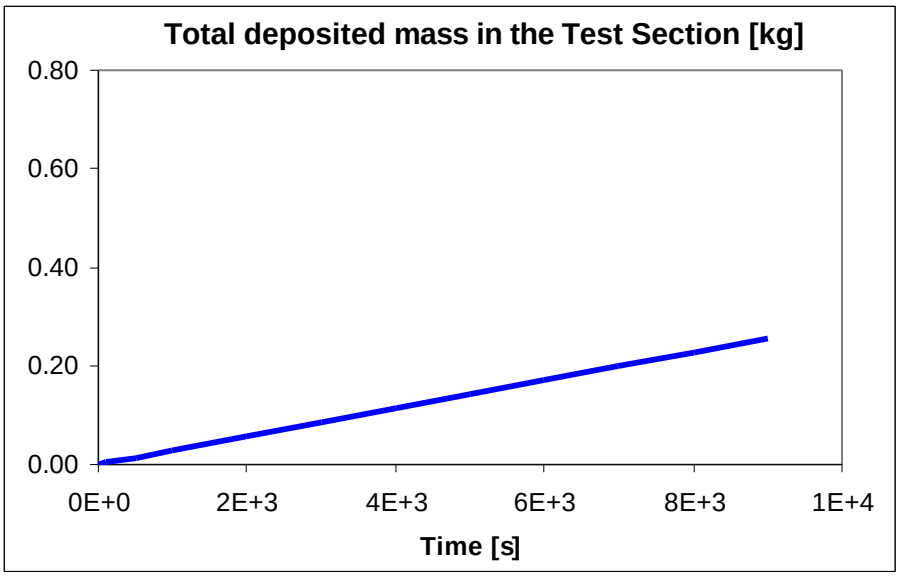

Fig. 51 - Time evolution of deposition (CEA/IPSN/DRS)

According to the results of the calculation, thermophoresis was the dominant deposition mechanism, being responsible for 77% of the total deposition, while eddy impaction caused 22% of the deposition and sedimentation the remaining 1%. This distribution among deposition mechanisms was constant in time, and the importance of thermophoresis increased slightly from the entrance to the exit of the test pipe (Fig. 52).

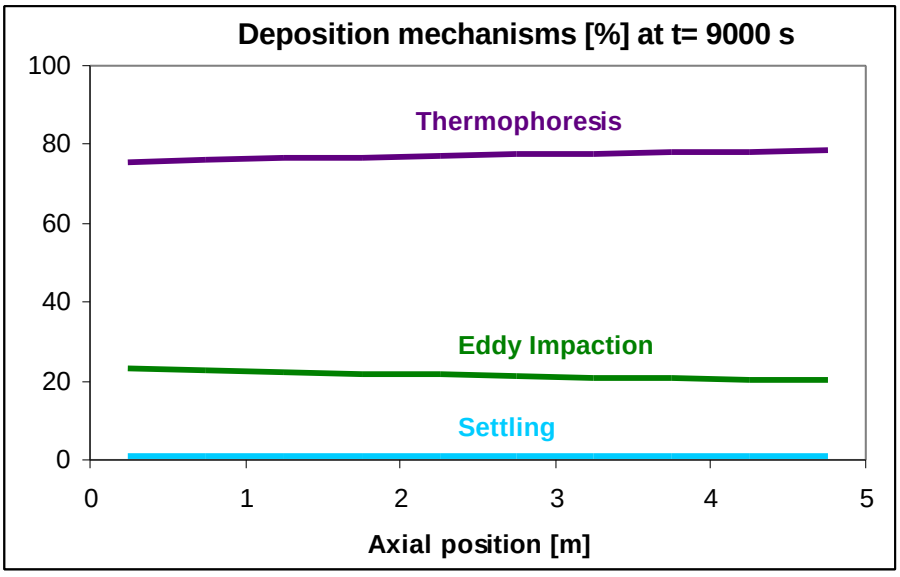

Fig. 52 - Deposition mechanisms along the test pipe (CEA/IPSN/DRS)

The particles that did not deposit left the test pipe with a geometric mean diameter of 0.44 µm and a geometric standard deviation of 1.7.

3.9.2.2. Sensitivity calculations

The dominance of thermophoresis is mainly linked to the particle size distribution characterised by a small geometric mean radius and a small geometric standard deviation, and to the presence of tin dioxide particles with a low apparent density. So, the influence of this estimated parameter was investigated. A decrease by 50% of the aerosol density leads to a decrease of about 15% of the total deposition in the test pipe and thermophoresis becomes more dominant (92%). On the other hand, the opposite trend is observed when the aerosol density is increased by 50%. The total deposition increases by about 20% and the contribution of eddy impaction, helped by the presence of aerosol agglomeration in the circuit, increases (36%) to the detriment of thermophoresis (62%).

The influence of another estimated parameter -thermal conductivity of particles- was investigated and showed little on the total deposition for the conditions studied in the ISP40.

3.9.3. GRS

The results submitted by GRS were calculated with version 1.4 GRS of Sophaeros with the Liu-Agarwal model for eddy impaction [63].

For this particular problem, the restriction in the Sophaeros control file to pressures greater or equal to 10^6 dyne/cm^2 and to aerosol densities greater or equal to 1 g/cm^3 were removed, and the SnO_2 non-volatile species was added to the Sophaeros databank.

3.9.3.1. ISP calculation

The ISP calculation submitted by GRS was performed on an IBM workstation. It took 56.35 seconds to run, which is 99 times more than the reference *linpackd* code.

The test pipe was divided into 10 identical control volumes and a total of 183 time steps were used, with up to three iterations per time step. The time step was shorter in the first 4 steps and constant afterwards, due to the steady-state character of the problem.

The aerosol size distribution was discretised into 20 bins, covering the range between 0.025 and 500 μm.

Since the Sophaeros code does not contemplate the possibility of having the same mixture of gases that was used in the tests, some modifications were made to the composition of the carrier gas for the calculations. Helium and argon were treated together, with the properties of argon, and the same was done with air and nitrogen, with the properties of nitrogen. Steam was replaced with oxygen, to allow the use of the *GKINETIC* option for the gas properties.

The total deposited mass in the test pipe was calculated to be 225 grams and is distributed practically uniformly along the test pipe (Fig. 53). The time dependence of the deposited mass is, as expected, linear (Fig. 54).

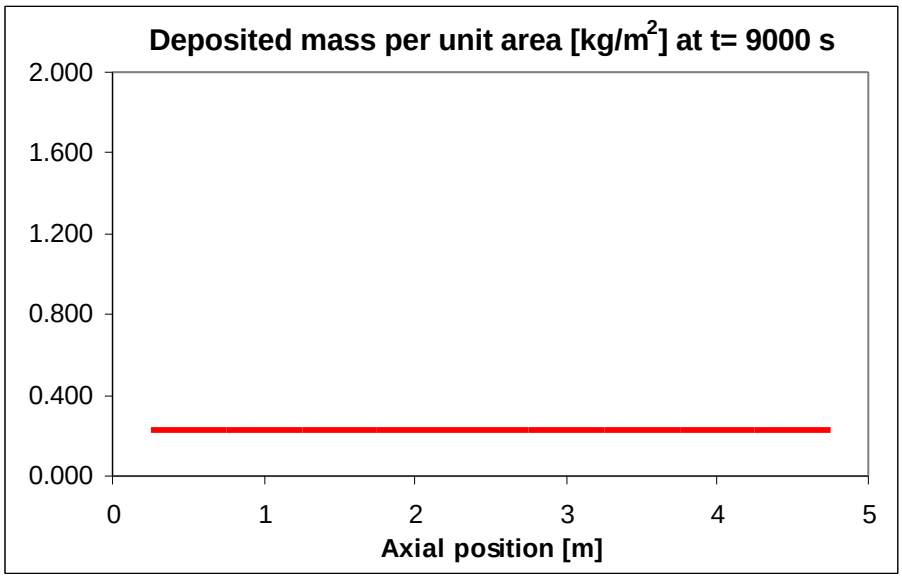

Fig. 53 - Spatial distribution of deposition (GRS)

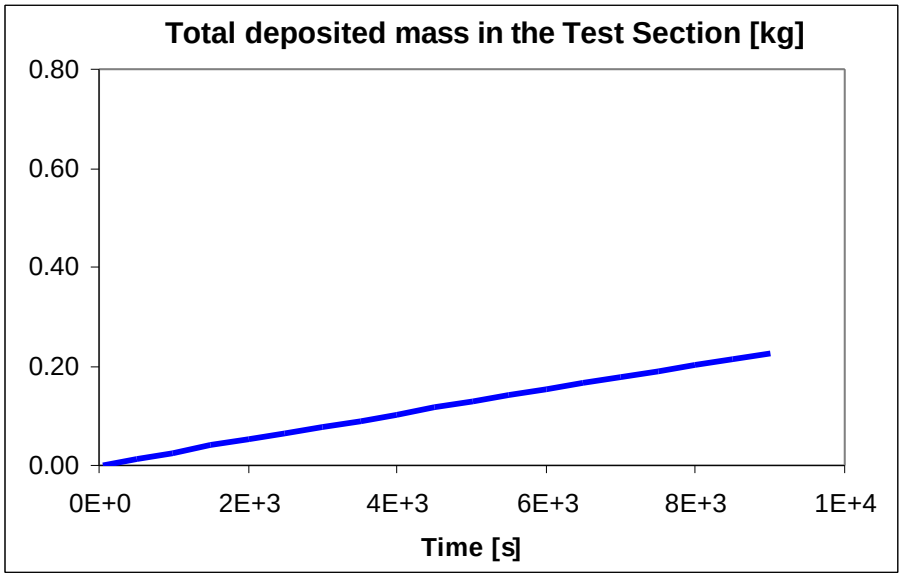

Fig. 54 - Time evolution of deposition (GRS)

Thermophoresis is calculated to be largely dominant as a deposition mechanism, being responsible for 94.6% of the total deposition. Eddy impaction accounts for 4.1% of deposition with gravitational settling and turbulent diffusion playing very minor roles. The dominance of thermophoresis as a deposition mechanism is practically constant along the test pipe (Fig. 55).

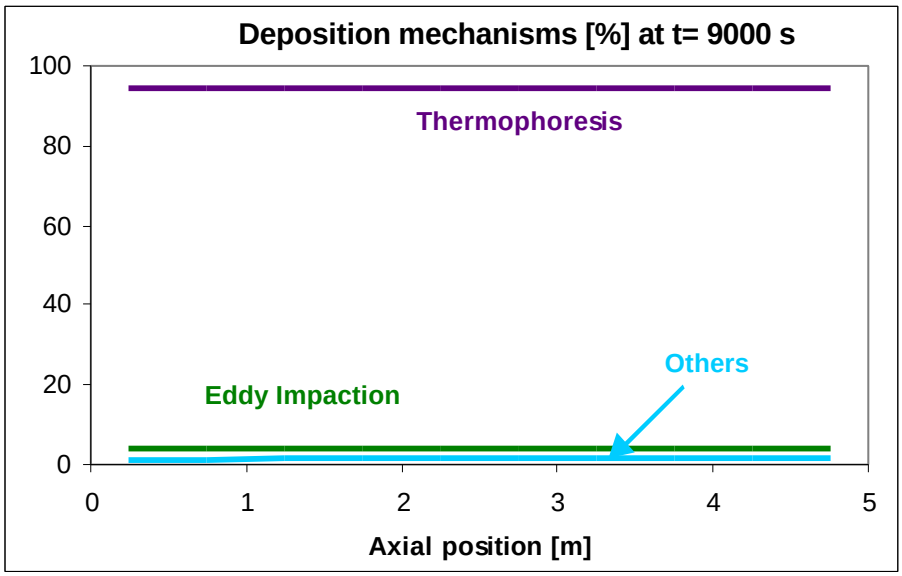

Fig. 55 - Deposition mechanisms along the test pipe (GRS)

The particles that exit the test pipe have a geometric mean diameter of 0.44 µm and a geometric standard deviation of 1.7. The mean particle size increases with time, but the increase is barely noticeable (about 0.05% for the whole duration of the test).

3.9.3.2. Sensitivity calculations

One calculation was done excluding the aerosol resuspension module. The calculated deposited mass increased to 237 grams for the whole test pipe and the spatial distribution of the deposit was less uniform, slightly decreasing along the test pipe. The distribution among deposition mechanisms was practically the same, with just a very small increase of thermophoresis, from 94.6 % to 94.8 %.

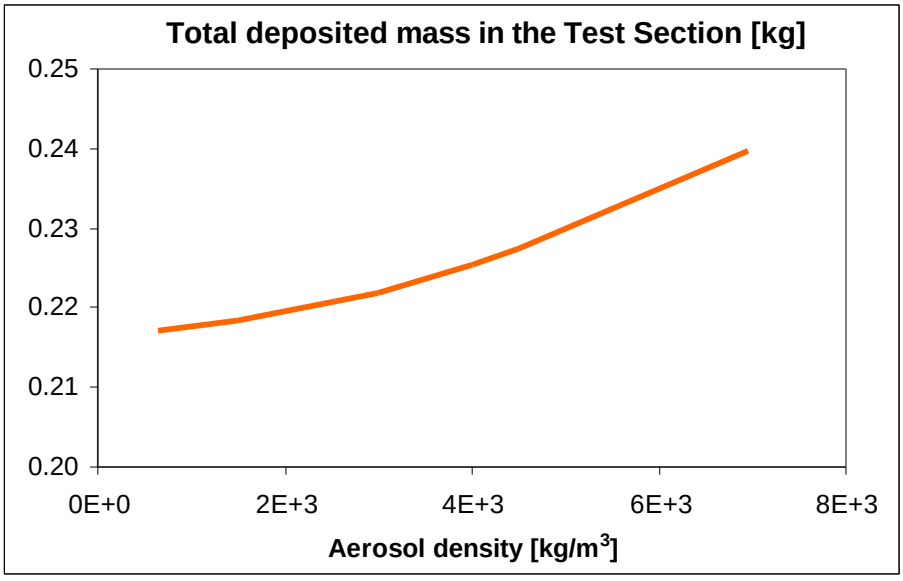

Fig. 56 - Variation of the deposited mass with the aerosol density (GRS)

The sensitivity of the results to the aerosol characteristics was also carefully examined. Calculations were done for particle densities ranging from 650 to 6950 kg/m3, showing only a variation of ± 5 % in the total mass deposited (Fig. 56) [77]. The relative importance of thermophoresis decreases with increasing density, with the inertial mechanisms - eddy impaction and gravitational settling - becoming more important.

Modifying the aerosol heat conductivity in the range of 5 to 17 W/m.K, on the other hand, did not produce any significant changes in the results.

3.9.4. JRC-3

The third calculation was done with version 1.1 of Sophaeros, without any specific changes for this problem [50].

3.9.4.1. ISP calculation

The Sophaeros calculation was done on a Sun SparcStation 10 workstation and took 39.9 seconds to run, which is 4.4 times more than the reference *linpackd* code.

The test pipe was divided into 9 control volumes of different lengths and the total time was divided into 302 time steps with 2 or 3 iterations per time step.

The particle size distribution was discretised into 20 bins, covering the range from 0.05 µm to 20 µm.

The total deposited mass was calculated to be 308 grams decreasing slightly along the test pipe (Fig. 57). The temporal evolution of deposition was calculated to be linear (Fig. 58).

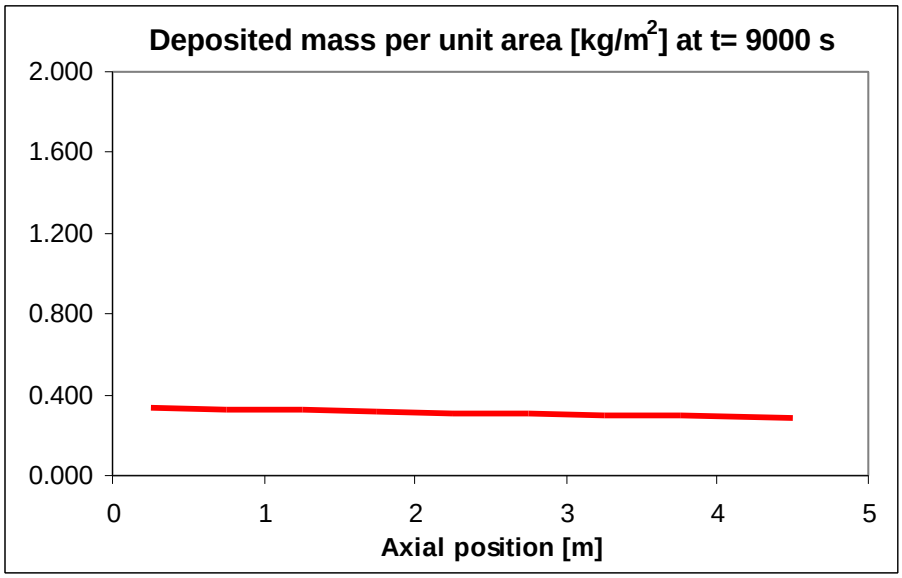

Fig. 57 - Spatial distribution of deposition (JRC-3)

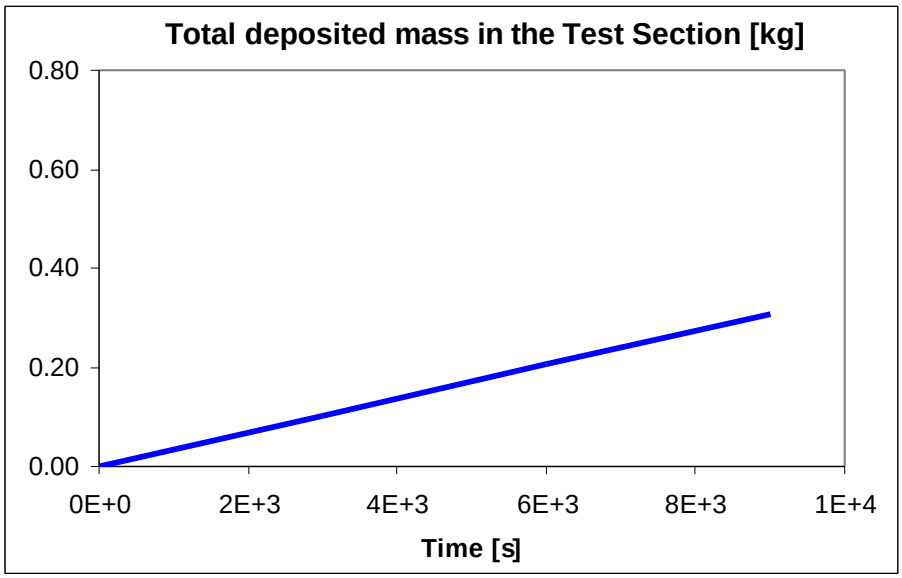

Fig. 58 - Time evolution of deposition (JRC-3)

Thermophoresis and eddy impaction are the dominant deposition mechanisms, being responsible for 54.2 % and 44.5 % of the total deposition, respectively. Gravitational settling is the only other significant deposition mechanism. The relative importance of thermophoresis increases along the test pipe, while that of eddy impaction decreases (Fig. 59).

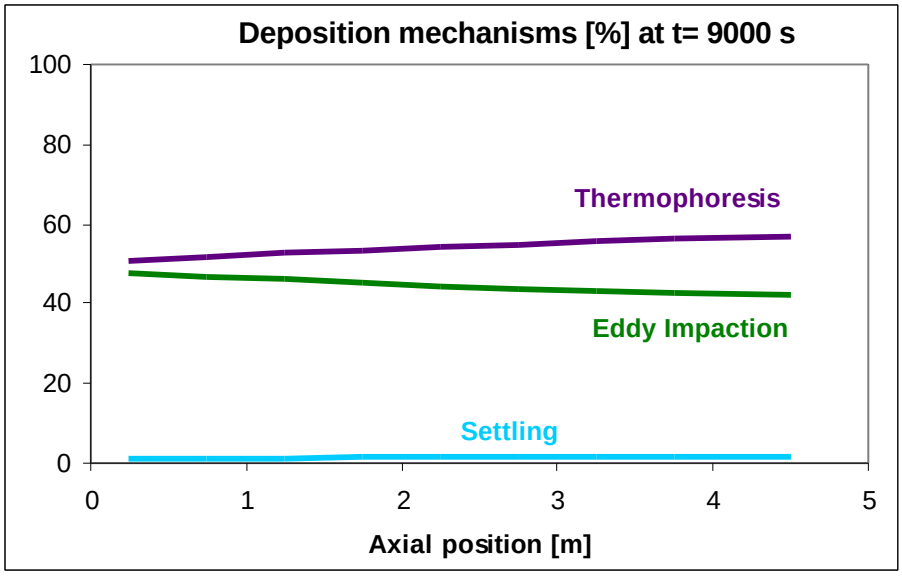

Fig. 59 - Deposition mechanisms along the test pipe (JRC-3)

The particles that do not deposit in the test pipe exit with a geometric mean diameter of 0.43 μm and a geometric standard deviation of 1.7.

3.10. Victoria

3.10.1. Introduction

Victoria is a USNRC code, developed originally by Sandia National Labs. and later also in collaboration with AEA Technology, to model the release, transport, deposition and resuspension of fission products during a severe reactor accident. It models chemistry in the vapour and condensed phases, assuming instantaneous chemical equilibrium [23].

Concerning aerosol transport, it models aerosol formation, agglomeration due to gravity, Brownian motion and turbulence, and deposition by gravitational settling, Brownian diffusion, turbulence (diffusion and impaction), thermophoresis and impaction in bends.

The thermophoretic deposition model uses Talbot's equation [75], with a user-specified thermal boundary layer thickness. For turbulent deposition, it takes the sum of eddy impaction, calculated with Sehmel's equation [68], and turbulent diffusion, using Davies' equation [7].

3.10.2. CIEMAT

The ISP calculation was performed with Victoria-92 [28]. To be able to simulate the ISP test, gaseous nitrogen had to be added to the chemical database, and the density and thermal conductivity of SnO_2 had to be changed to 4000 kg/m^3 and 11 W/m.K, respectively.

3.10.2.1. ISP calculation

The ISP calculation was run on a HP 715/100 workstation. Fifty identical computational cells were used and, since the convective term is solved explicitly in Victoria, the time step had to be selected according to the Courant condition for numerical stability. A time step of 10^{-3} seconds was therefore used. This led to an extremely long run time, of more than 47,000 seconds of CPU per real-time second. Since the conditions specified were steady state, the calculation was run only for a few seconds of real-time and the results were then extrapolated for the whole duration of the test. A full run would take of the order of 10^8 times longer to run than the reference *linpackd* code.

A second calculation was run with a rougher nodalisation - 10 computational cells - and, consequently, a longer time step - 0.02 seconds. Virtually the same results were obtained, and the run time was decreased by one order of magnitude - less than 5,900 seconds per real-time second, or $1.3*10^7$ times the reference *linpackd* code.

The particle size distribution was discretised in 40 bins, covering the range from 0.004 μm to 21.5 μm.

The total deposited mass in the test pipe was calculated to be 239 grams, uniformly distributed along the test pipe except for the first cell, where deposition was calculated to be smaller (Fig. 60). As mentioned before, the calculation was performed only for a few seconds of real time, and extrapolated linearly for the whole length of the test.

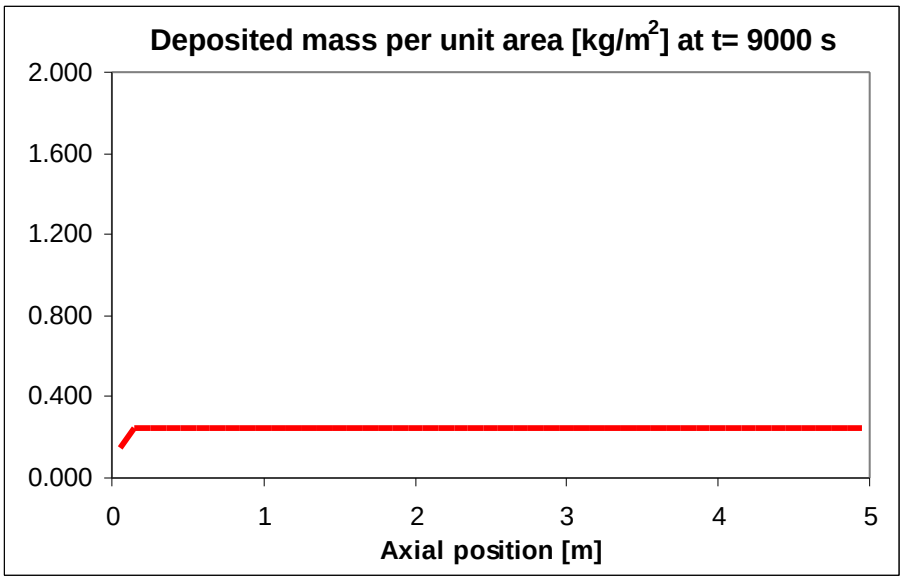

Fig. 60 - Spatial distribution of deposition (CIEMAT)

The Victoria calculation predicted thermophoresis to be largely dominant as a deposition mechanism, being responsible for 92.6% of the total deposition. The remaining 7.5% is mostly due to turbulent deposition (6.5%). The distribution among deposition mechanisms is assumed to be constant in time and decreases very slightly along the test pipe except for the first cell, where thermophoresis is responsible for about 98% of the deposition (Fig. 61).

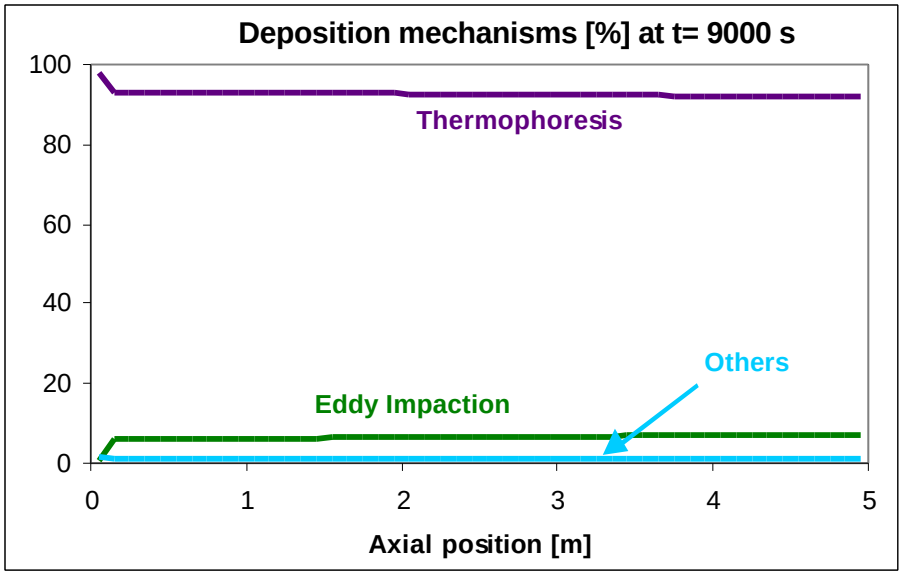

Fig. 61 - Deposition mechanisms along the test pipe (CIEMAT)

The particles that did not deposit left the test pipe with a geometric mean diameter of 0.44 µm and a geometric standard deviation of 1.7.

3.10.3. VEIKI-2

The second submission from VEIKI was done with version 92 of Victoria, which was also not modified specifically for this problem [40].

3.10.3.1. ISP calculation

The ISP calculation was performed on an IBM Risc 6000 workstation and took just over 3 hours to calculate the whole experiment, which is 2200 times more than the reference *linpackd* code.

The test pipe was divided into 10 almost identical control volumes, with a time step of 0.2 seconds. Although this is 10 times higher than the Courant limit, additional calculations performed with smaller time steps show that there were no numerical problems and the same results were obtained.

The particle size distribution was divided into 12 bins. The mass median radius, which is the parameter accepted by Victoria for the definition of the particle size distribution was given as 1 μm, which is almost twice as large as the suggested value - the geometric mean diameter of 0.4348 μm corresponds to a mass median radius of 0.5062 μm.

Since nitrogen is not in the Victoria database, the nitrogen flow rate was replaced with a mixture of oxygen and helium, so that the gas density was maintained.

The total mass deposited in the test pipe was calculated to be 303 grams, slightly higher at the beginning of the pipe, then practically uniform and finally lower in the last control volume (Fig. 62). Time evolution of the deposit was practically linear (Fig. 63).

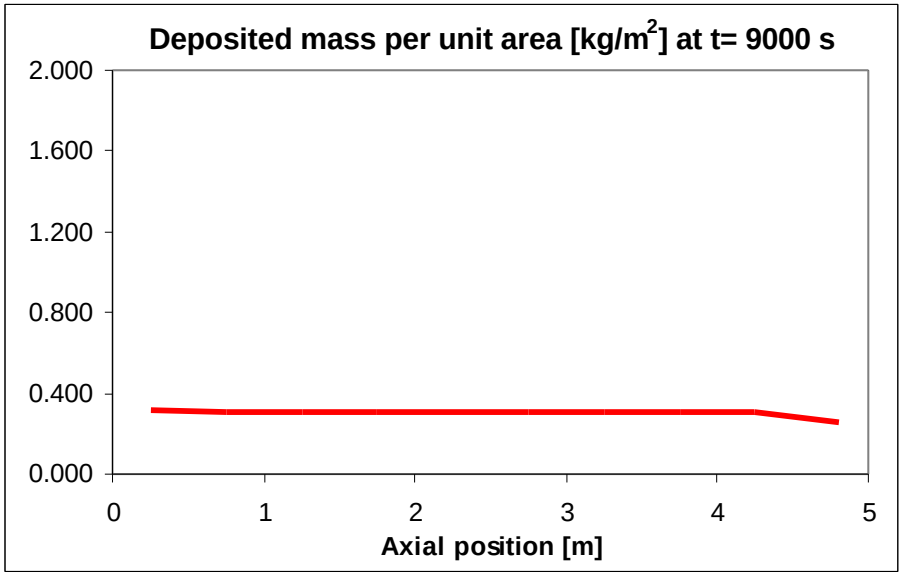

Fig. 62 - Spatial distribution of deposition (VEIKI-2)

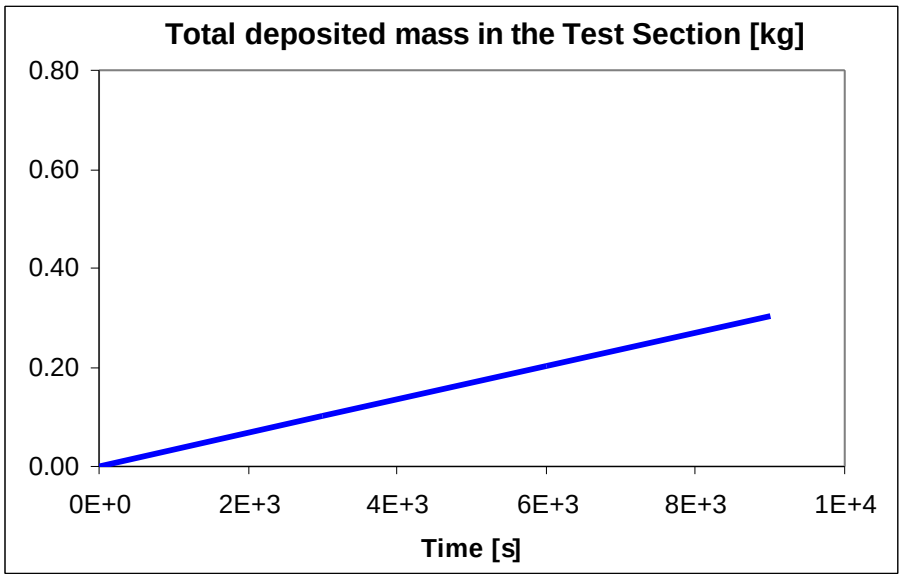

Fig. 63 - Time evolution of deposition (VEIKI-2)

Thermophoresis is the dominant deposition mechanism, with 72.0 % of the total deposition, while 21.5 % of the deposition was calculated to be due to eddy impaction and 6.5 % to gravitational settling. Except for the first control volume, in which the contributions of thermophoresis and gravitational settling are considerably higher to the detriment of eddy impaction, the distribution among deposition mechanisms remains practically constant along the test pipe (Fig. 64).

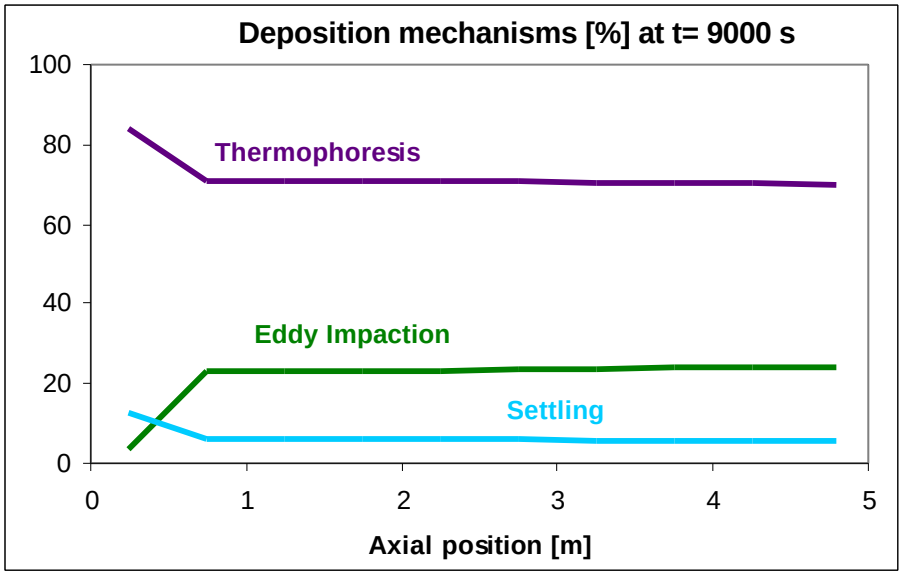

Fig. 64 - Deposition mechanisms along the test pipe (VEIKI-2)

The particles exiting the test pipe are characterised by a geometric mean diameter of 2.4 μm and a standard deviation of 2.0.

3.11. Comparison

3.11.1. Computer codes used

Twenty-otwo different submissions were received from fifteen different organisations. Additionally, several of these organisations also presented results of sensitivity analysis they performed on parameters considered particularly relevant or insufficiently known.

Although the difference between two submissions from the same organisation and one submission plus sensitivity analysis is not always clear, they are presented as separate submissions only when the results submitted had comparable detail. That is the reason why the calculation performed by GRS excluding the resuspension module is presented as a sensitivity calculations while the calculations performed by JAERI and the University of Pisa with and without activating the resuspension model are presented as separate submissions.

Nine different computer codes were used, and two of them - Melcor and Sophaeros - in two or three different versions. Athlet-CD was not counted as a separate code since its aerosol module is a version of the Sophaeros code. If the number of submissions reflects the present situation in the severe accident research community, Melcor is the most used severe accident code, with almost 1/3 of the total number of submissions.

While a large majority of the participants used codes currently used in severe accident analysis, in which the equations are solved in an Eulerian way, assuming well-mixed conditions in each computational cell, two submissions concerned computer codes that are still under development but take a substantially different approach. The two codes - DeNiro and Marie - use particle tracking to follow the trajectories of individual particles associated with a Monte-Carlo approach to calculate the global parameters.

In terms of models used for the main deposition mechanisms, which are, in this case, thermophoresis and eddy impaction, the dispersion is much smaller. With only two exceptions - Raft and Art, but this one only for large Knudsen numbers - the Brock-type equation for thermophoretic deposition [3] is used by all codes. In most cases, the coefficients used are those proposed by Talbot [75], while in Melcor the coefficients can be specified by the user, allowing the use of the original Brock coefficients as well as Talbot's or others.

The Liu-Agarwal correlation for eddy impaction [42] is preferred by most codes, although the Friedlander-Johnstone correlation [17] and the Sehmel [68] correlation are also used. The aerosol module in Melcor, having been developed primarily for containment conditions, does not include a model for eddy impaction.

3.11.2. Computational effort

A reference number-crunching code, *linpackd,* was supplied to all participants so that they could run it on their computers, in order to allow a more significant comparison of the CPU times needed to solve the ISP-40 problem. It must be noted, however, that the reference code was distributed as Fortran source and compiled in each computer. The speed of execution could, therefore, be influenced by the parameters used for the compilation, which can be different even for the default installation of different compilers, which have, for example, different levels of optimisation of the executable

code. Even if the comparison is more meaningful than just by comparing run times, it should still be seen critically. In addition, it should be noted that there is only a weak relationship between the CPU time needed to calculate a simple experiment and the CPU time needed for a full plant calculation. This relationship depends strongly on the options chosen by the user in terms of discretisation and time step.

Most of the ISP participants used Unix workstations to perform their calculations. The *linpackd* results given by the Kurchatov Institute, however, show that even a relatively slow 90 MHz Pentium personal computer can perform as well as most workstations and even considerably better than some of them.

Tab. 5- Computational effort (deposition exercise)

Organisation	Code	Computer	linpackd (s)	ISP-40
CEA/IPSN/DRS	Sophaeros	Sun Sparc 10	8.0	13 sec
CEA/IPSN/DPEA	Aerosols-B2	Sun Sparc 5	10.0	116 min
CIEMAT	Victoria	HP 715/100	4.08	13.5 yrs
ENEA	Melcor	IBM Risc 6000/375	6.8	118.5 hrs
ENEL	Ecart	IBM 486	14.44	32.9 hrs
GRS	Sophaeros	IBM workstation	0.57	56 sec
JAERI-1	Art	AS5080	2.0	40 hrs
JAERI-2	Art	AS5080	2.0	40 hrs
KINS	Melcor	Sun Center 2000	7.0	70 hrs
Kurchatov	Melcor	Peacock Pentium 90	4.11	11.5 hrs
Tractebel-1	Melcor	HP workstation	9.83	15.3 hrs
Tractebel-2	Melcor	HP workstation	9.83	15.3 hrs
Univ. Bochum-1	Athlet-CD	Sun Sparc 10	7.9	40 min
Univ. Bochum-2	Melcor	Sun Sparc 10	7.9	32 hrs
Univ. Karlsruhe	Marie			
Univ. Pisa-1	Ecart	IBM Risc 6000/250	1.672	60 min
Univ. Pisa-2	Ecart	IBM Risc 6000/250	1.672	62 min
VEIKI-1	Melcor	Intel 80486 100 MHz		2.5 hrs
VEIKI-2	Victoria	IBM Risc 6000	5.0	3 hrs
JRC-1	DeNiro	Sun Sparc 10	9.1	11.5 days
JRC-2	Raft	Sun Sparc 10	9.1	37 sec
JRC-3	Sophaeros	Sun Sparc 10	9.1	40 sec

The range of CPU times needed to solve the deposition phase of ISP-40 is extremely wide and depends not only on the computer or code used, but also on some user

options, namely in terms of discretisation - nodalisation, time step and number of particle size bins (Tab. 5).

In average terms, and already taking into account the different speed of the computers used, Sophaeros and Raft (and, to a lesser extent, Athlet-CD, which uses Sophaeros) are faster than the other codes used, with run times in the order of seconds or minutes. This is due to the numerical methods used, mostly implicit and therefore avoiding the Courant limit and allowing for considerably larger time steps. In the case of Raft, it also excludes all time derivatives from the equations if the problem is specified as steady state. Athlet-CD is slower than Sophaeros due to the coupling between the Sophaeros module for aerosol physics and the other modules of the code.

For Ecart, Victoria, Melcor and Art, the run times were of the order of 1 hour up to a few days. The influence of user-specified parameters, and namely of the discretisation used, is clear in several submissions, but the most striking case is the CIEMAT submission with Victoria. Using a very fine nodalisation, and consequently a very small time step - the Courant limit was strictly observed - associated with a large number of particle size bins, led to a run time of the order of years to calculate 2.5 hours of real time.

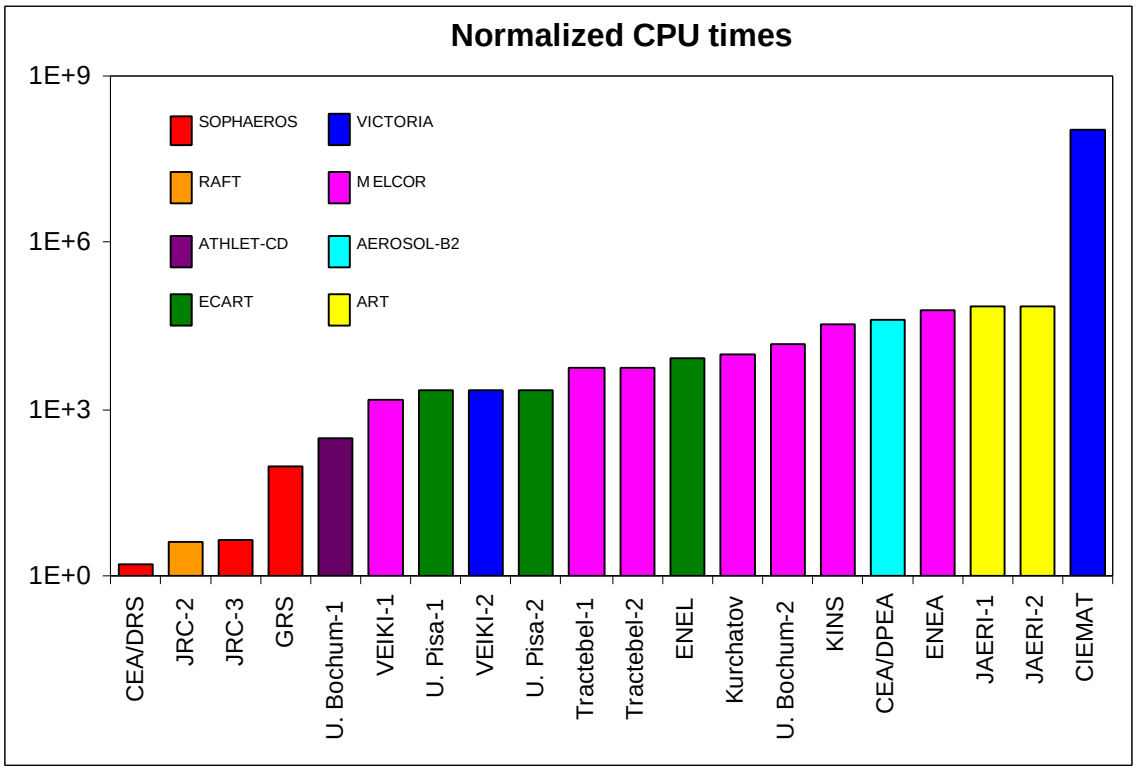

Fig. 65 - Normalised CPU times (deposition exercise)

3.11.3. Total aerosol deposition

The total deposited masses calculated by the participants, and, when available, their distribution among deposition mechanisms are shown in Fig. 66.

While the tendency seems to be to over-estimate the total deposition, the notable exception is Melcor, which consistently under-estimates deposition. While this can be

attributed in part to the fact that eddy impaction is not modelled in Melcor, even thermophoresis is severely under-predicted. The sensitivity calculation performed by Tractebel, in which different parameters for the Brock equation were used seems to indicate that the default parameters in Melcor might not be the most appropriate. Replacing the default coefficients with others within the range proposed by Brock changed the total deposition calculated by Tractebel from 57 to 130 grams, much closer to the actual deposition. Another possibility is to use the Talbot formulation which, again, uses the Brock equation with coefficients modified by Talbot to agree with the theoretical limit for high Knudsen numbers. This was done in the Melcor submission from the University of Bochum, again leading to a total deposited mass in the test pipe much closer to the experimental value (139 grams).

The Springer equation for thermophoresis, used by Raft, over-predicts deposition. According to Dumaz et al. [14], the Springer equation should predict higher thermophoretic deposition velocities than the Talbot formulation when the Knudsen number exceeds 0.2. For the small particles used in STORM and at the temperature of the gas in the test pipe, the Knudsen number is approximately 1 and hence the over-prediction of thermophoretic deposition is consistent with the theoretical results.

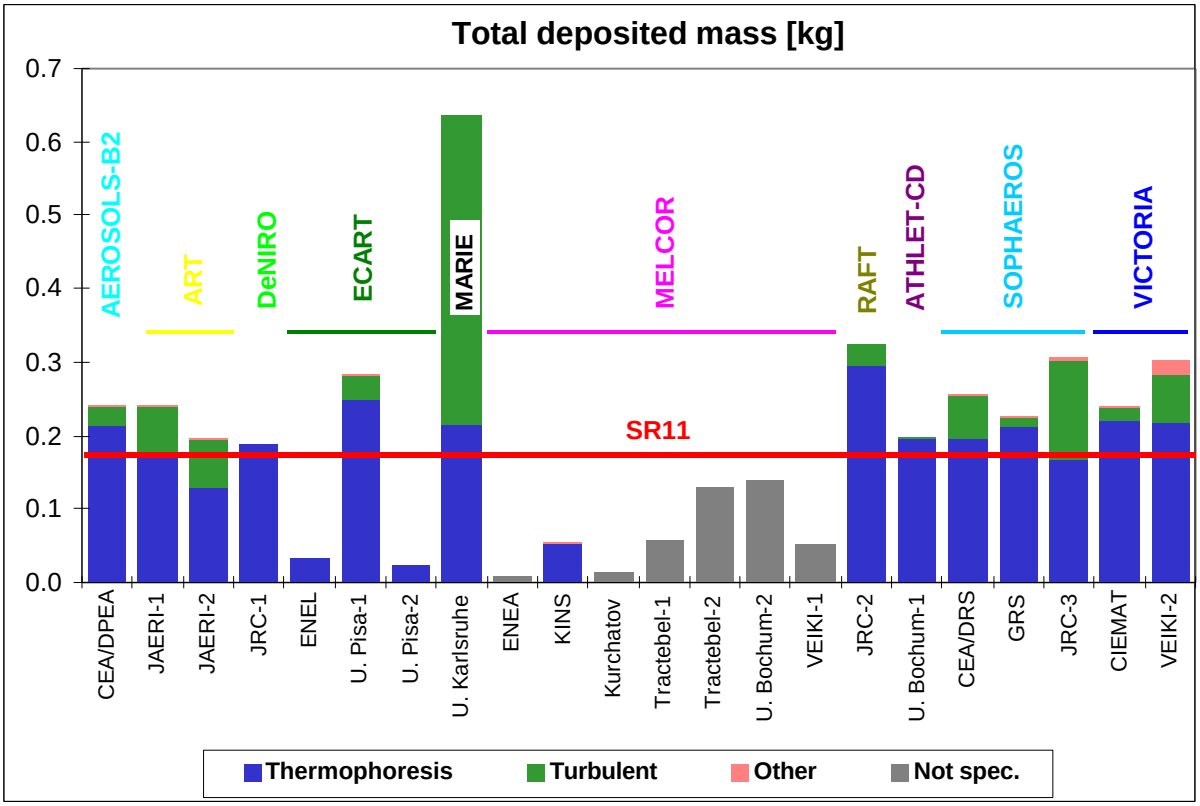

Fig. 66 - Total deposited mass (deposition exercise)

It should be noted that several errors were made in the specification of the initial particle size distribution. Although one measure of the mean particle size (geometric mean diameter, aerodynamic mass median diameter or other) and the geometric standard deviation are specified in the input to all codes, the actual size distribution used also depends on the minimum and maximum sizes allowed and on the number of size bins used in the calculation. Some of the participants selected a minimum and

maximum value for the particle sizes that lead to actual size distributions that are quite different from the one specified.

In the case of the submission from the University of Karlsruhe, the given geometric mean diameter was used as if it was a mass median diameter. This means that the actual geometric mean diameter used was less than half the correct value. Although it is not clear how the contribution of thermophoresis and eddy impaction to the total deposition was calculated in the particle tracking code used, this smaller initial particle size seems to be in contradiction with the largely excessive deposition calculated by eddy impaction.

A similar error was done by VEIKI in their calculation with Victoria, where they used the geometric mean diameter as if it was a geometric mean radius, using particles that were two times larger than specified. This is reflected in the amount of deposition calculated by eddy impaction and gravitational settling, much higher than those calculated with CIEMAT with the same code.

Finally, the two Ecart calculations that included resuspension or inhibition of deposition clearly under-predicted the amount of aerosols remaining in the deposit, which seems to indicate that the coupling between deposition and resuspension is still not accurate enough. Deposition is inhibited mainly for large particles, and hence inertial deposition mechanisms like eddy impaction or gravitational settling practically disappear. The submission by JAERI, also including resuspension, showed a much smaller effect.

It should be noted that, in this phase, the experimental data were compared with the results of calculations done with the wrong thermal-hydraulic conditions. Although the qualitative conclusions are generally valid, this is not always the case quantitatively.

3.11.4. Spatial distribution of deposition

The actual spatial distribution of aerosol deposition in the experiment is not known, since the test pipe was not opened between the deposition and the resuspension phases. However, the distribution of the deposit in previous tests with only deposition can give a qualitative indication of the expected distribution in the deposition phase of this particular test. The quantity of aerosols deposited can therefore be expected to have decreased along the test pipe. The mass deposited by unit area near the outlet is thought to have been about 30 % lower than near the inlet.

Most of the ISP participants predicted a similar trend, but with a smaller decrease of the deposition rates along the test pipe. The detailed evolution depends strongly on the way the supplied thermal-hydraulic conditions were specified for each calculation. Several participants had to change the thermal characteristics of the pipe walls and the composition of the carrier gas because of the limitations of codes that were developed to be used for actual reactor conditions, and not for reproducing experiments. This difficulty was enhanced by the incorrect thermal-hydraulic parameters that had been specified. The fact that most still obtained a reasonably good agreement with the deposition distribution in the test pipe shows that the approximations made were correct.

The Victoria calculations and most of the Melcor ones show slightly different deposition rates near the entrance of the test pipe - generally lower than in the rest of the pipe, but in one case higher - that are attributed to entrance effects. Although the

effect is significant, it would be negligible in a reactor calculation, in which the length of the piping available for deposition is much higher.

The same cannot be said about the two particle tracking submissions, which predict very important deposition near the entrance, decreasing very sharply along the pipe. This is probably due to the initial distribution of particles in the inlet cross section, which is assumed to be uniform and does not correspond to an "equilibrium" profile of particle concentrations. The addition of a certain length of pipe before the test pipe itself, to allow for a stabilisation of the concentration cross-sectional profile would certainly reduce this effect.

Finally, three of the ISP submissions predict increasing deposition rates towards the end of the test pipe. These are the calculations in which the resuspension modules were used. The calculation performed with Art still shows an almost constant deposition rate along the pipe, which is consistent with the conclusion drawn in the previous section that the effect of resuspension was small. The two calculations with Ecart show a similar behaviour, with limited deposition in the first half of the test pipe and a significant increase of deposition in the second half of the pipe. This is also consistent with the previous conclusion that in the Ecart calculation resuspension - or inhibition of deposition - played a much more significant role. The deposition longitudinal profile also seems to indicate that there was some actual resuspension, with relocation of some of the deposit from the first half of the pipe to the second. This is not apparent, however, from the evolution of deposition mechanisms along the pipe, since thermophoresis remains practically the only active mechanism in the whole pipe.There is no increase of inertial processes towards the end of the pipe as would be the case if some of the largest particles resuspended in the first section re-deposited towards the exit.

3.11.5. Temporal evolution of the deposit

All the ISP results submitted either assumed the growth rate of the deposit to be constant in time or actually calculated a time evolution that was also linear. This could be expected, since the thermal-hydraulic conditions are practically constant during the whole test and so is the aerosol production rate.

The measurements obtained with the radiation system, even if they are restricted to one particular cross section, however, indicate that there are two distinct deposition phases. In each one of them the growth of the aerosol deposit on the test pipes is approximately linear with time, but the growth rates are different. After a few minutes of faster growth, the growth rate decreases and stays constant until the end of the test. This has been observed in all STORM tests and has been linked to the change of surface conditions after a first layer of deposit is created. Although the change in rate is not dramatic, it is easily seen in the plots of the radiation system measurements.

Although Ecart includes a time-varying wall roughness, it did not predict this change of deposition rate. This is probably due to the fact that the change is due not to a different roughness but to a different sticking efficiency between, on one hand, the particles hitting the wall and the stainless steel, and, on the other hand, between the particles and the pre-existing deposit layer.

3.11.6. Particles exiting the test pipe

In the STORM tests, the aerosol size distribution is normally measured upstream of the test pipe in the deposition phase and downstream of the test pipe in the resuspension phase. In a deposition-only test, however, the two sampling stations were run almost simultaneously, to verify the assumption that the particle size distribution does not change significantly along the test pipe.

This is also confirmed by most of the participants in the ISP, who calculate that the particle size distribution at the outlet of the test pipe is very similar to the one imposed at the inlet. Agglomeration is calculated to be practically negligible and only a very small fraction of the injected aerosols deposit in the test pipe, hence the size distribution remains practically unchanged. When errors were made in the inlet size distribution, they are obviously reflected in the outlet size distribution.

For those submissions in which a small number of size bins were used, associated in some cases with a narrow range of allowed particle sizes, the actual size distribution at the inlet can be quite different from the one specified. Only Tractebel supplied the re-calculated parameters of the actual size distribution. A minimum diameter of 0.13 μm and a maximum of 3.8 μm yield a log-normal distribution in which the geometric mean diameter and the geometric standard deviation are very similar to the specified values of 0.4348 μm and 1.7003 respectively. From the minimum and maximum sizes, which are the only information available for the other cases, the initial distribution adopted by KINS (0.4 to 10 μm) seems to be on the high side and that used by the University of Bochum (0.08 to 0.8 μm) on the low side. The particle size distributions at the outlet agree with this conclusion.

4. Open calculations - Deposition

4.1. Introduction

Several of the participating organisations have decided to perform new calculations after the intermediate workshop which took place in Ispra in March 1998. This was done in part to evaluate the effect of the error in the steam mass flow rate - and consequent error in the gas and wall temperatures - that was announced at the workshop. In other cases, these open calculations were used to correct errors detected only after the submission of the blind results or to evaluate the sensitivity of the results to additional parameters.

This section is divided into two sub-sections, including:

- new calculations with the correct thermal-hydraulic conditions and without additional changes, in some cases accompanied by sensitivity analysis on specific parameters
- new calculations with the correct thermal-hydraulic conditions and additional changes

4.2. New calculations with correct thermal-hydraulic conditions

4.2.1. GRS

A new set of calculations was run by GRS with version 1.4 GRS of Sophaeros using the correct thermal-hydraulic data [16].

The nodalisation used in the calculations was the same as in the previous ones, and the same is true for the time step and the discretisation of the particle size distribution. The carrier gas was also described in the same way as in the blind calculations.

As for the calculations described before, the effect of the increased temperature difference between the carrier gas and the pipe wall was stronger than the effect of the decrease of the carrier gas velocity, leading to a prediction of higher deposition by 33% (Fig. 67). The spatial distribution of the deposit remains practically uniform along the test pipe, and the distribution among deposition mechanisms changes only slightly, with thermophoresis becoming even more dominant, being responsible for 97% of the total resuspension.

Additional sensitivity calculations were run by GRS to study the effect on the calculated deposition of several parameters and code options.

In one calculation, the resuspension module of Sophaeros was disabled, as had been done in the previous, blind calculations. As before, this led to a slight increase of the deposition - 308 instead of 300 grams.

The effect of the adhesion coefficient used in the calculation of the cohesive forces was also studied in detail [4]. The conclusion of this work was that practically no resuspension was calculated by the code for values of H above 10^{-5} N/m, corresponding to extremely smooth clean surfaces. Lowering the value of H down to 10^{-6} N/m led to an increase of resuspension, but below this value, resuspension

became independent of H. The default value in Sophaeros, 10^{-6} N/m, was therefore used in all other calculations.

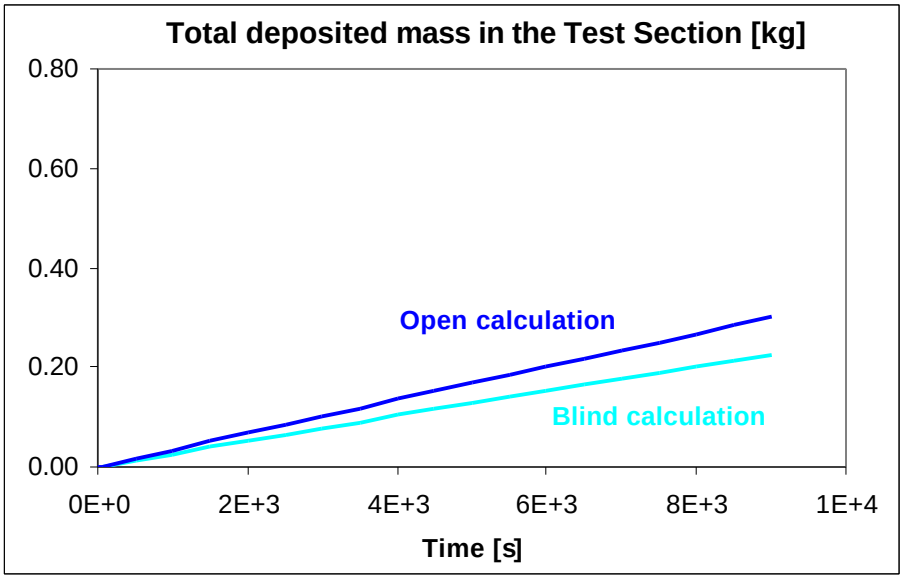

Fig. 67 - Time evolution of deposition (GRS)

Finally, the code was modified to take into account the effect of surface roughness, by replacing the undisturbed Fanning friction factor in Sophaeros with a flow resistance coefficient that depends on the surface roughness. The value of the surface roughness was varied between 10 µm and 1 mm, with a negligible effect (less than 1%) on the calculated deposited mass, which decreases very slightly for increasing surface roughness.

4.2.2. JAERI - without resuspension

The corrected thermal-hydraulic data supplied by the JRC was used for a new calculation with Art mod. 2 [25]. Since the steam mass flow rate, and consequently the carrier gas velocity, was lower than previously indicated, the time step used in the calculation was 0.02 seconds instead of the 0.01 seconds used in the previous calculation.

The decrease in the carrier gas velocity led to a reduction of the deposition by eddy impaction (Fig. 68) but this reduction was compensated by the increased temperature difference between carrier gas and wall, resulting in a total deposition in the test pipe which is 11% higher than in the previous calculation (Fig. 69).

The spatial distribution of deposition is practically the same as in the previous calculation, and the same is true for the size distribution of the particles exiting the test section.

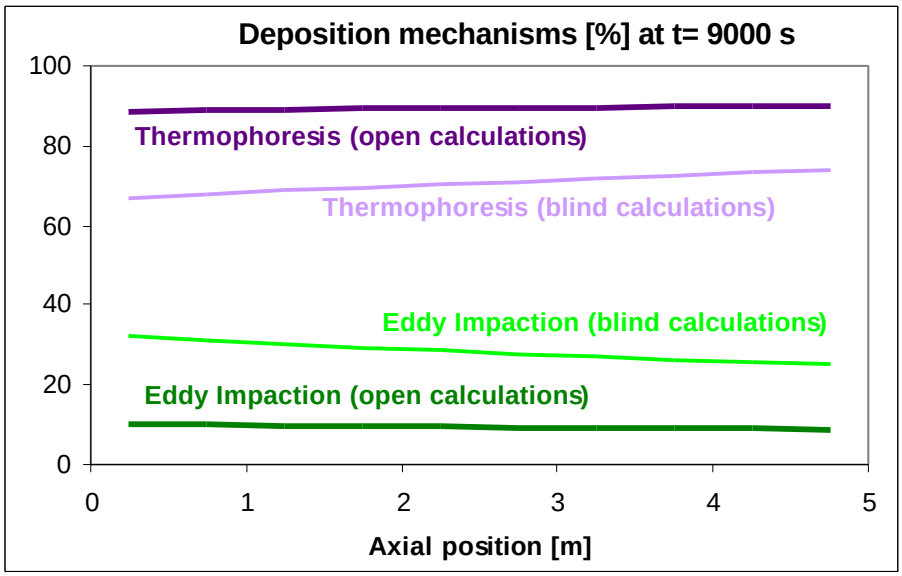

Fig. 68 - Deposition mechanisms along the test pipe (JAERI-1)

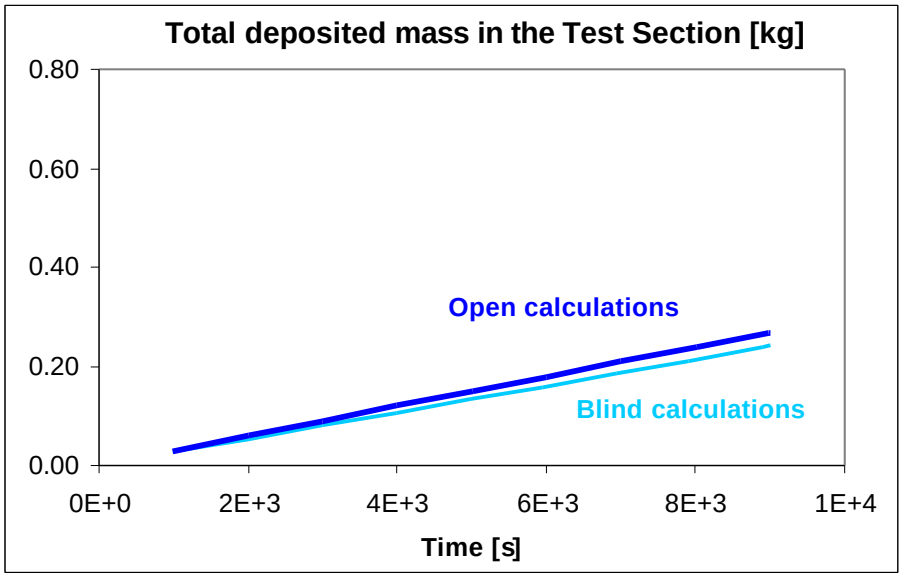

Fig. 69 - Time evolution of deposition (JAERI-1)

4.2.3. JAERI - with resuspension

A similar calculation was performed by JAERI enabling the resuspension module of Art [25]. As in the calculations performed in blind conditions, the effective deposition is slightly lower than in the calculation without resuspension, but in this case the difference between the open and blind calculations is higher, with an increase of effective deposition in the test section of 27% (Fig. 70). This is due to the fact that, in addition to the reduction in deposition by eddy impaction (Fig. 71), the reduced carrier gas velocity also leads to a reduction of resuspension, which, together with the increased thermophoretic deposition, leads to a considerable increase of the effective deposition.

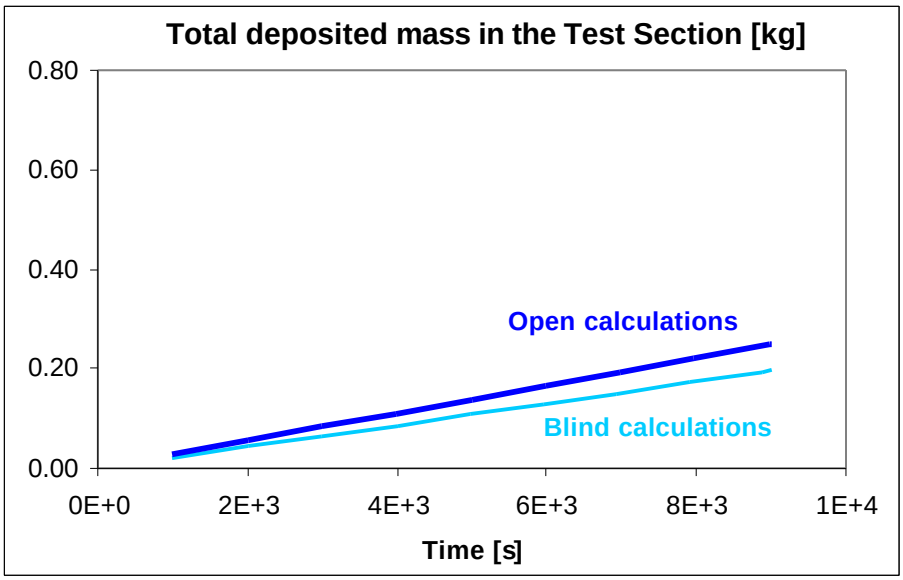

Fig. 70 - Time evolution of deposition (JAERI-2)

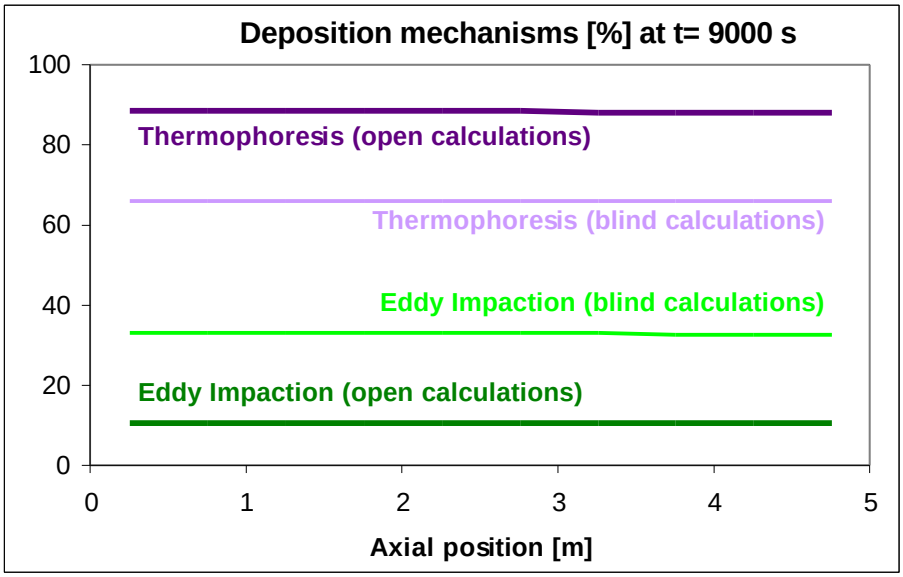

Fig. 71 - Deposition mechanisms along the test pipe (JAERI-2)

Due to the reduced resuspension, the spatial distribution of the deposit becomes slightly different from the one in the blind calculation. Although in both cases the distribution is practically uniform along the test pipe, it increases slightly along the test pipe in the blind calculation, while it decreases slightly in the open calculation.

The particle size distribution at the outlet of the test section is calculated to be the same as in the case without resuspension, and also the same as calculated in the blind calculation.

4.2.4. JRC-Raft

The calculation performed with the JRC with version 1.1/JRC of Raft was repeated with the correct thermal-hydraulic data [2].

Due to the semi-lagrangian method used in Raft, the actual nodalisation is set internally by the code. Also, as in the previous calculation, the problem was calculated as steady-state and therefore the time step is irrelevant. The discretisation of the particle size distribution was the same as in the blind calculation.

The total deposition calculated for the correct thermal-hydraulic conditions is, as mentioned before, a balance between the increased thermophoretic deposition due to a larger temperature difference between the carrier gas and the wall and the reduced deposition by eddy impaction due to the lower velocity of the carrier gas. In the case of the Raft calculation, this resulted in an increase of the total deposition of the order of 7% (Fig. 72).

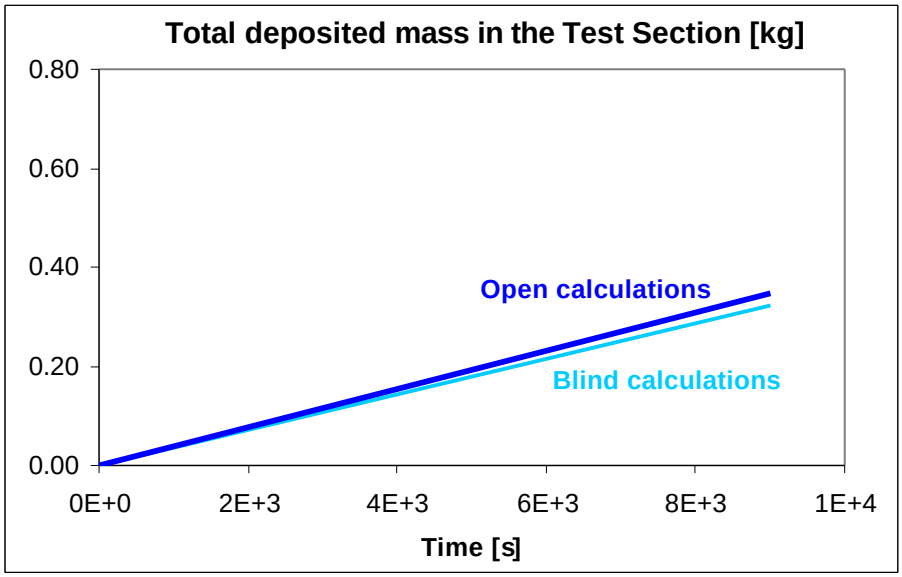

Fig. 72 - Time evolution of deposition (JRC-Raft)

In terms of deposition mechanisms, thermophoresis became even more dominant, with more than 95% of the total deposition, and the spatial distribution of the deposit remained the same, slightly decreasing along the test section. The particle size distribution at the outlet of the test section also remains unchanged, with a geometric mean diameter of 0.44 µm and a geometric standard deviation of 1.7.

4.2.5. University of Pisa - without resuspension

The University of Pisa submitted two new calculations with the corrected thermal-hydraulic conditions [55]. As in the blind calculations previously submitted, the aerosol resuspension module was activated only in the second calculation.

The calculations were performed with version 98.1 of Ecart, while the previous blind calculations had been done with version 97.2 of the same code. However, the previous calculations had also been repeated with the newer version of the code producing results that were identical to those submitted to ISP-40.

The nodalisation, time step and discretisation of the particle size distribution were kept unchanged, and the same is true for the composition of the carrier gas and the initial roughness of the pipe wall.

As in the calculations presented above, the effect of the increased temperature difference between the carrier gas and the pipe walls exceeded the effect of the reduced velocity of the carrier gas, leading to an increase of the total deposition in the test section of about 27% (Fig. 73).

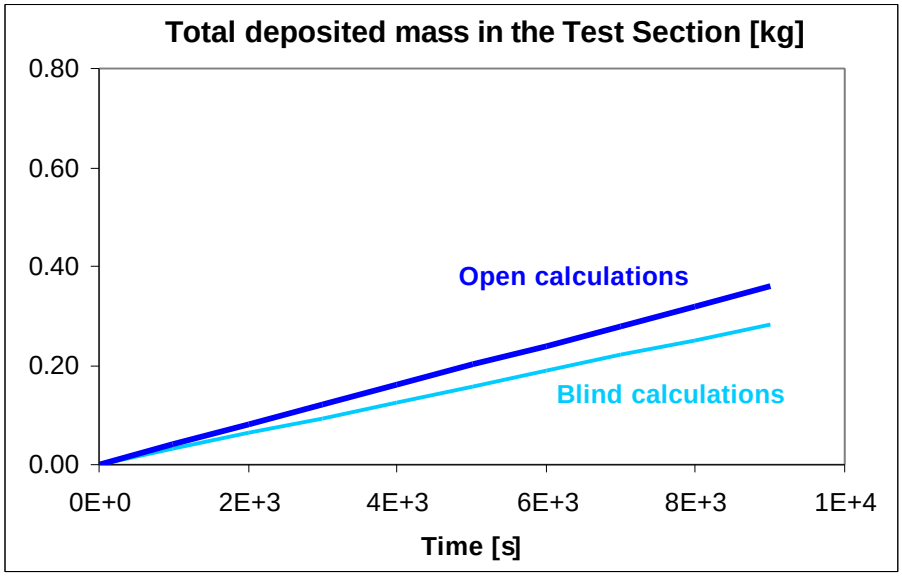

Fig. 73 - Time evolution of deposition (U. Pisa-1)

The spatial distribution of the deposit in the test pipe remains unchanged, decreasing slightly along the pipe and the particle size distribution at the outlet also remains practically unchanged.

4.2.6. University of Pisa - with resuspension

As mentioned in the previous section, the second calculation submitted by the University of Pisa was done enabling the resuspension module in Ecart. In this case, and similarly to the JAERI calculations discussed above, the reduction of the carrier gas velocity leads to an increase of calculated effective deposition in the test section considerably higher than when the resuspension module is not used.

The total deposition calculated by the University of Pisa was 92 grams, which is more than 3.5 times higher than in the blind ISP-40 calculation (Fig. 74).

The reduced effect of resuspension is also highly visible in the modified deposition profile. While in the blind calculations the aerosol deposition clearly increased towards the end of the test section, the deposition profile calculated with the correct thermal-hydraulic data is much flatter, decreasing slightly along the test section, similar to the profile in the calculations without resuspension.

The particle size distribution remained practically unchanged, with only a negligible increase of the geometric standard deviation.

Additional calculations were performed to evaluate the effect of the number of size bins, the adhesion coefficient in the Brockman equation [4] and the collisional shape factor on the total deposition predicted by Ecart.

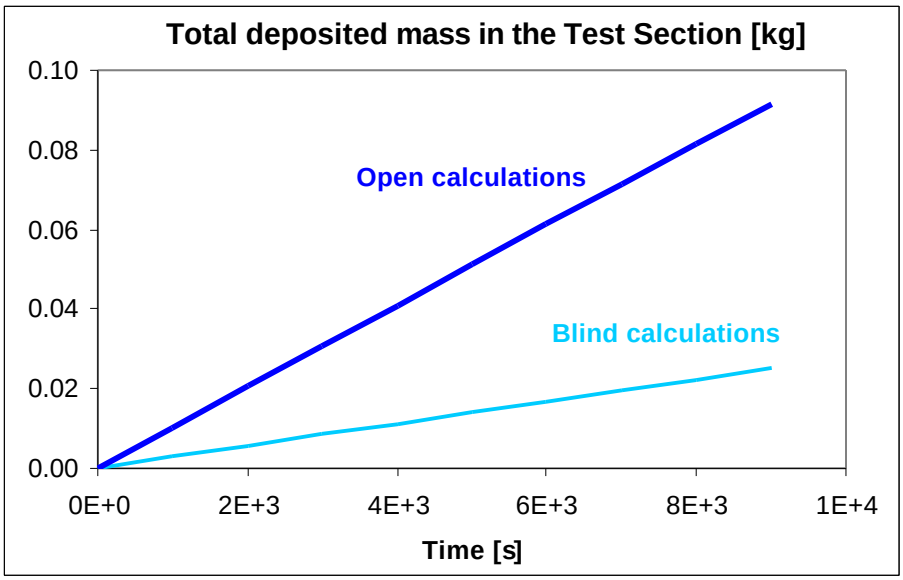

Fig. 74 - Time evolution of deposition (U. Pisa-2)

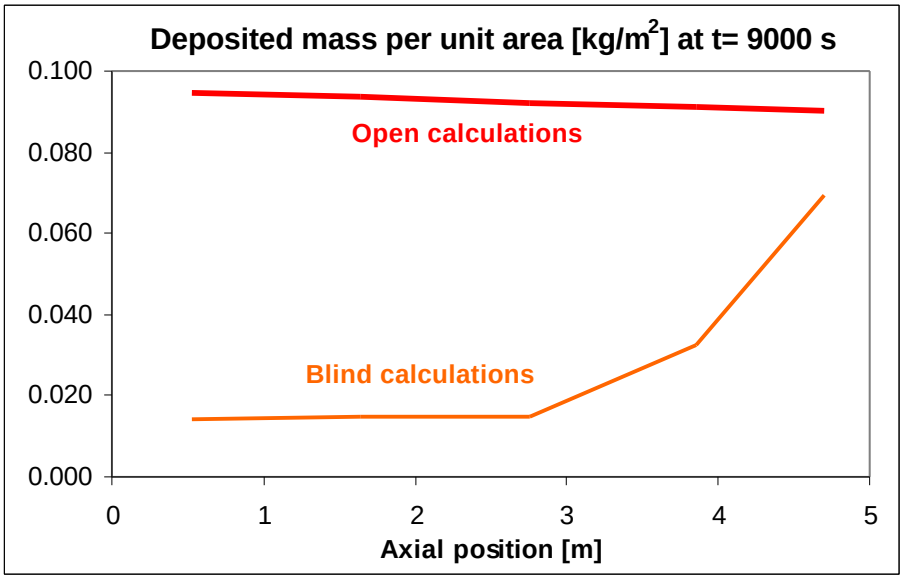

Fig. 75 - Spatial distribution of deposition (U. Pisa-2)

In the first sensitivity calculation, the number of size bins used in the discretisation of the particle size distribution was doubled to 40, to reduce the discontinuities created by the model between the size bins for which resuspension is active and those on which it does not have any effect. The results of this calculation was an increase of the effective total deposition of more than 28%, relative to the case with only 20 size bins. A similar analysis performed on the original blind calculation led to a proportionally even larger increase in the total deposition.

During the intermediate ISP-40 workshop, the different adhesion coefficients used in the Ecart and Sophaeros calculations had been identified as the reason for the considerably different effects of adding resuspension to the aerosol deposition calculations. The University of Pisa therefore repeated its previous calculation with an adhesion coefficient of 10^{-6} N/m, as used by CEA/IPSN/DRS, instead of the default

value in Ecart, $4x10^{-7}$ N/m. This led to a sharp reduction of the effect of resuspension, and consequently to a large increase of the effective deposition, and the predicted total deposition is 161 grams, in excellent agreement with the experimental value of 162 grams. However, if the same value of the adhesion coefficient is used with the correct thermal-hydraulic conditions, the increased deposition calculated by Ecart (309 grams) is much higher than the experimental value. This is possibly due to the fact that the value of 10^{-6} N/m for the adhesion coefficient had been estimated by CEA/IPSN/DRS based on the results of previous STORM tests in which the same error in the measurement of the steam mass flow rates also occurred.

Finally, for the revised thermal-hydraulic conditions, it was found that, by increasing the collisional shape factor from the default value of 1.0 to 1.24, the experimental results in terms of total deposition could be reproduced almost exactly. It should be noticed that, with the original thermal-hydraulic data, a value of 2.2 had to be used for the collisional shape factor in order to create the adequate initial conditions for the blind resuspension calculation.

4.3. New calculations with correct thermal-hydraulic conditions and additional changes

4.3.1. CIEMAT

A new calculation was done by CIEMAT mainly with the objective of evaluating the effect of the modified thermal-hydraulic conditions [29]. However, since the very high CPU time needed for the previous calculation was due to the fine nodalisation and discretisation of the particle size distribution, the opportunity was taken to reduce the number of computational cells and of size bins.

The new calculation was therefore performed with 10 cells instead of 50, and with 20 size bins instead of 40, while the time step was kept at 10^{-3} seconds. Although this nodalisation and particle size discretisation are still finer than those that would be used in reactor calculation, they already allowed a reduction of the computational time by a factor of more than 25.

As in the new calculations described above, the effect of the increased temperature difference between the carrier gas and the pipe wall exceeded the effect of the reduced eddy impaction due to a lower velocity of the carrier gas. The total deposition calculated was 228.7 grams, which is 21% higher than in the previous calculation.

The spatial distribution of the deposited aerosols remained practically uniform, and the entrance effect seen in the previous calculation is also present, with a significantly lower deposition in the first computational cell. The distribution among deposition mechanisms remains qualitatively the same, but the dominance of thermophoresis is, as expected, even stronger, with more than 95% of the deposition. The particle size distribution at the outlet of the test section remains practically unchanged.

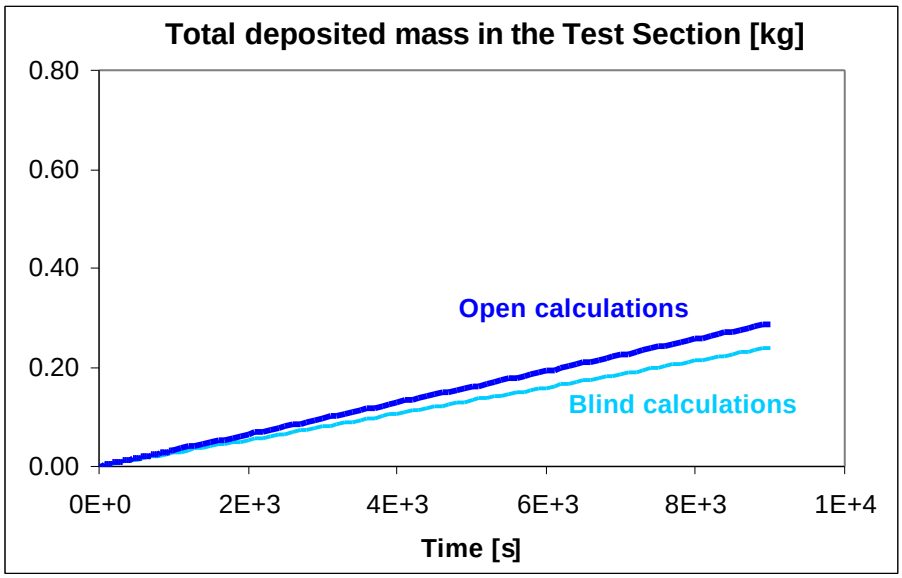

Fig. 76 - Time evolution of deposition (CIEMAT)

4.3.2. JRC-Sophaeros

The results submitted by the JRC for the blind phase of the exercise were considerably different from those submitted by other participants using different versions of the same code. A close examination of the calculation performed brought to light one error in the input deck, concerning the definition of the physical properties of the carrier gas. The new Sophaeros calculation submitted by the JRC [51] therefore includes not only a correction of the thermal-hydraulic boundary conditions as presented in the intermediate ISP-40 workshop but also a correction of the input error mentioned above. For this reason, the new results cannot be compared directly with the ones submitted previously.

The total deposition in the test pipe was calculated to be 309 grams (Fig. 77), decreasing slightly along the test section. The contribution of the different deposition mechanisms, however, was calculated to be significantly different of the one obtained in the previous calculation, with thermophoresis being responsible for 95.2% of the total deposition, eddy impaction contributing with 3.8% of the total, gravitational settling with 0.9% and turbulent diffusion with 0.1% of the total deposition.

No significant changes are seen in the size distribution of the aerosols exiting the test section.

Comparing the new results obtained by the JRC with Sophaeros with the results of the blind calculations - with the wrong thermal-hydraulic data - previously submitted by the other participants who used different versions of Sophaeros, the JRC results show 21% more deposition than calculated by CEA/IPSN/DRS and 30% more deposition than calculated by GRS when the resuspension module is excluded.

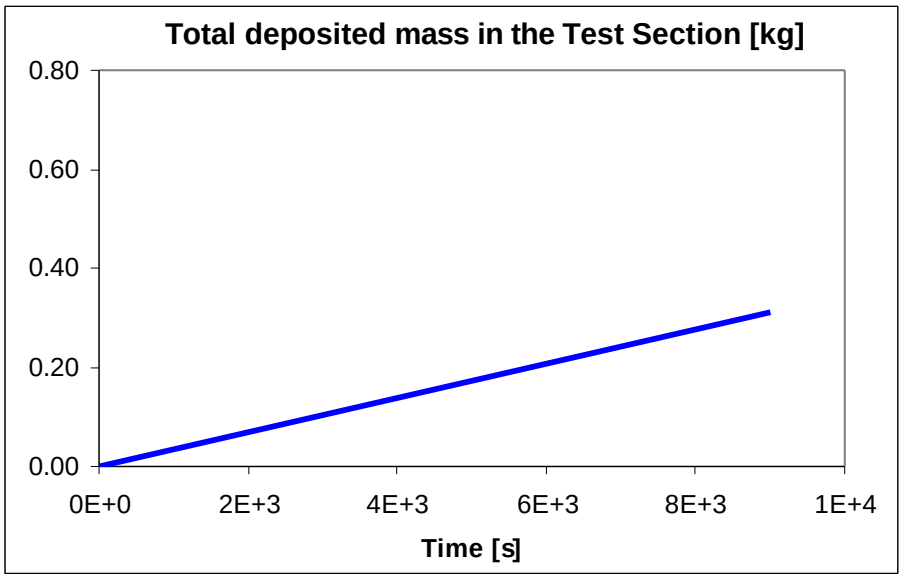

Fig. 77 - Time evolution of deposition (JRC-Sophaeros)

4.3.3. KINS

A new calculation, performed in open conditions, was submitted by KINS [33]. Version 1.8.3 of Melcor was used again, including the modification introduced to print out the contribution of each mechanism to the total deposition. The same nodalisation was used in the test pipe, but with four additional cells instead of just two, to represent the sources and sinks. The maximum time step was again 0.1 second, and the particle size distribution was discretised into 10 size bins, covering the range between 0.05 μm and 90 μm. The error that had been done in the specification of the particle size distribution was corrected, and the specified values for the geometric mean diameter and the geometric standard deviation were used.

The default coefficients for the calculation of the thermophoretic deposition were replaced by the ones determined by Talbot [75]. In the description of the carrier gas, air was treated as a mixture of nitrogen, oxygen, argon and carbon dioxide.

The correct thermal-hydraulic parameters, distributed after the second ISP-40 workshop, were used in this open calculation.

The calculation was again done on a Sun Center 2000 workstation, and took 81.5 hours to run, which is about $4.2*10^4$ times more than the reference *linpackd* code.

The total deposition calculated was 59 grams (Fig. **Error! Not a valid link.**), only slightly higher than in the blind calculation submitted earlier. The spatial distribution of the deposit was still practically uniform along the test pipe, but the addition of a source node upstream of the test section considerably reduced the entrance effects seen in the previous calculation. The aerosol deposition calculated in the first cell of the test section is now slightly higher than in the rest of the pipe.

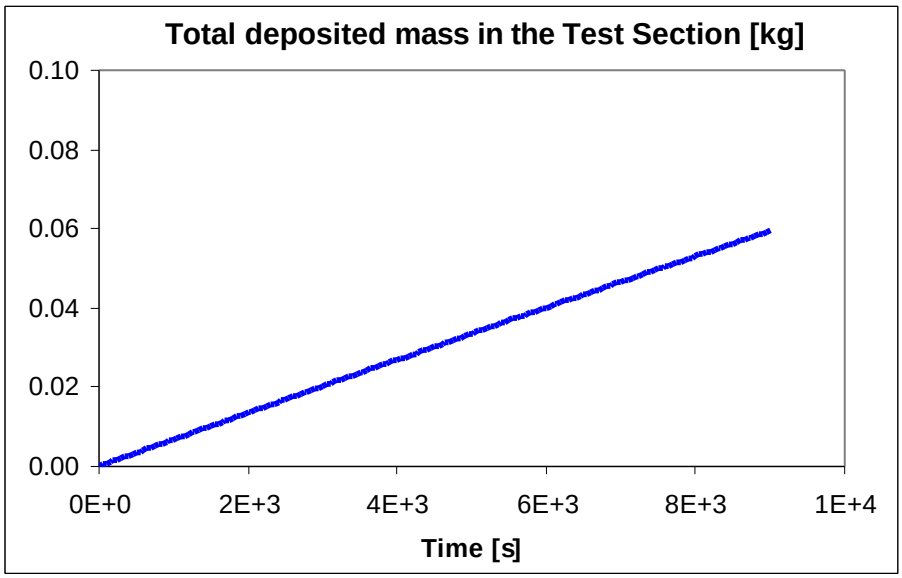

Fig. 78 - Time evolution of deposition (KINS)

Due to the modification of the particle size distribution at the inlet, the relative importance of the different deposition mechanisms changed significantly, with gravitational settling becoming more important and the contribution of thermophoresis decreasing from 93% to under 80% of the total deposition.

4.3.4. Kurchatov Institute

The new calculation was still performed with version 1.8.2 of Melcor, using the same nodalisation, time step and discretisation of the particle size distribution [70].

An error in the gas and wall temperatures used in the blind calculation was detected, meaning that the actual temperature difference between the gas and the wall was considerably smaller than in the experiment. For this new calculation, the Kurchatov Institute used the corrected values of the gas and wall temperatures distributed after the 2nd workshop.

The calculation was done on a faster personal computer (a 166 MHz Pentium, instead of the 90 MHz Pentium used before) but the calculation took a longer CPU time to perform. When related to the time needed to run the reference *linpackd* code, the CPU time used was more than 16,000 times larger, instead of the 10,000 times of the previous calculation.

Since eddy impaction is not modelled in Melcor, the modification of the thermal-hydraulic conditions affects only the amount of aerosols deposited by thermophoresis, due to the increased temperature difference between the carrier gas and the wall. The increase of the total deposition is therefore more significant than for the cases described above, and the total deposition is calculated to be 79,9 grams, which is almost 6 times more than in the previous calculation (Fig. 79).

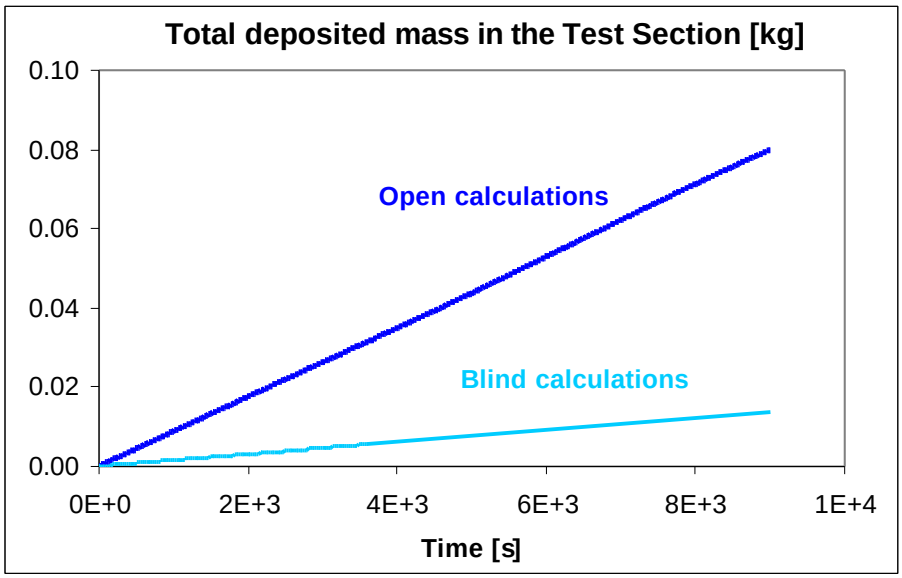

Fig. 79 - Time evolution of deposition (Kurchatov)

The spatial distribution of the deposit remains practically as before, with the amount of deposition decreasing slightly along the test section, and the particle size distribution at the outlet remains unchanged.

4.3.5. University of Bochum-Athlet-CD

The University of Bochum submitted new results, calculated, as before, with version 1.1D/0.2E of Athlet-CD [72]. In addition to the correction of the steam flow rate and consequently of the thermal-hydraulic boundary conditions, the discretisation of the particle size distribution was changed, as well as the thermal conductivity of the pipe walls.

In the previous blind calculations the particle size distribution was discretised into 10 size bins, with a minimum and a maximum diameters of 0.1304 µm and 0.739 µm, respectively, which led to an actual distribution that was much narrower than the one specified. This was modified for the new calculations, and the new minimum and maximum diameters were set to 0.088 µm and 2.12 µm, respectively.

The heat transfer coefficient for the outer pipe surface was reduced, but even so, the gas and wall temperatures distributed to the participants were not reached. The temperature difference between the carrier gas and the wall that was used in the calculation was 48% lower than the one specified.

As for the JRC calculations with Sophaeros, the new results obtained by the University of Bochum with Athlet-CD cannot be directly compared with their previous results.

The total deposition in the test pipe was calculated to be 172.6 grams (Fig. 80), with the same spatial distribution as previously, i.e. slightly decreasing along the test pipe but with considerably higher deposition in the cells that correspond to the flanges of the test pipe.

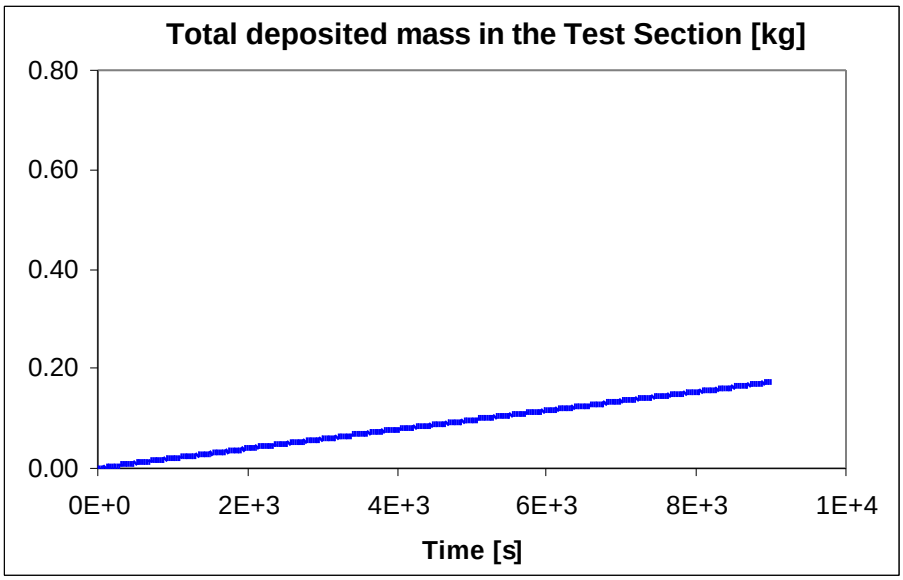

Fig. 80 - Time evolution of deposition (U. Bochum-Athlet-CD)

Even if the carrier gas velocity is lower, the increase of the particle sizes leads to a higher contribution of eddy impaction and gravitational settling to aerosol deposition. Consequently, the contribution of thermophoresis changes from 98.5% to 93.5%.

Due to the modified particle size distribution used at the inlet, the particle size distribution at the outlet of the test section is also different from the one previously calculated, and more consistent with the experimentally observed distribution. It is characterised by a geometric mean diameter of 0.43 μm and a geometric standard deviation of 1.7.

To evaluate the effect of the minimum and maximum diameters on the deposition results, the University of Bochum performed a sensitivity analysis on these parameters. Five different calculations were performed, with the combinations of minimum and maximum diameters indicated in Tab. 6.

Tab. 6 - Sensitivity calculations from U. Bochum

Case	Minimum diameter [mm]	Maximum diameter [mm]	Deposited mass [kg]	
			Athlet-CD	Melcor
1	0.088	2.12	0.1726	0.12151
2	0.02	2.00	0.1728	0.12166
3	0.02	20.0	0.1847	0.12439
4	0.02	200.0	0.1844	0.12644
5	0.13	0.739	0.1833	-
6	0.078264	0.791336	-	0.13459

The results obtained in terms of total deposition in the test pipe show an increase of almost 7% between the first two cases and the last three. While the similarity between

cases 1 and 2 and between cases 3 and 4 could be expected, the increased deposition in cases 3/4 relative to cases 1/2 could be due to the fact that the very large particles (in the order of tens of microns) that can be present in cases 3 and 4 are truncated from the distribution in cases 1 and 2. Although negligible in terms of number of particles, these might be significant in terms of mass, which depends on the third power of the diameter.

The total deposition calculated in case 5, which is only slightly smaller than in cases 3 and 4 and larger than in cases 1 and 2 is probably due to the fact that in case 5 a significant part of the lower end of the distribution is truncated, and the corresponding mass is re-distributed over the larger sizes. The lower deposition of the small size particles is more than compensated with the additional deposition of larger particles, even if the very large particles mentioned before are also excluded.

4.3.6. University of Bochum-Melcor

The second calculation submitted by the University of Bochum for the corrected thermal-hydraulic conditions was performed with Melcor [60]. The additional modifications mentioned above for the Athlet-CD calculation were also included in the new Melcor calculation.

As in the new Athlet-CD calculation, the gas and wall temperatures were also not well reproduced in this Melcor calculation, and the temperature difference between the carrier gas and the pipe walls considered in the calculation was 42% lower than specified.

The total deposition in the test section was calculated to be 121.5 grams, slightly decreasing along the test section.

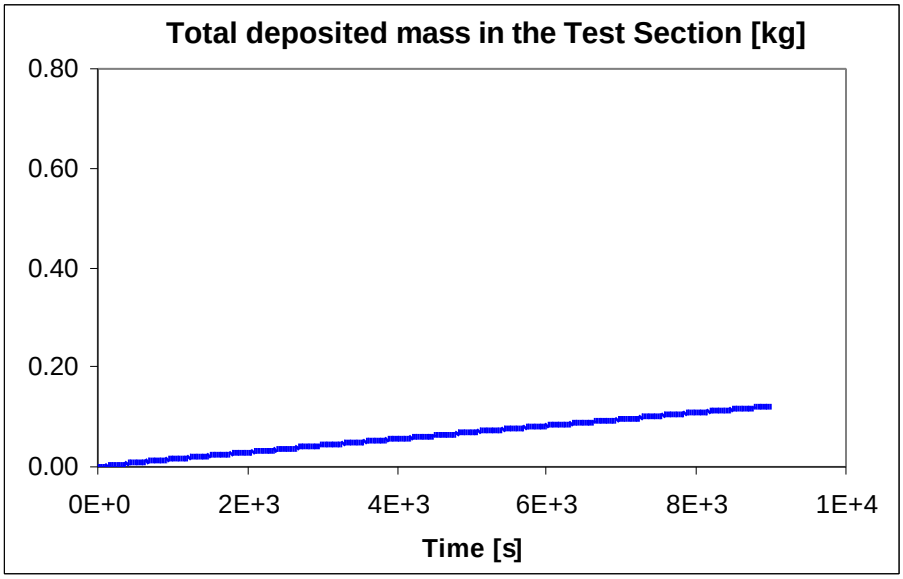

Fig. 81 - Time evolution of deposition (U. Bochum-Melcor)

As in the Athlet-CD calculation, the extended range of particle sizes allowed is expected to lead to a more accurate discretisation of the suggested particle size distribution, which should in turn lead to a better agreement of the particle size distribution at the outlet. For this Melcor calculation, no information was given on the

geometric mean diameter of the particles exiting the test section, but the geometric standard deviation was 1.6, which is much closer to the value of 1.7 specified at the inlet.

A sensitivity analysis similar to the one performed with Athlet-CD was also carried out with Melcor, and the results, although quantitatively different, seem to be qualitatively similar. The total deposition calculated for cases 1 and 2 (see Tab. 6) is still similar and lower than calculated in cases 3 and 4, although only by 2 to 4%. The deposition calculated in case 4 is higher than in case 3, which was not the case in the Athlet-CD analysis, but the reason could again be the presence of a very small number of very large particles.

The deposition calculated in case 6, with the narrowest distribution, is the highest of all five cases and, again, this could be due to the re-distribution of the particles in the low end of the size spectrum among the larger particles allowed in the distribution.

4.4. Conclusions

The analysis of the new calculations performed with the correct thermal-hydraulic conditions - including the one performed by CIEMAT, in which the additional modifications introduced are not supposed to have any effect on the results - indicate that, for most of the computer codes used, the correction of the steam mass flow rate and, consequently, the temperatures of the gas and wall, generally led to an increase of the calculated total deposition that varies between 7 and 33%.

As expected, the increase in the calculated deposition is stronger in the calculations that include a resuspension model, due to the fact that a reduction of the effect of resuspension, due to the lower carrier gas velocity, is superimposed on an increase of deposition due to the larger temperature difference between the carrier gas and the pipe wall. This is the case with the Art calculation performed by JAERI, but even more in the Ecart calculation by the University of Pisa. This could also be expected, since the previous Ecart calculation already predicted the effect of resuspension to be much stronger.

5. ISP-40 calculations - Resuspension

5.1. Art

5.1.1. Introduction

Art is a code developed by JAERI for the calculation of fission product transport in the coolant circuit and containment of an LWR under severe accident conditions [32].

The Art code models aerosol growth by agglomeration and vapour condensation on the particle surface, aerosol deposition, resuspension and revaporisation.

The aerosol resuspension module in Art uses the Paress model proposed by Fromentin [20], which calculates the mass remaining in the deposit as a function of the friction velocity and time.

5.1.2. JAERI

The calculation submitted by JAERI was performed with the Mod2 version of Art [24].

The Paress model was developed for gas flows considerably slower than those used in this experiment and led to extremely quick resuspension of the whole deposit - less than 2 seconds at the lowest gas velocity used in the experiment. Since this was attributed to the fact that the ratio between the thickness of the deposited layer and the friction velocity is much lower than in the tests for which the model was developed, it was decided to use a modified Paress model that includes a dependence of the resuspension rate on the deposited mass.

5.1.2.1. ISP calculation

The ISP calculation was performed on an AS7000 workstation (SparcStation 20 compatible) and took 60 hours to run, which is 72,000 times more than the reference *linpackd* code.

The test pipe was divided into 10 identical computational cells and the time used was 0.0025 seconds.

Vaporisation of SnO_2 was not considered.

The initial conditions used and the results obtained are summarised in Tab. 7 and Fig. 82. The resuspension rate increases from the first to the last step, with larger carrier gas velocities (Fig. 83). In each velocity step, the aerosol resuspension occurs practically only in the first few seconds, independently of the duration of the step.

Tab. 7 - Summary of results for resuspension phase (JAERI)

Step	Mass remaining (g)	Particles exiting the test pipe	
		Geometric mean diameter (μm)	Geometric standard deviation
Start	162		
1	31	1.05	3.22
2	2	1.21	2.86
3	~0	1.47	2.96
4	~0	1.64	3.31
5	~0	1.70	3.84
6	~0	1.74	4.43

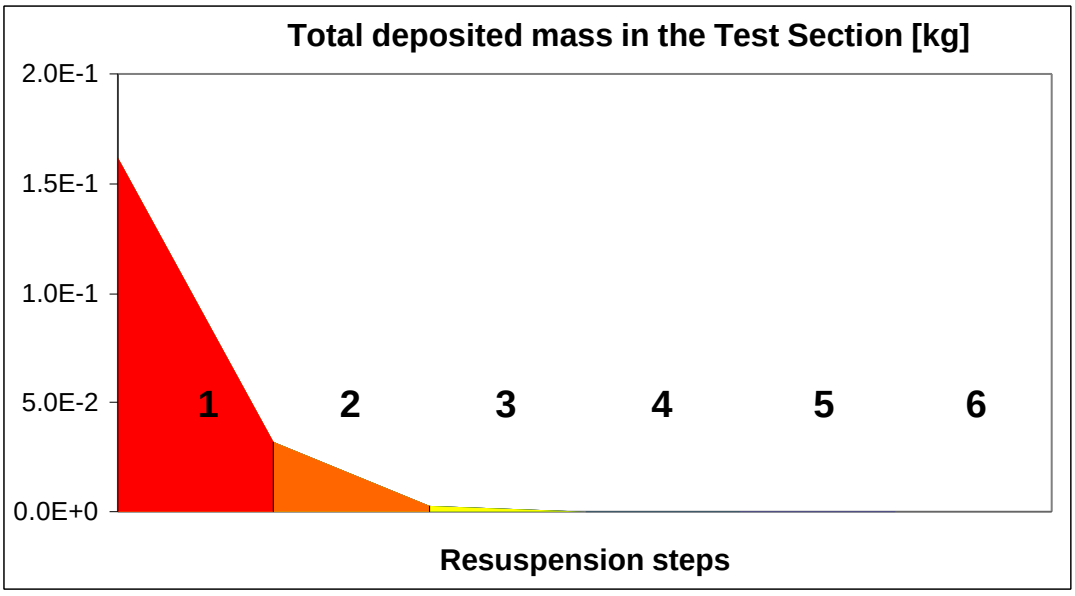

Fig. 82 - Mass remaining in the test pipe (JAERI)

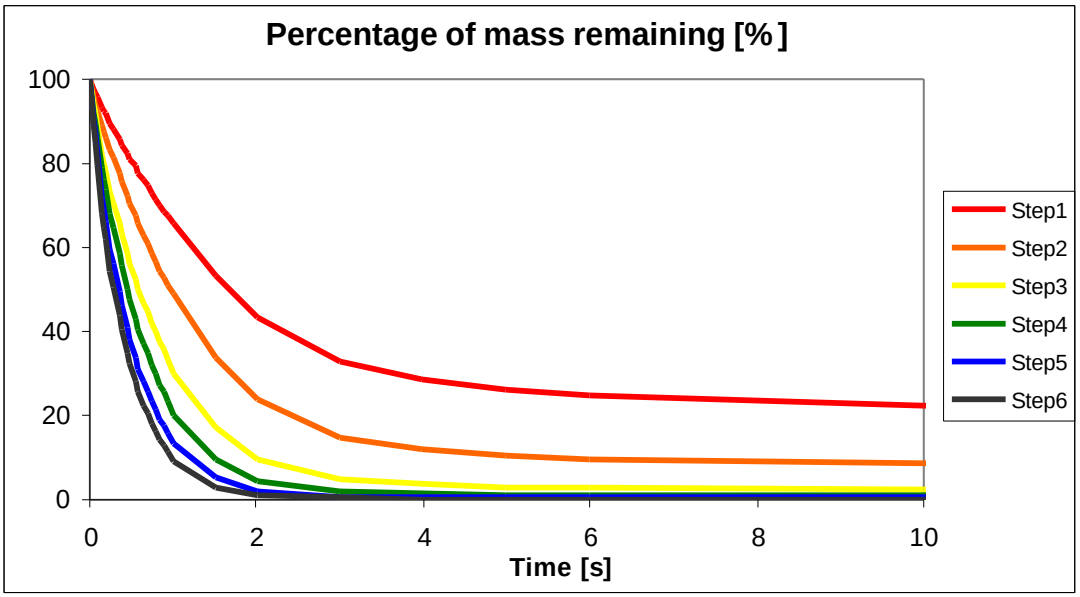

Fig. 83 - Resuspension rate in each velocity step (JAERI)

Calculating resuspension of practically all the deposited aerosols in the first two steps, the spatial distribution of resuspension necessarily follows very closely the initial distribution of the deposited aerosols (Fig. 84). It is therefore higher near the entrance of the test pipe and decreases towards the exit. Some of the material resuspended from the beginning of the test pipe re-deposits downstream, adding to the decreasing trend of effective resuspension along the pipe.

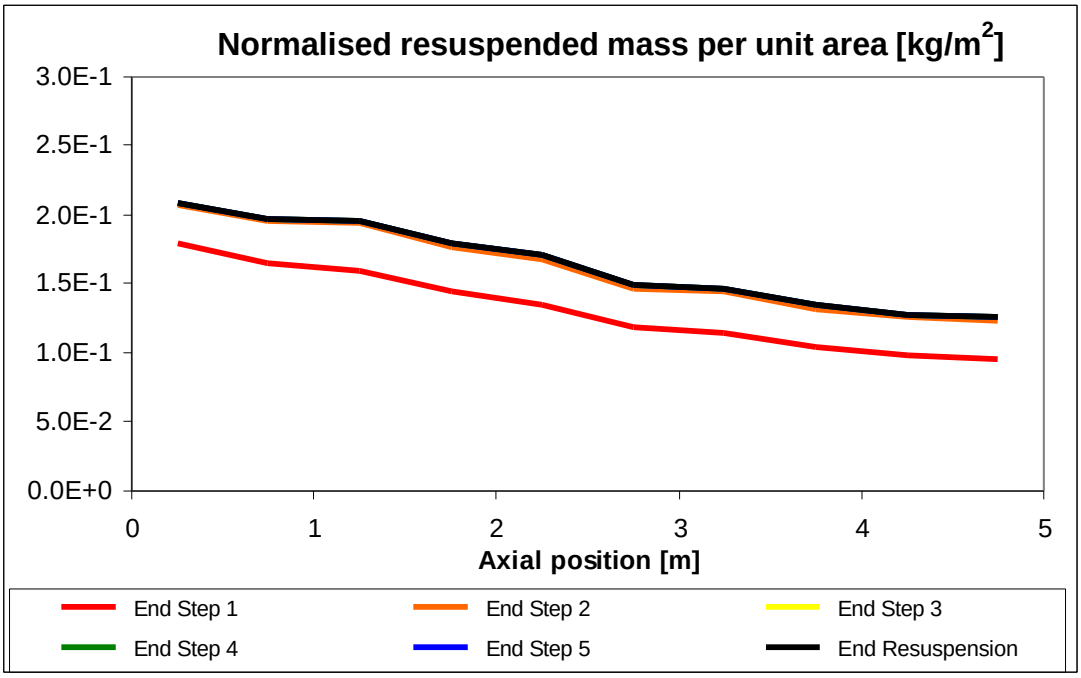

Fig. 84 - Spatial distribution of resuspension (JAERI)

The resuspension model used is independent of the particle size, and leads to an equally distributed resuspension rate in each size bin considered. While there is a

significant mass in the deposit, this leads to an increase of the mean size and a narrower distribution of the particles remaining in the deposit - and available for resuspension in the next step. After the second velocity step the initial deposit becomes extremely small and the size distribution information becomes practically irrelevant (Fig. 85).

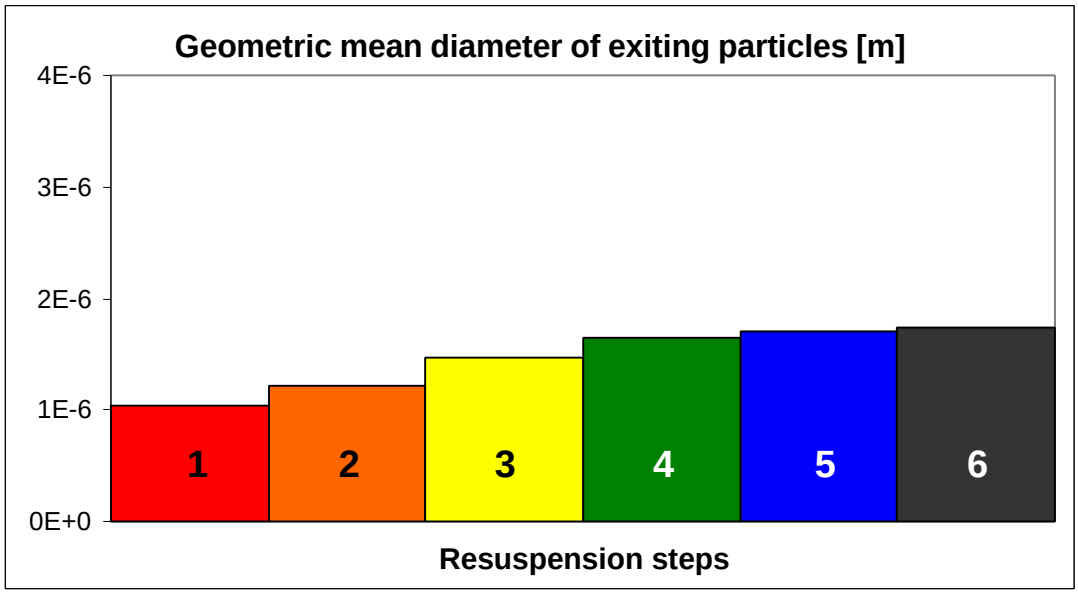

Fig. 85 - Mean particle size at the outlet of the test pipe (JAERI)

5.2. Cæsar

5.2.1. Introduction

The Cæsar computer code is a particle tracking code for the calculation of dry aerosol resuspension created originally at the JRC and presently under joint development by the JRC, the Consejo de Seguridad Nuclear and CIEMAT [9], [10].

The balance between the adhesive forces that tend to attach a particle to the wall and the aerodynamic forces, which tend to move it away from the wall is calculated for each single particle. The resulting force may lead to movement inside the laminar sub-layer of the turbulent boundary layer, in which case the particle tracking continues, or to its movement away from the laminar sub-layer, in which case the particle is considered as resuspended and the particle tracking stops.

The adhesive forces keeping the particles attached to the pipe walls are the resultant of the inter-molecular attractive and repulsive forces. The aerodynamic forces are a drag force, calculated using Stokes' formulation [21], with corrections for gas-particle slip, the effect of a bounded flow and inertial effects, and a lift force, calculated with Cherukat & McLaughlin's formulation [5].

Both calculations submitted with Cæsar were done with the most recent version, which includes the effect of surface roughness in the calculation of the adhesive forces.

5.2.2. CIEMAT-JRC-CSN

A joint CIEMAT-JRC-CSN calculation was submitted, using the Cæsar computer code without any specific changes for this problem [11].

5.2.2.1. ISP calculation

The calculation submitted was performed on a Cray. The calculation of one of the six velocity steps was done for 10,000 particles and the others for 500 particles each. Extrapolating the time used for the 10,000 particles calculation, the total time needed if that number of particles had been used in all steps would be of the order of 50 days, which would be about $6*10^6$ times more than the reference *linpackd* code.

In each velocity step, the supplied initial particle size distribution was used.

The results obtained by CIEMAT-JRC-CSN are summarised in Tab. 8 and Fig. 86. The resuspension rate increases with increasing carrier gas velocity (Fig. 87). In each velocity step, resuspension happens only for a fraction of a second, reaching a new equilibrium situation, after which nothing happens until the velocity is increased again.

Tab. 8 - Summary of results for resuspension phase (CIEMAT-JRC-CSN)

Step	Mass remaining (g)	Particles exiting the test pipe	
		Geometric mean diameter (μm)	Geometric standard deviation
Start	162		
1	140	3.50	1.42
2	81	3.12	1.92
3	22	3.34	3.86
4	4	2.92	3.20
5	0	2.79	3.37
6	0	2.81	4.95

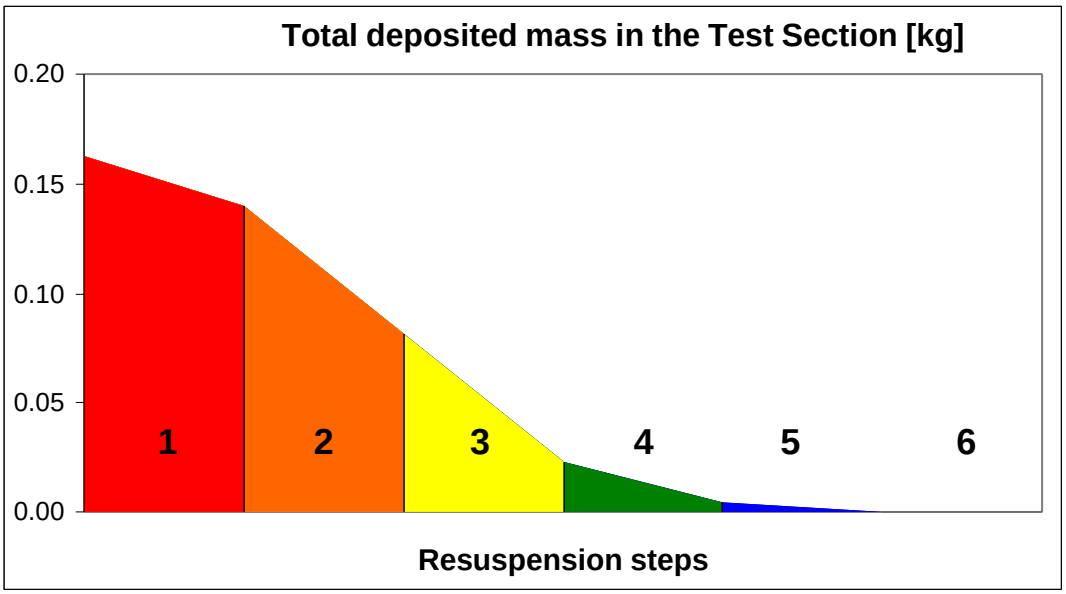

Fig. 86 - Mass remaining in the test pipe (CIEMAT-JRC-CSN)

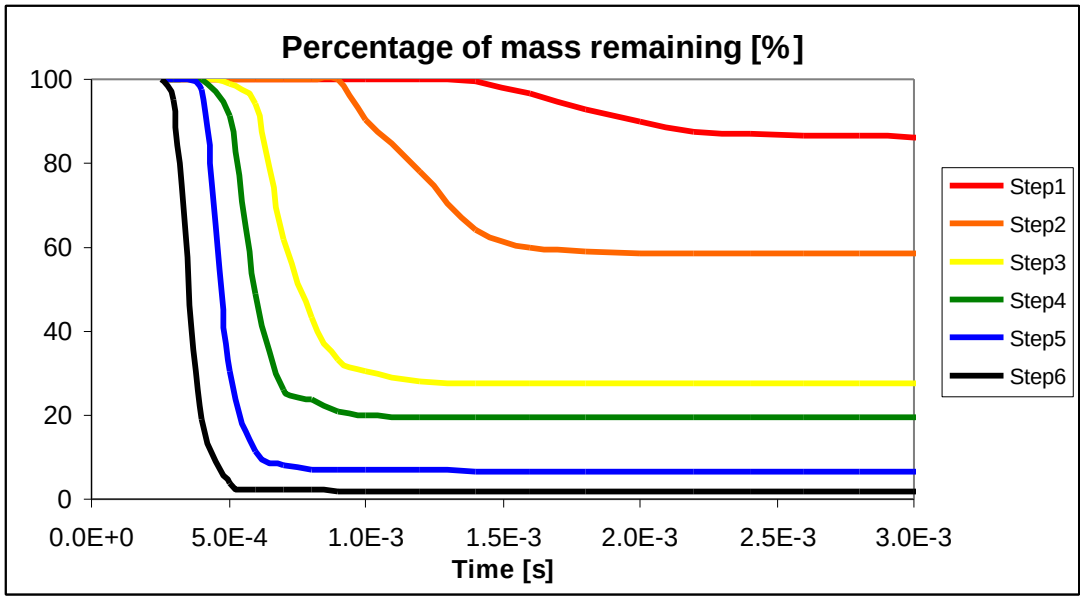

Fig. 87 - Resuspension rate in each velocity step (CIEMAT-JRC-CSN)

The aerosol particle size at the outlet follows closely the specified initial particle size. The geometric mean diameter is lower than the initial size but the spreading is considerably wider (Fig. 88).

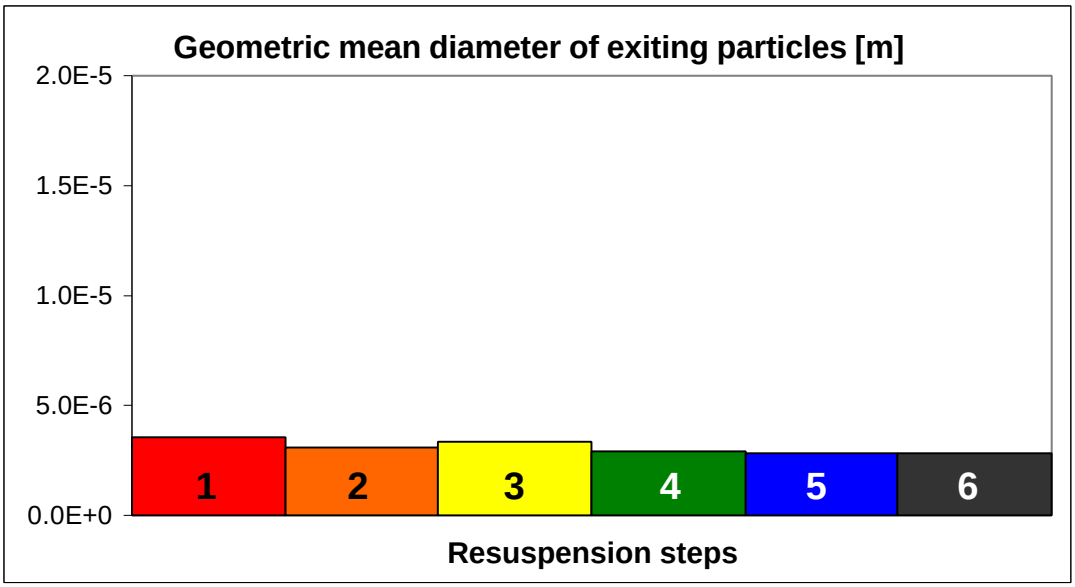

Fig. 88 - Mean particle size at the outlet of the test pipe (CIEMAT-JRC-CSN)

5.2.3. JRC-CSN

The JRC-CSN calculation was performed with the Cæsar computer code, without any specific changes for this problem [11].

5.2.3.1. ISP calculation

The JRC-CSN submission was performed on a Cray and took almost 59 hours to run, which is $3*10^5$ times more than the reference *linpackd* code.

Since Cæsar is a particle tracking code, there is no spatial nodalisation involved. The time step used is calculated internally by the integration subroutine and is not known, and 500 particles were tracked in this calculation. The particle diameters were generated to simulate the bi-modal particle size distribution measured in the first velocity step of the experiment. The velocity steps were run in sequence and hence the particle size distribution at the beginning of each step is the one remaining in the deposit at the end of the preceding step.

The initial conditions and the results obtained are summarised in Tab. 9 and Fig. 89. The resuspension rate, expressed in terms of rate of decrease of the initial deposit in each step, increases with increasing carrier gas velocity (Fig. 90).

Tab. 9 - Summary of results for resuspension phase (JRC-CSN)

Step	Mass remaining (g)	Particles exiting the test pipe	
		Geometric mean diameter (μm)	Geometric standard deviation
Start	162		
1	161	16.66	1.00
2	142	14.52	1.05
3	108	11.10	1.08
4	71	8.85	1.06
5	13	6.29	1.15
6	1	4.00	1.18

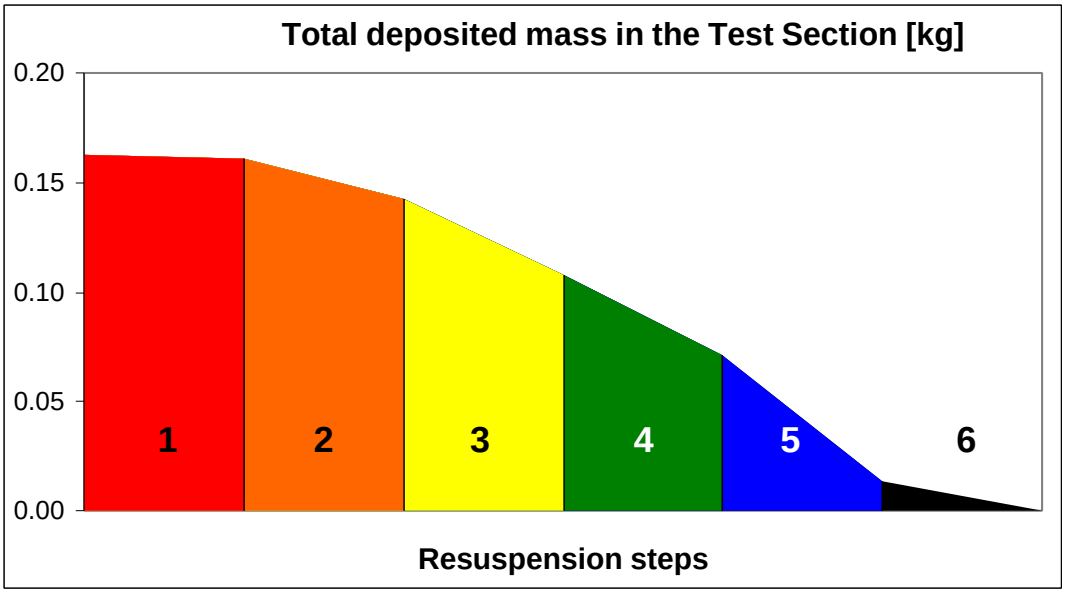

Fig. 89 - Mass remaining in the test pipe (JRC-CSN)

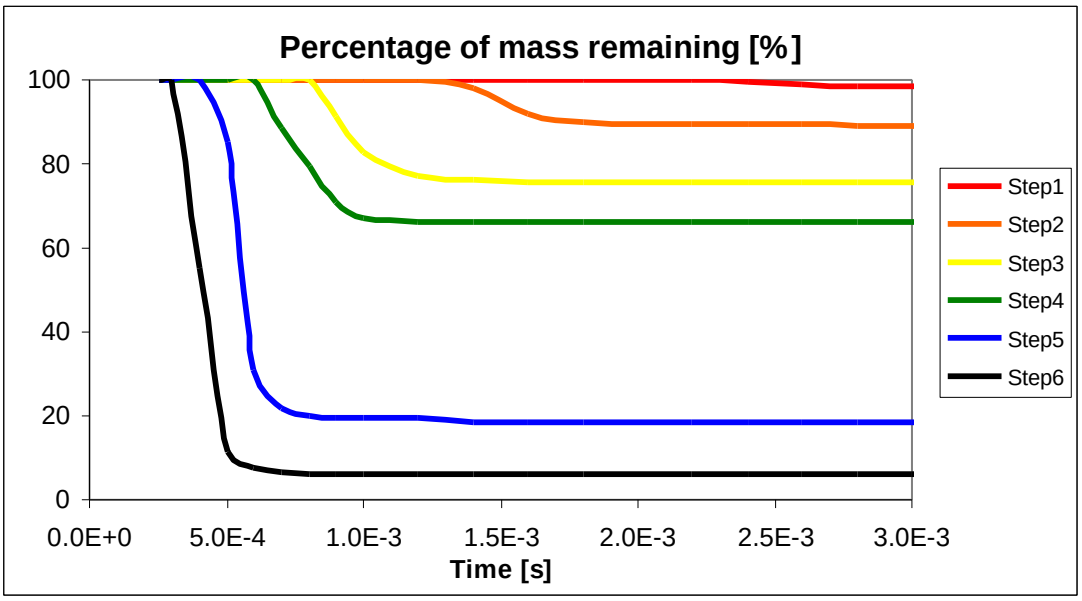

Fig. 90 - Resuspension rate in each velocity step (JRC-CSN)

In the calculation performed with Cæsar, the particle tracking stops when each particle leaves the laminar sub-layer of the turbulent boundary layer and is therefore counted as resuspended. The movement of the particle down the test pipe is not calculated and hence re-deposition is not considered. In this way, the aerosol mass resuspended from each location is proportional to the mass deposited there and any spatial analysis of resuspension is meaningless.

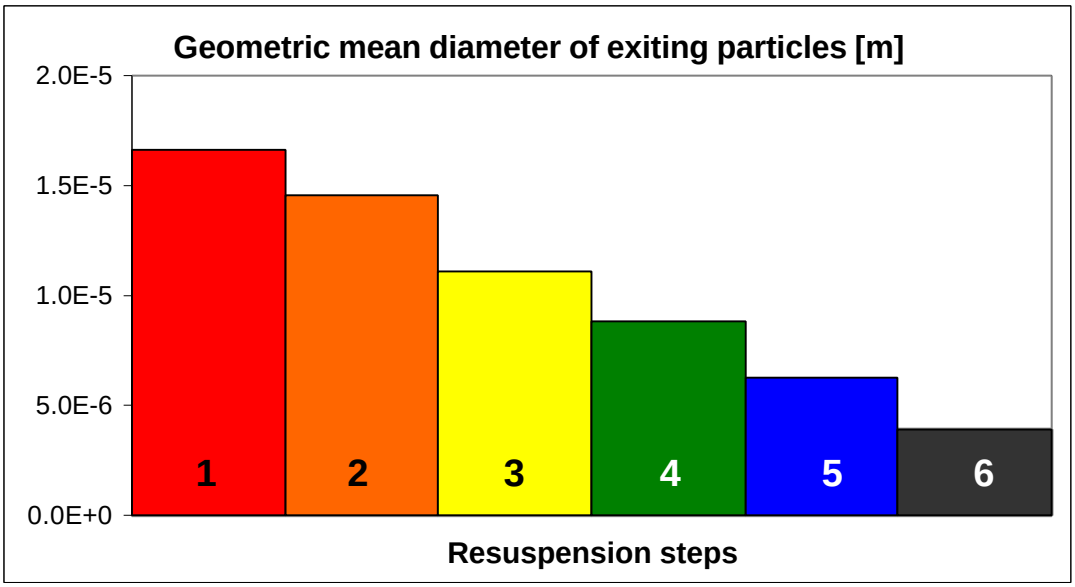

Fig. 91 - Mean particle size at the outlet of the test pipe (JRC-CSN)

The Cæsar calculation predicts a clear correspondence between the diameter of the single resuspended particles and the carrier gas velocity. For each velocity, there is a diameter above which practically all particles resuspend and below which practically no particles resuspend. The geometric standard deviation of the resuspended particles in each velocity step is therefore small because only the particle having sizes between

the limits corresponding to that step and the preceding one are resuspended. The geometric mean diameter of the particles calculated to exit the test pipe decreases sharply with increasing gas velocity (Fig. 91).

5.2.3.2. Sensitivity analysis

Additional calculations were run for different initial particle size distributions. Instead of focussing in the calculated resuspension, which changed with the particle size distribution, the objective of these calculations was more that of verifying the conclusion obtained with the initial calculation that there was a direct relationship between the carrier gas velocity and the minimum diameter of the resuspended particles. The results obtained are shown in Fig. 92 and show an almost linear decrease of the minimum diameter with the carrier gas velocity.

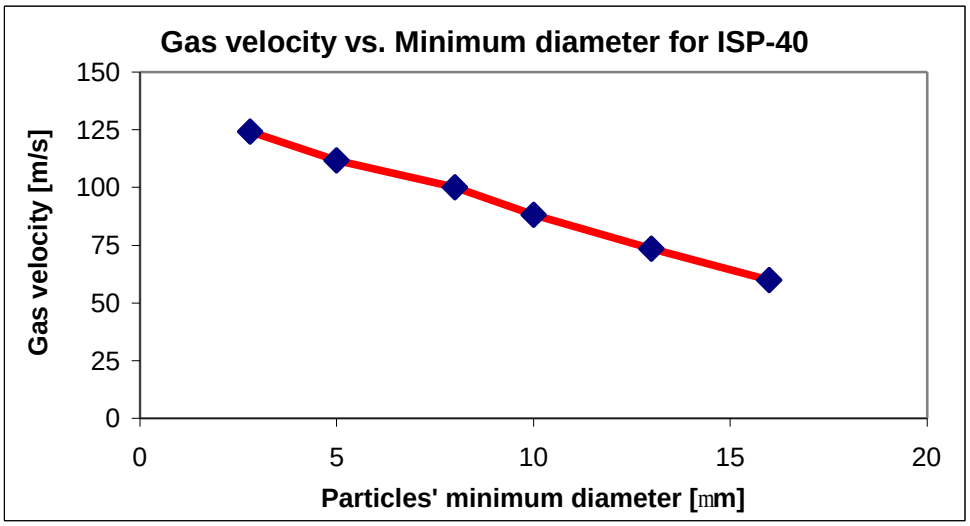

Fig. 92 - Dependence of the minimum diameter of the resuspended particles on the carrier gas velocity (JRC-CSN)

5.3. Ecart

5.3.1. Introduction

The Ecart code is a joint ENEL-EDF code for severe accident simulation that fully couples aerosol and vapour transport with thermal-hydraulics and chemical equilibrium [58], [59]. It includes models for particle agglomeration by gravity, Brownian motion and turbulence, and for particle deposition by thermophoresis, diffusiophoresis, gravitational settling, Brownian diffusion, turbulent diffusion, eddy impaction and impaction in bends.

The Ecart code includes a semi-empirical resuspension model, based on a force balance concept. It considers the individual particle to be subjected to the combined action of adhesive and aerodynamic forces. The comparison of these forces results in a criterion for the onset of resuspension. The extent of resuspension is calculated with a semi-empirical rate equation developed by fitting experimental resuspension data (Oak Ridge Series 2 ART [78], PARESS T-10 [20] and Winfrith Tests n° 53-54).

Resuspension occurs when the following conditions are observed simultaneously:

- The Reynolds number of the carrier gas flow exceeds 2,300.
- The system is dry (environment characterised by a superheated steam atmosphere and subcooled solid phase of the aerosol deposit).
- The aerodynamic forces acting on the particle exceed the adhesive forces between the particle and the wall.

The approach adopted by this resuspension model implies the following assumptions and limitations:

- Deposition and resuspension occur onto and from homogeneous deposits uniformly distributed.
- Particles undergoing resuspension have the same size distribution that they had at the time of their deposition (no agglomeration or fragmentation in the deposit is taken into account).

The adhesive forces taken into account are the inter-molecular attractive forces, the gravitational force and friction. The aerodynamic forces are a drag force and a lift force.

5.3.2. ENEL

The calculation submitted by ENEL was performed with version 97.2 of Ecart without any specific changes for this problem [57].

5.3.2.1. ISP calculation

No information is available on the computer used, the run-time necessary to calculate the resuspension exercise, the time step or the number of size bins used to discretise the aerosol particle size distribution.

Only one computational cell was used to simulate the whole test pipe.

Since there is no possibility in Ecart of imposing an initial deposit and solving only the deposition phase, the ISP calculation had to include a deposition phase followed by a resuspension phase. A large number of deposition calculations were done to reach the appropriate initial conditions for resuspension.

The initial conditions and the results obtained are summarised in Tab. 10 and Fig. 93. The resuspension rate increases steadily from one step to the next, following the increase in the carrier gas velocity (Fig. 94).

Tab. 10 - Summary of results for resuspension phase (ENEL)

Step	Mass remaining (g)	Particles exiting the test pipe	
		Geometric mean diameter (μm)	Geometric standard deviation
Start	173	0.13	1.7
1	166	0.13	1.7
2	146	0.13	1.7
3	130	0.13	1.7
4	114	0.13	1.7
5	94	0.13	1.7
6	86	0.13	1.7

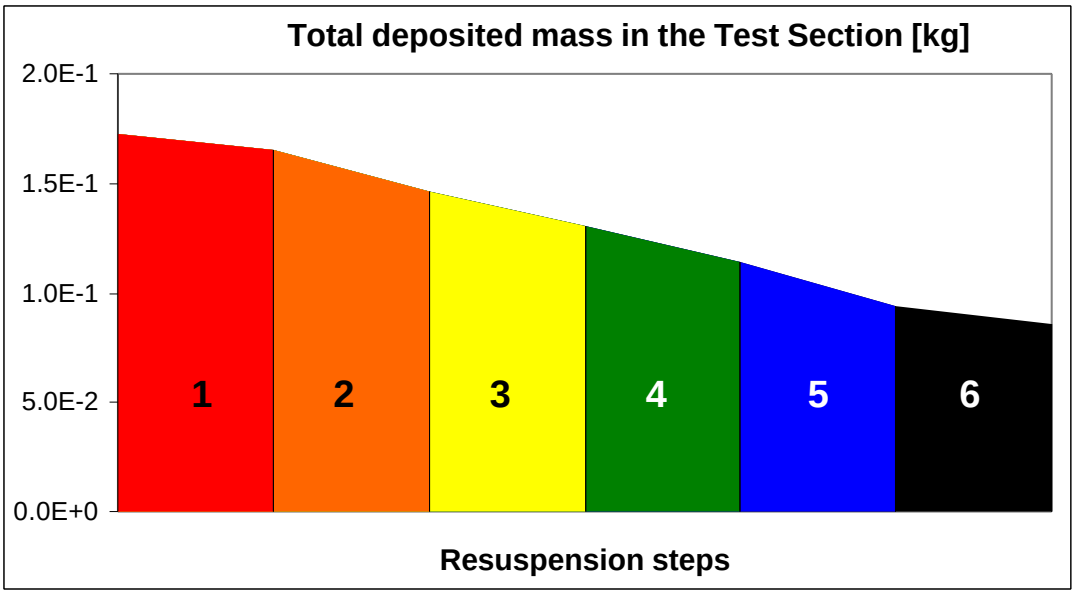

Fig. 93 - Mass remaining in the test pipe (ENEL)

Since only one computational cell was used in the resuspension calculation, there is no information on the spatial distribution of resuspension.

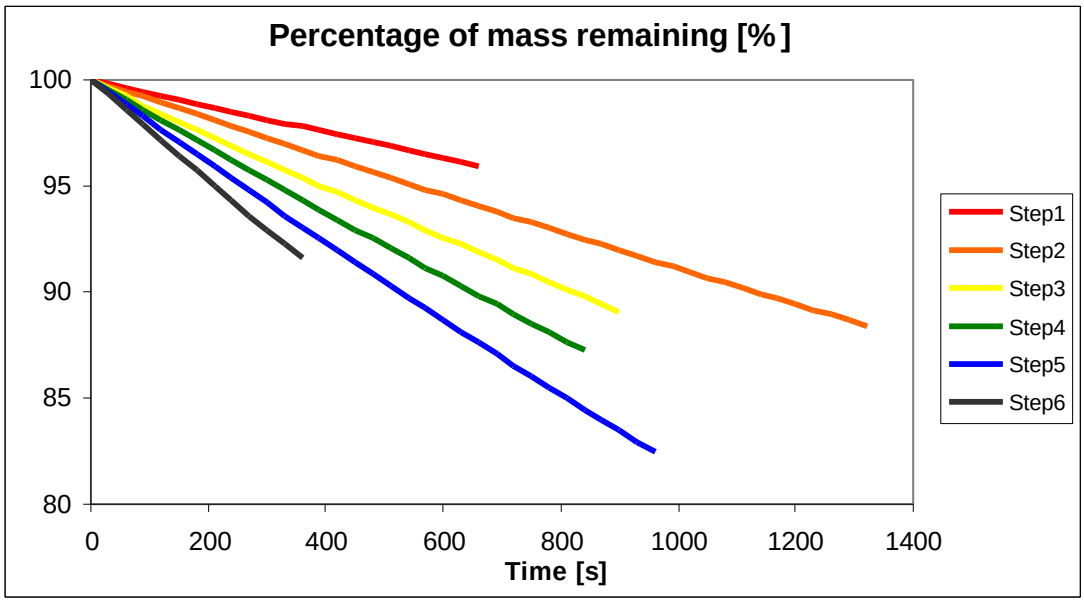

Fig. 94 - Resuspension rate in each velocity step (ENEL)

In Ecart, the particle sizes at the time of deposition are memorised. If those particles are later resuspended, they still have the same size as when they deposited, which means that agglomeration and fragmentation in the deposit are not considered. The results submitted for the particle size distribution at the outlet are constant for the whole resuspension exercise (Fig. 95). They seem to assume that not only the individual particle sizes remain the same but also the global statistical distribution of the particles that resuspend is exactly identical to the distribution during deposition.

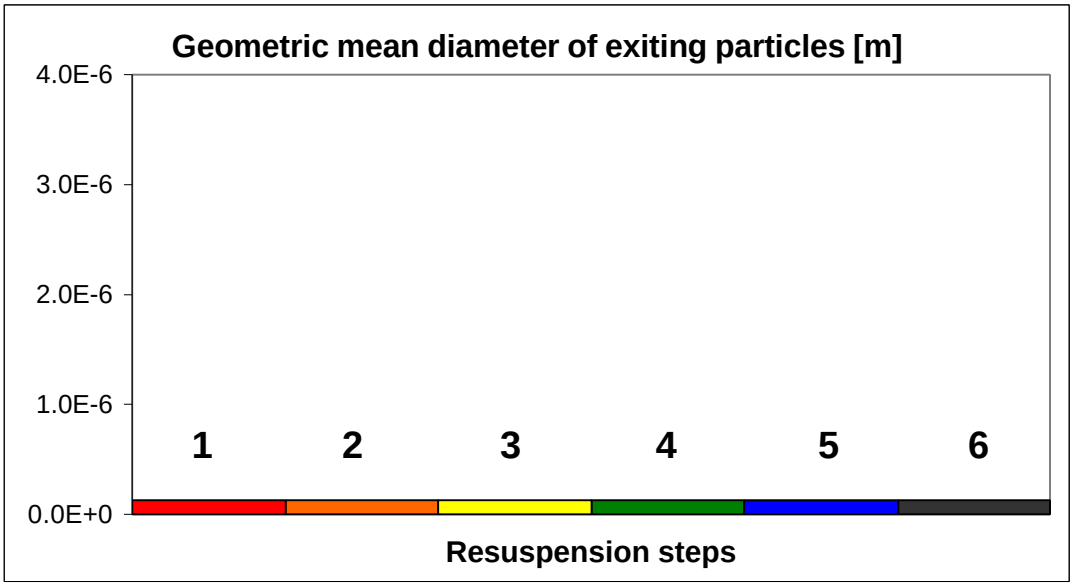

Fig. 95 - Mean particle size at the outlet of the test pipe (ENEL)

5.3.3. University of Pisa

The calculation submitted by the University of Pisa was performed with version 97.2 of Ecart, without any specific changes for this particular problem [55].

5.3.3.1. ISP calculation

The calculation was run on an IBM Risc 6000/250 workstation and took more about 4.6 hours to run the resuspension phase, which is 9,900 times more than the reference *linpackd* code.

The test pipe was divided into five control volumes of different lengths, chosen to accommodate the physical units (pipes and flanges) in the experimental set-up. To obtain the desired flow conditions, two additional control volumes were added, one upstream and the other one downstream of the test pipe.

The time step used in the calculation was 0.01 second, which is up to four times higher than the Courant limits in some control volumes. Additional runs with smaller time steps confirmed that this violation of the Courant limit did not create numerical problems, while considerably reducing the run time.

The particle size distribution was discretised into 40 size bins. In order to save CPU time, agglomeration was not modelled.

It is not possible in Ecart to start from a given deposit and run only the resuspension phase. A large number of deposition calculations were therefore performed to reach satisfactory initial conditions for the resuspension phase, which were reach by setting the collisional shape factor to 2.2.

The initial conditions and the results obtained are summarised in Tab. 11 and Fig. 96. The resuspension rate increases from the first to the last velocity step, following the increase in the velocity of the carrier gas (Fig. 97).

Tab. 11 - Summary of results for resuspension phase (U. Pisa)

Step	Mass remaining (g)	Particles exiting the test pipe	
		Geometric mean diameter (μm)	Geometric standard deviation
Start	162	0.44	1.70
1	156	0.66	1.52
2	139	0.75	1.43
3	125	0.73	1.44
4	110	0.71	1.46
5	91	0.70	1.47
6	84	0.70	1.47

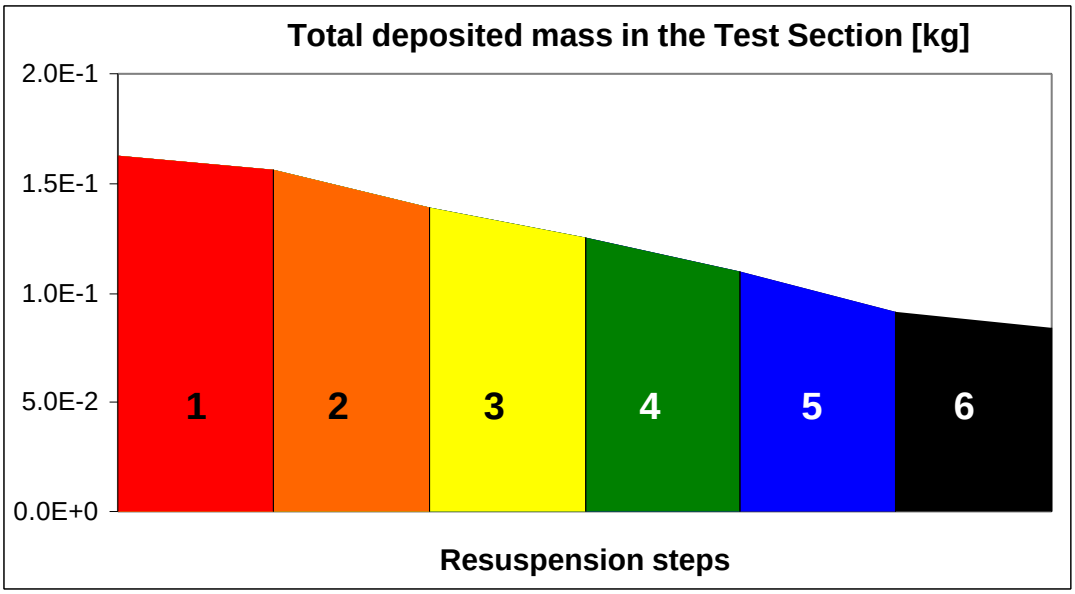

Fig. 96 - Mass remaining in the test pipe (U. Pisa)

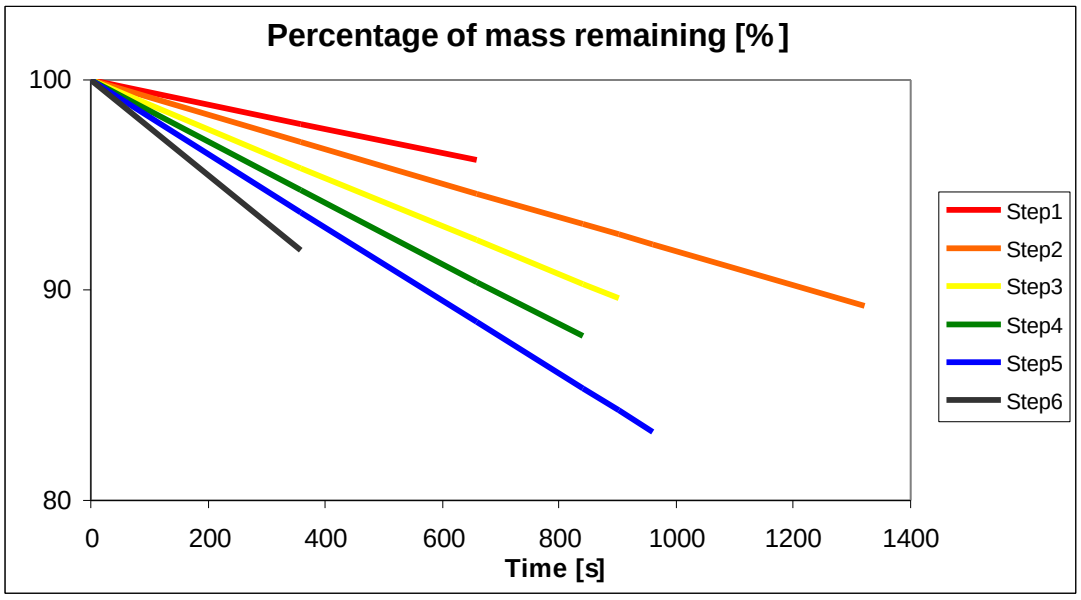

Fig. 97 - Resuspension rate in each velocity step (U. Pisa)

The spatial distribution of resuspension follows closely the distribution of the deposited mass, as can be seen in Fig. 98.

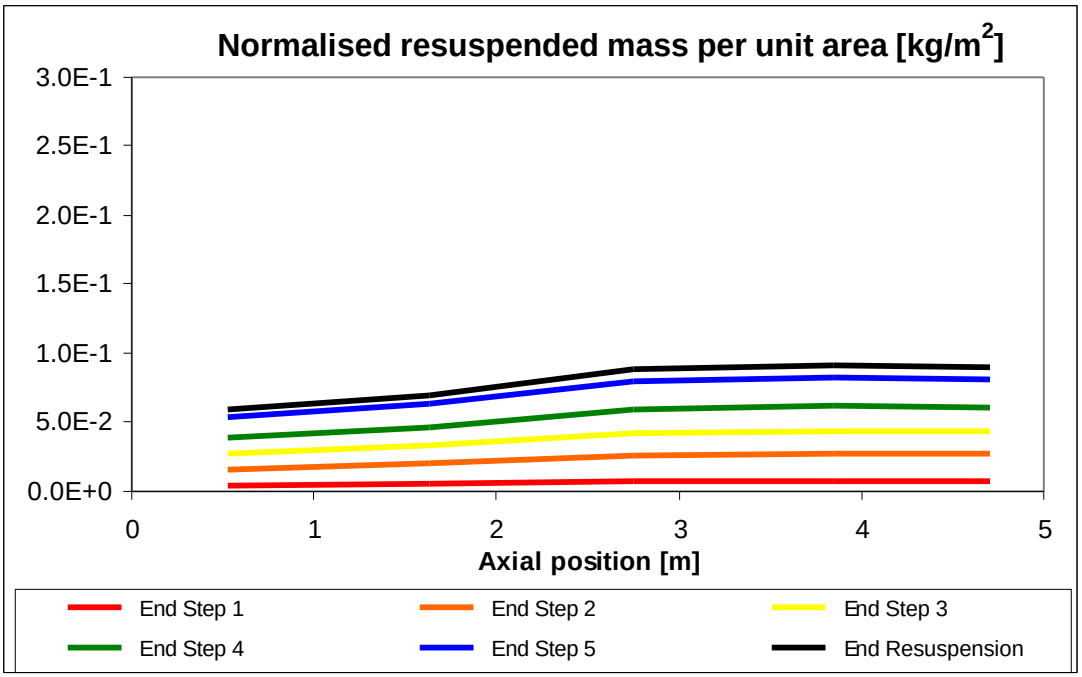

Fig. 98 - Spatial distribution of resuspension (U. Pisa)

The mean particle size calculated by the University of Pisa for the particles exiting the test pipe decreases with increasing carrier gas velocity, after an initial sharp increase from the mean particle size in the deposition phase (Fig. 99).

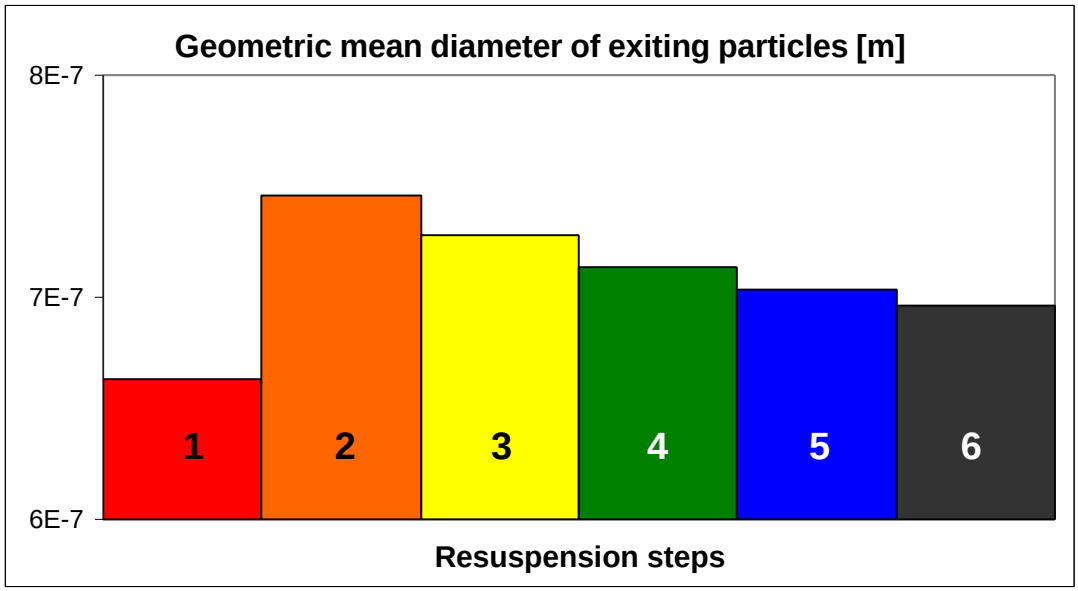

Fig. 99 - Mean particle size at the outlet of the test pipe (U. Pisa)

5.4. ETH model

5.4.1. Introduction

The resuspension model under development at ETH is based on a simulation of random particle beds on a microscopic level. In addition to the "traditional" input parameters used by resuspension models, this model contains a structural parameter (the bed porosity) distinguishing "fluffy" from "crusty" deposits (when all traditional parameters are the same) [19].

At each moment, all "topologically removable" substructures of a particle bed are considered as "potential agglomerates". The time evolution of the system is determined by resuspension probabilities per unit time assigned to these potential agglomerates. In the current implementation, the identification of potential agglomerates is restricted to a simple subclass, liable to underestimate strongly the effect of agglomerate formation. Resuspension probabilities are derived from a generalisation of Fromentin's model [20].

In addition to the physical input parameters (mass load, particle density and size distribution, bed porosity, fluid properties, friction velocity), the model contains only one adaptable parameter which should depend only on the chemical composition, shape etc. of the aerosols.

5.4.2. ETH

The ISP submission was performed using the model under development at ETH [18]. Some of the components of the computer code were written specifically to represent the ISP conditions, including the transport of the resuspended material along the pipe and the space-dependent mass load in the deposit.

5.4.2.1. ISP calculation

The calculation was performed on a 200 MHz Intel Pentium personal computer. The full calculation took slightly more than 8 hours, of which only the last 7.5 minutes were used to calculate resuspension, after the generation of the deposit and the topological analysis. If the topological analysis and the calculation of resuspension are considered together, the calculation took just over 4.5 hours, which is about $5*10^3$ times more than the reference *linpackd* code.

It should be noted, however, that the topological analysis is independent of the gas flow conditions. For the same initial configuration of the deposit, additional resuspension calculations can be carried out in just 7.5 minutes.

The results submitted are for a total of 450,000 particles. The CPU time needed for the calculation is roughly proportional to the number of particles used in the simulation.

The test pipe was divided into 54 cells, so that the initial deposited masses could be used directly as specified.

The model contains one adaptable parameter (loosely speaking, the ratio of "typical" burst force to "typical" adhesion force) which is known only very roughly for the time

being. Since the model response essentially depends on the product of this parameter by the size of deposited particles, the geometric mean diameter of deposited particles was arbitrarily chosen to be 1 µm, and the model parameter was then adapted so that the resulting critical flow velocity for resuspension approximately equals 100 m/s. This procedure makes the ratio of deposited to exiting particle size easily readable from exiting particle sizes. As Tab. 12 and Fig. 103 show, this size ratio is systematically predicted to be greater than 1, which is a consequence of the mechanism of agglomerate formation incorporated in the model. On the other hand, the predicted size ratio is still below the experimental one, which can be attributed to the simplicity of the model.

The evolution of resuspended mass (Tab. 12 and Fig. 100) can be interpreted as follows: In step 1, the surface structure is relatively fragile, corresponding to a relatively large amount (28 g) of loose material being resuspended in the first puff. In step 2, the surface is more robust, which accounts for the relatively small amount of resuspended material (12 g). In steps 3, 4, 5, the effect of approaching and exceeding the "critical velocity" becomes dominant, and the resuspended mass increases. Finally, towards the end of the experiment, the deposit becomes exhausted causing the resuspended mass to drop.

Tab. 12 - Summary of results for resuspension phase (ETH)

Step	Mass remaining (g)	Particles exiting the test pipe	
		Geometric mean diameter (µm)	Geometric standard deviation
Start	162	1	2.12
1	134	1.55	2.03
2	122	1.22	2.25
3	98	1.27	2.27
4	50	1.28	2.28
5	3	1.28	2.30
6	0	1.29	2.28

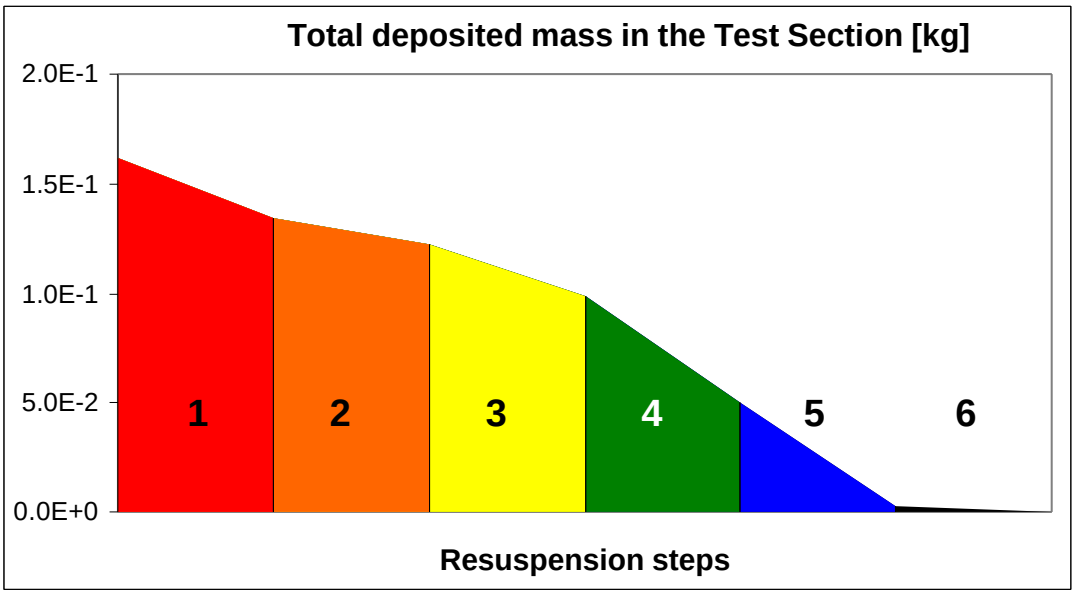

Fig. 100 - Mass remaining in the test pipe (ETH)

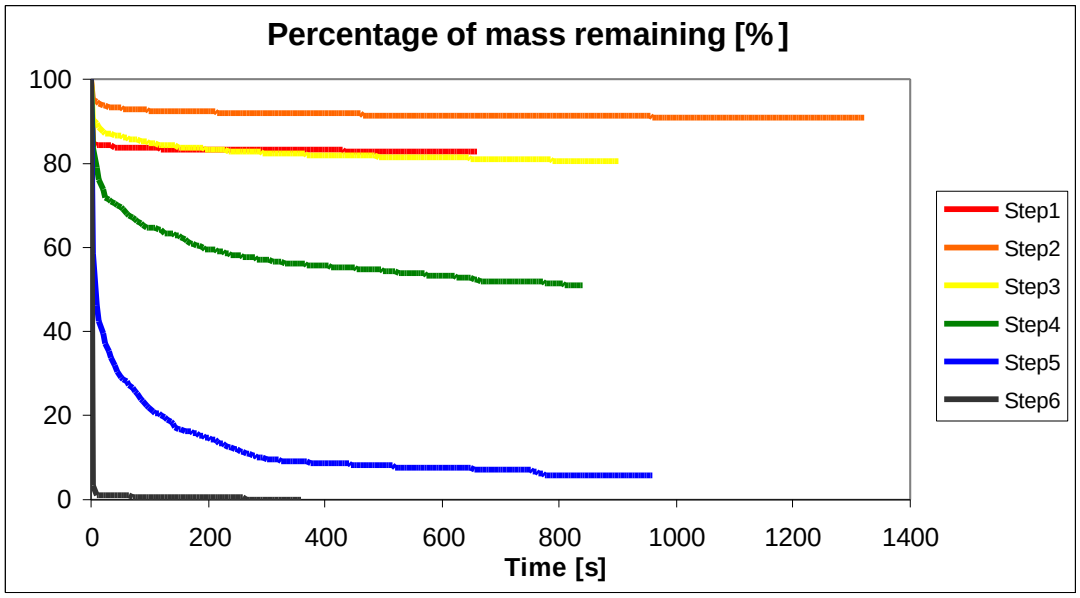

Fig. 101 - Resuspension rate in each velocity step (ETH)

In terms of spatial distribution, resuspension is practically constant along the test pipe in the first three velocity steps and decreases along the pipe for the last three (Fig. 102). This is due to the fact that for a thick deposit - compared with the particle size - the resuspension rate is practically independent of the quantity of aerosols deposited. The particles below a certain depth are not exposed to the flow and hence do not affect the resuspension rate. When the thickness of the deposit becomes smaller, the effective resuspension rates depend on the availability of material in the deposit and are therefore higher where the mass load is higher.

It should be noted that re-deposition of particles was not considered in the calculation and the resuspended particles are simply taken by the carrier gas towards the exit of the test pipe.

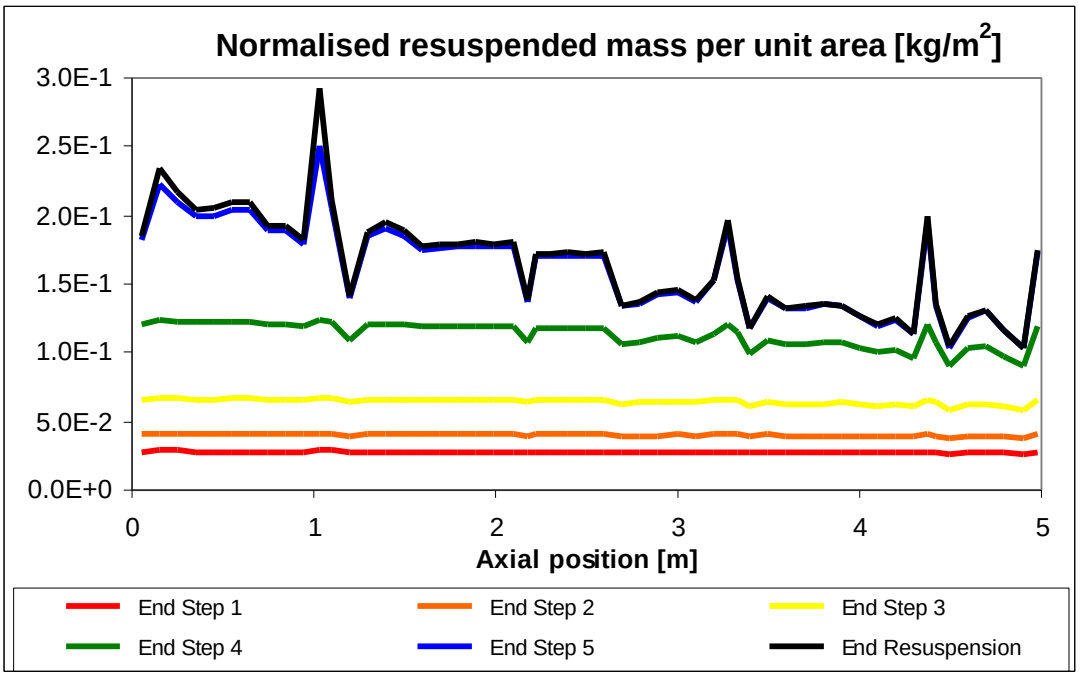

Fig. 102 - Spatial distribution of resuspension (ETH)

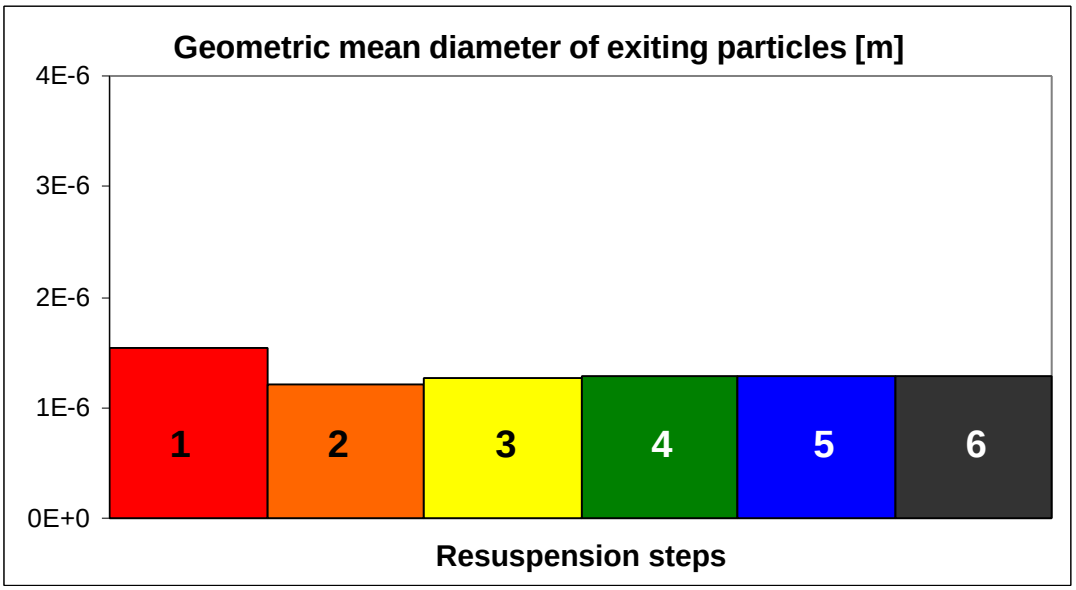

Fig. 103 - Mean particles size at the outlet of the test pipe (ETH)

5.4.2.2. Sensitivity calculations

Although the particle size distribution is measured during the deposition phase, there is a real possibility of creation and break-up of agglomerates in the deposit that depend on the conditions during deposition and on the physical and chemical characteristics of the deposited aerosols. The experimental determination of the sizes of the deposited particles is therefore practically impossible except in the simplest cases of mono-layer deposits and/or non-cohesive particles, i.e. those for which the particle-particle adhesion is always much lower than the particle-wall adhesion, so

that it can be safely assumed that each single particle will detach from the deposit independently, without forming any agglomerates.

Given this practical difficulty in the characterisation of the sizes of the deposited particles, ETH considered that it was particularly important to perform a sensitivity analysis on the variation of calculated resuspension due to a modification of the assumed size distribution. The geometric mean diameter used in the ISP-40 calculation was first doubled and then halved while all other parameters in the calculation were kept constant.

The results (Fig. 104) show a huge variation of the calculated aerosol resuspension for a relatively narrow uncertainty margin in the specified mean particle size, highlighting the importance for modelling of a correct characterisation of the deposit. It should be noted, however, that the ETH model depends on one user-adaptable parameter, that represents, loosely speaking, the ratio of the typical burst force to the typical adhesion force. In the basic calculation, the geometric mean diameter was set to 1 µm and this adaptable parameter was set to a value that yielded a critical flow velocity for resuspension that reproduced reasonably well the previous STORM tests. Since there is no reason to assume that the size distribution in the deposit in test SR-11 was considerably different from that of other STORM tests, the assumption of a different mean particle size would also lead to a revision of the adequate adaptable parameter. It would be interesting to know whether the necessary change of this parameter would make physical sense or would lead to un-physical values.

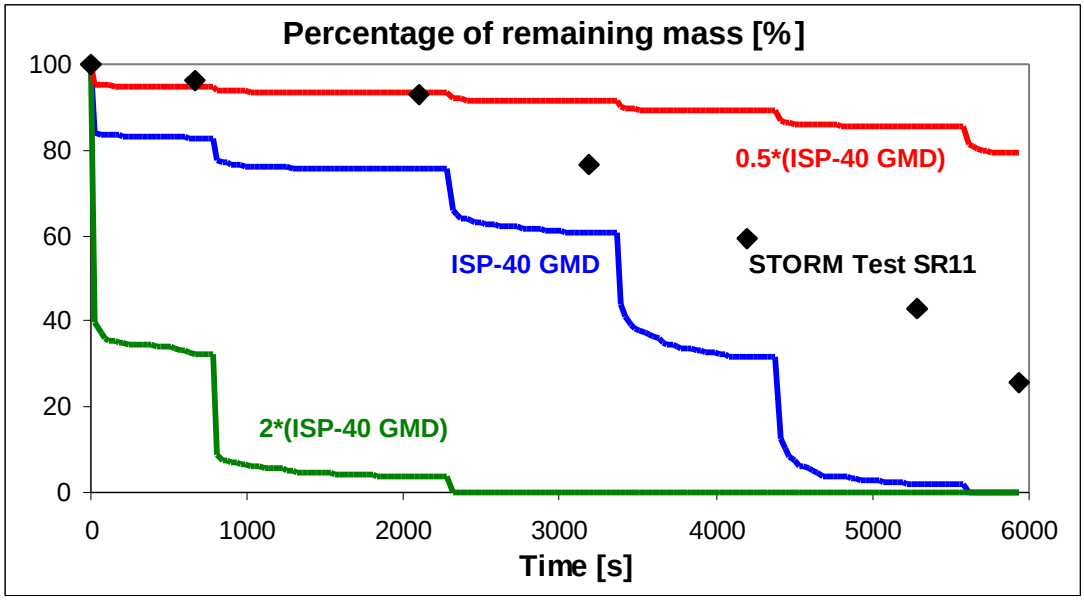

Fig. 104 - Analysis of sensitivity to mean particle size of the deposit (ETH)

5.5. Sophaeros

5.5.1. Introduction

The Sophaeros code was developed by IPSN to predict in a mechanistic way the fission product (f.p.) physical behaviour in LWR primary circuits during severe

accidents [46], [47], [48]. The modular structure of the code allows a versatile choice of defining input thermal-hydraulic data, circuit geometry, and physical description of aerosol/vapour deposition, with possible switching on/off of all transport mechanisms.

The main phenomena modelled by the code are interaction of f.p. vapours with aerosols (condensation/evaporation), interaction of vapours with walls (condensation and sorption), aerosol fallback and coagulation, aerosol deposition on circuit walls and aerosol resuspension.

The resuspension model included in Sophaeros [65], [66] is based on the Ecart model described above [56].

5.5.2. CEA/IPSN/DRS

The results submitted by CEA/IPSN/DRS were calculated with version 2.0 of Sophaeros [45], [49]. The module that calculates vapour-phase chemistry and homogeneous nucleation was not activated.

5.5.2.1. ISP calculation

The calculation was run on a Sun SparcStation 10 workstation and took 109 seconds to run, which is less than 14 times more than the reference *linpackd* code.

A total of 10 practically identical control volumes were used and the time of the test was divided into 60 time steps, with three or four iterations per time step.

It is not possible in Sophaeros to specify an initial deposit layer. The initial conditions for the ISP resuspension exercise had to be generated by repeating the calculation already done for the deposition phase. The boundary conditions were adjusted iteratively in order to obtain a good agreement with the total mass of aerosols in the deposit and its spatial distribution at the beginning of the resuspension phase, as well as with the size distribution of the resuspended aerosols at the end of the first resuspension step. A duration of 7000 seconds was chosen for the preliminary deposition phase (with the resuspension model enabled) using a cohesive coefficient for the resuspension model of 30.0 μN/m instead of the default value of 1.0 μN/m. Finally, the resuspension phase is calculated as continuation of this preliminary deposition calculation in one SOPHAEROS run.. It was impossible to reproduce exactly the initial conditions specified for the resuspension exercise but the agreement obtained was considered good enough for the purpose of the ISP. In particular, the initial deposited mass considered in the calculations was 199 grams instead of the specified 162 grams.

The results obtained, together with the initial conditions, are summarised in Tab. 13 and Fig. 105. The resuspension rate, expressed in terms of rate of decrease of the initial deposit in each step, increases steadily from the first to the last step, following the increase of the carrier gas velocity in the test pipe (Fig. 106).

Tab. 13 - Summary of results for resuspension phase (CEA/IPSN/DRS)

Step	Mass remaining (g)	Particles exiting the test pipe	
		Geometric mean diameter (µm)	Geometric standard deviation
Start	199	17.7	1.02
1	195	3.5	1.30
2	184	2.94	1.26
3	171	2.27	1.39
4	159	2.03	1.36
5	145	1.65	1.45
6	137	1.53	1.45

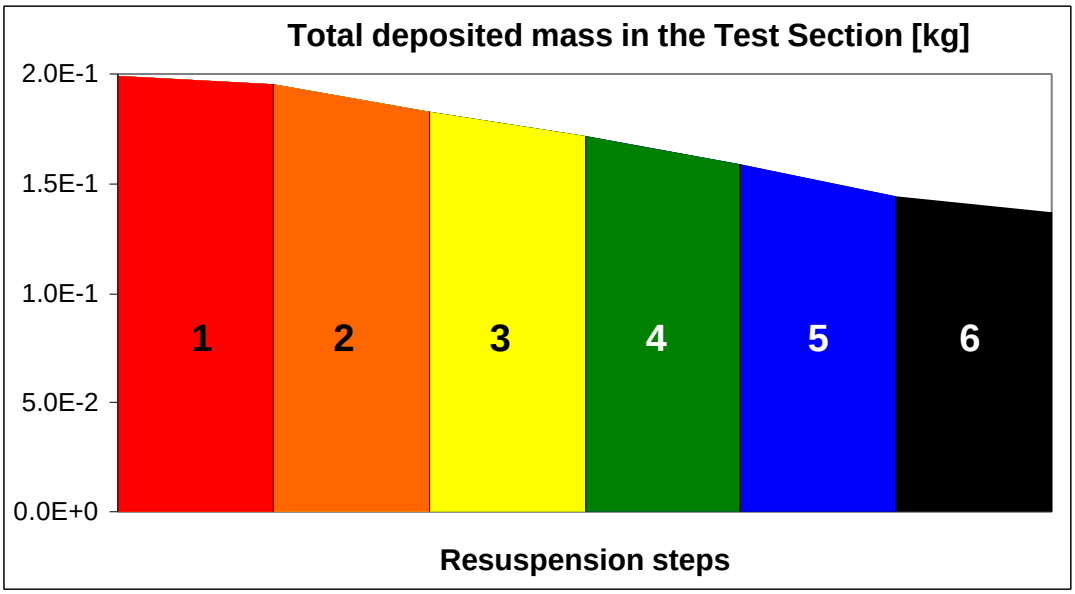

Fig. 105 - Mass remaining in the test pipe (CEA/IPSN/DRS)

In terms of the spatial distribution, resuspension is stronger near the entrance of the test pipe and decreases towards the exit (Fig. 107).

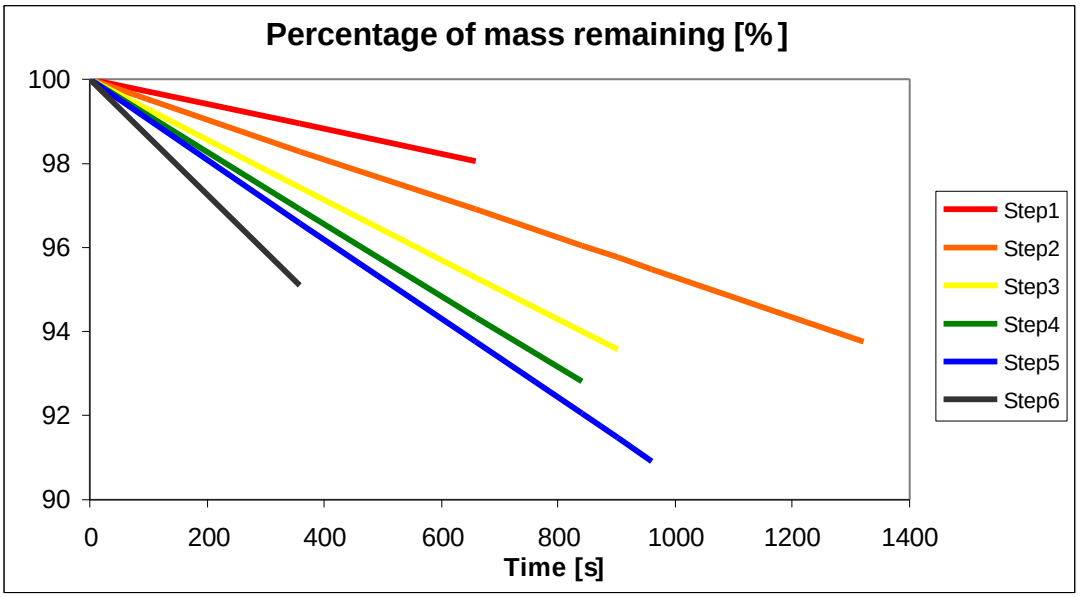

Fig. 106 - Resuspension rate in each velocity step (CEA/IPSN/DRS)

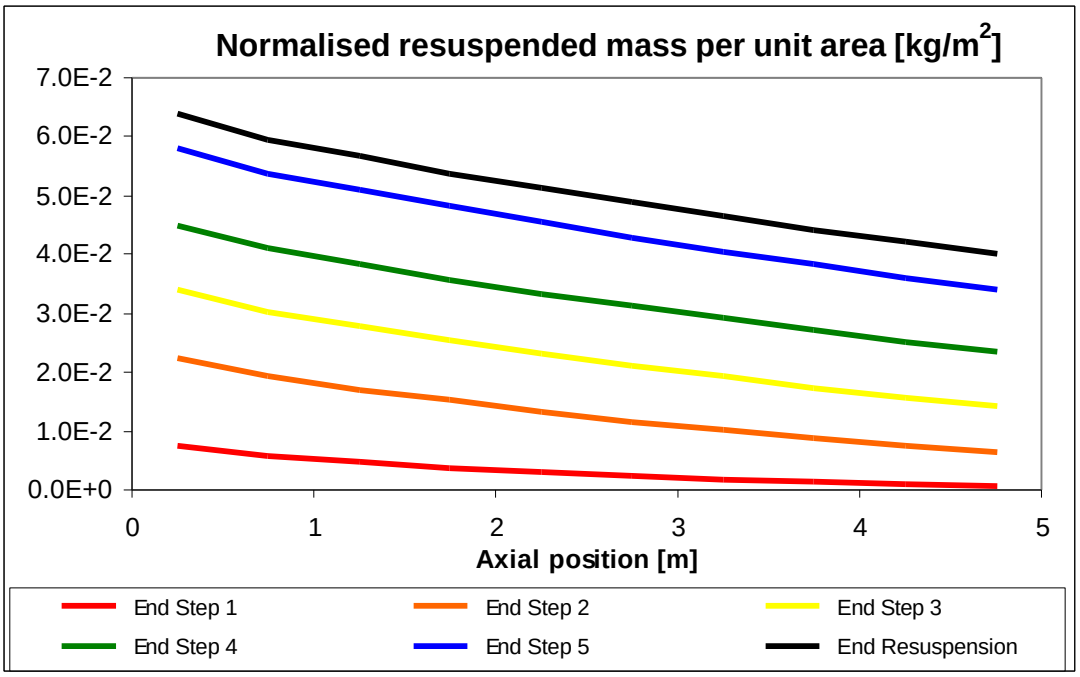

Fig. 107 - Spatial distribution of resuspension (CEA/IPSN/DRS)

The particle size distributions at the test pipe outlet calculated by Sophaeros are characterised by relatively small geometric standard deviations, higher towards the last velocity steps (Tab. 13). The geometric mean diameter decreases consistently from one velocity step to the next, indicating that the large particles are easier to resuspend. According to the calculation, there was no resuspension at all for particles of less than 0.5 µm, even in the last velocity step.

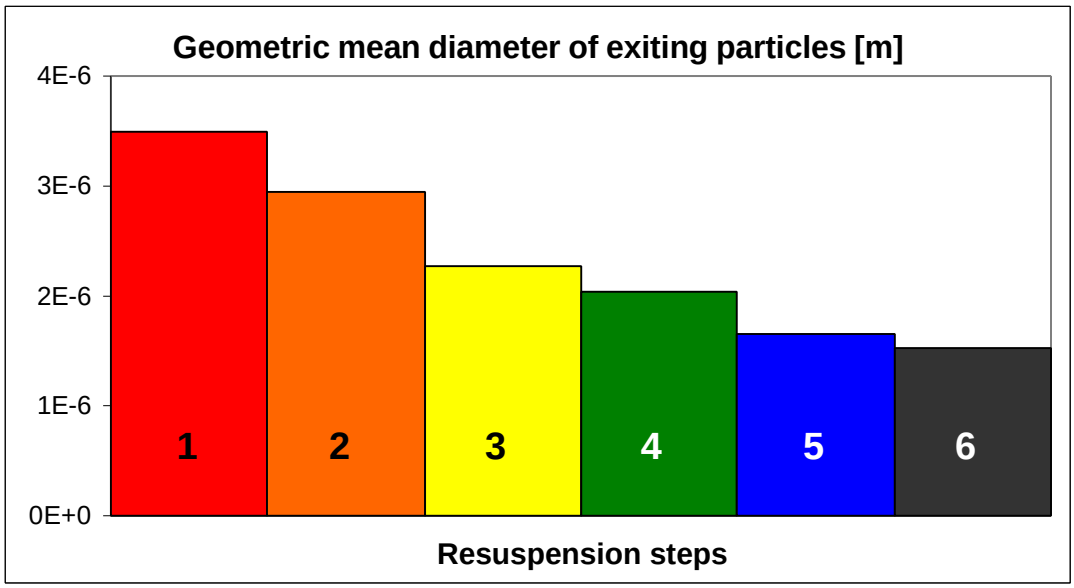

Fig. 108 - Mean particle size at the outlet of the test pipe (CEA/IPSN/DRS)

The results obtained by CEA/IPSN/DRS show that, according to the model in Sophaeros, there is a clearly identifiable and particle size dependent threshold velocity above which resuspension occurs for particles of that particular size.

5.5.3. GRS

The ISP submission from GRS was performed with version 1.4 GRS of Sophaeros [67]. As for the deposition exercise, the non-volatile species SnO_2 had to be added to the Sophaeros database and the restriction for pressures larger or equal to 10^6 dyne/cm^2 was removed. Additionally, some inconsistencies in the resuspension module that caused negative resuspension rates for large particle sizes were removed.

5.5.3.1. ISP calculation

The calculation for the ISP was run on an IBM workstation and took 110 seconds for the resuspension phase, which is about 180 times more than the reference *linpackd* code.

The test pipe was divided into 10 identical control volumes and the maximum time step was set to 50 seconds. The actual time step is calculated by the code, and a total of 330 time steps, with 3 or 4 iterations per time step, were used to represent the whole duration of the resuspension phase.

The aerosol particle size distribution was discretised into 20 bins covering the range between 0.005 µm and 25 µm.

Since Sophaeros cannot start from a known deposit to calculate only aerosol resuspension, the initial conditions had to be generated by running a deposition phase followed by the resuspension phase in one single calculation. The calculation performed for the ISP-40 deposition phase exercise was modified in order to obtain the specified initial aerosol deposition for the resuspension phase.

The initial conditions and the results obtained, in terms of mass of aerosols remaining in the test pipe and of the size distribution of the particles exiting the test pipe, are

summarised in Tab. 14 and Fig. 109. The resuspension rate, expressed in terms of rate of decrease of the initial deposit in each step, increases steadily from the first to the last step, following the increase of the carrier gas velocity in the test pipe (Fig. 110).

Tab. 14 - Summary of results for resuspension phase (GRS)

Step	Mass remaining (g)	Particles exiting the test pipe	
		Geometric mean diameter (µm)	Geometric standard deviation
Start	163	0.44	1.70
1	152	0.74	1.61
2	129	0.70	1.61
3	113	0.66	1.59
4	98	0.63	1.58
5	83	0.60	1.56
6	77	0.58	1.55

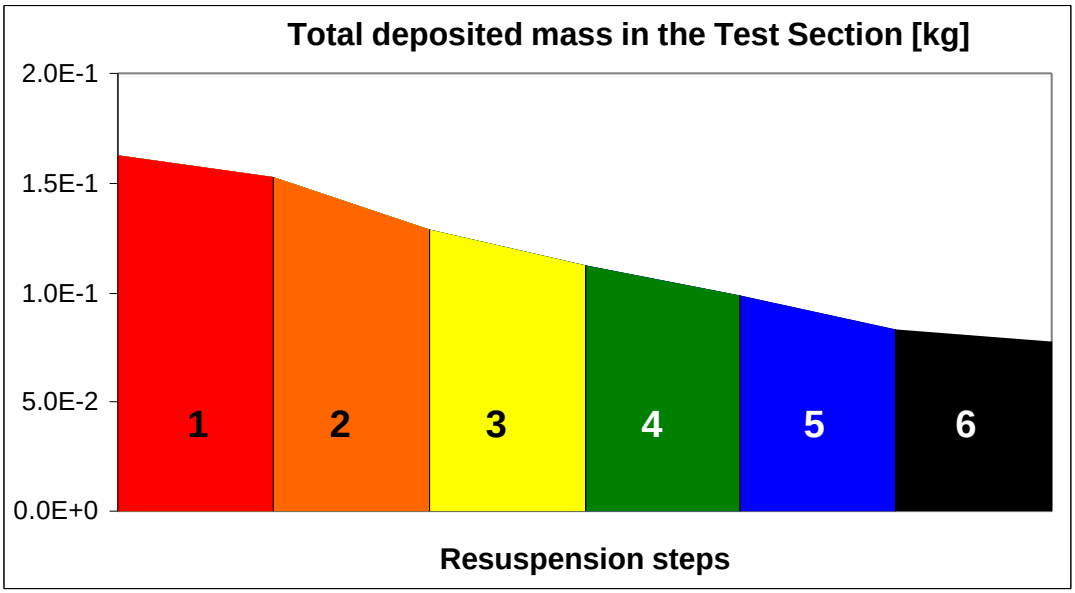

Fig. 109 - Mass remaining in the test pipe (GRS)

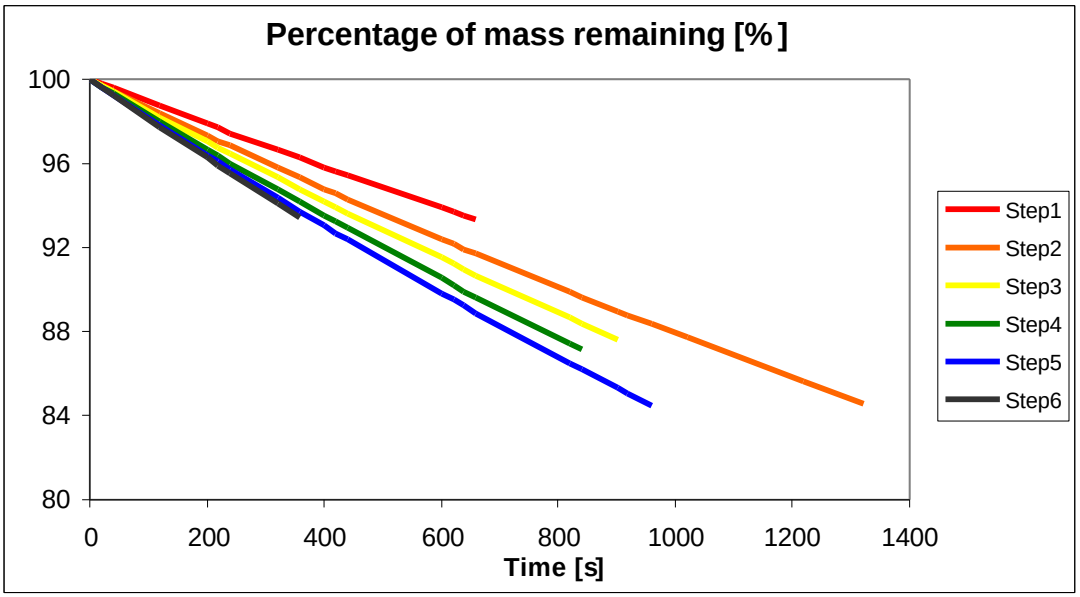

Fig. 110 - Resuspension rate in each velocity step (GRS)

The incidence of resuspension is stronger near the entrance, where the initial deposit is larger, and decreases steadily along the test pipe (Fig. 111). The rate of decrease is higher for higher carrier gas velocities.

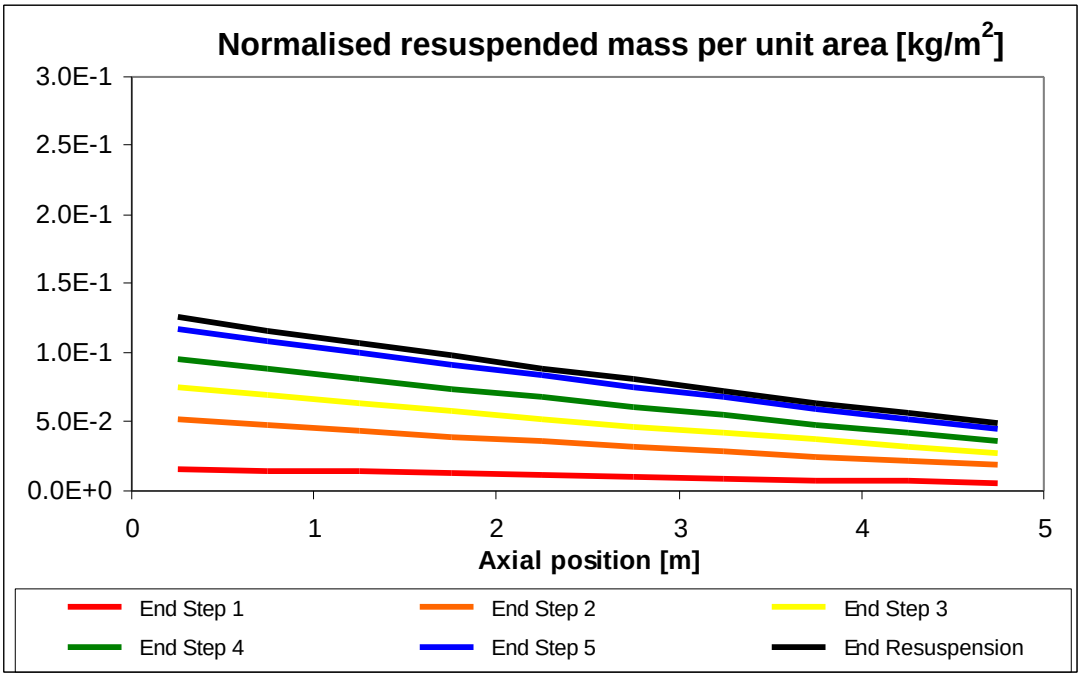

Fig. 111 - Spatial distribution of resuspension (GRS)

The particle size distribution at the outlet is strongly conditioned by the initial distribution. Since Sophaeros does not calculate any agglomeration of fragmentation in the deposit, the particle size distribution at the beginning of resuspension was the same that resulted from the previous deposition calculation. The particles that were resuspended have a considerably larger mean diameter and a somewhat narrower

distribution relative to the initial conditions (Fig. 112). The geometric mean diameter and geometric standard deviation decrease slightly from one step to the next.

Although it is not visible from the spatial profile, some of the material resuspended from the pipe re-deposits due mainly to eddy impaction. This affects 23% of the total resuspended mass.

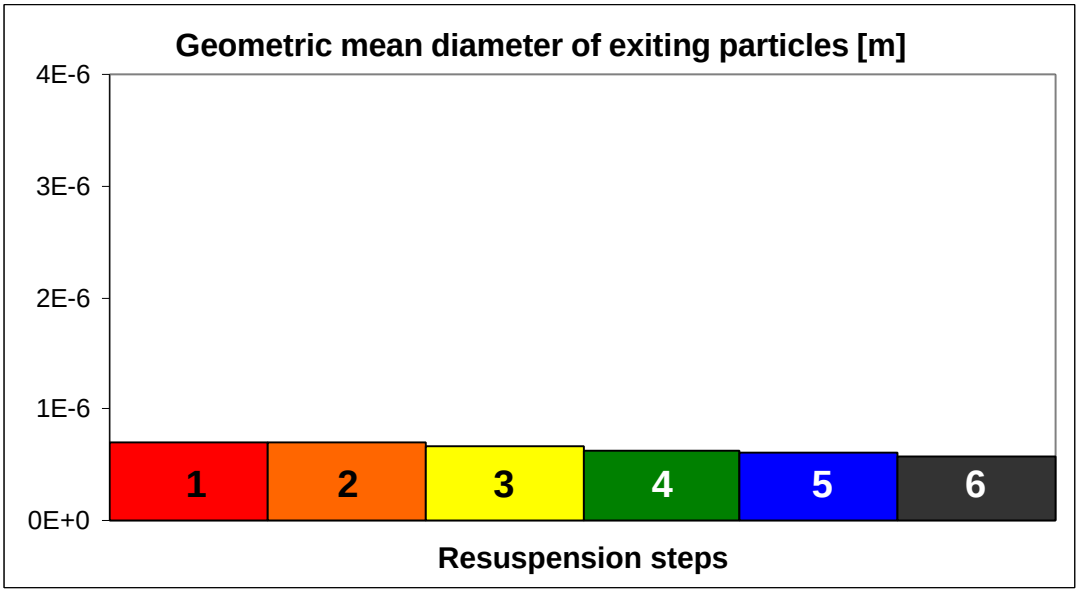

Fig. 112 - Mean particle size at the outlet of the test pipe (GRS)

5.5.3.2. Sensitivity calculation

The results obtained for aerosol resuspension were strongly dependent on the aerosol size distribution considered in the calculation. Since Sophaeros allows the use of a bi-modal log-normal distribution, this feature was used to add larger particles to the initial distribution. A second mode, with a geometric mean diameter of 0.75 µm and a geometric standard deviation of 1.7 was added to the initial particle size distribution in the deposition phase. Depending on the mass fraction attributed to this second distribution, the total mass remaining in the deposit went from the previous 77 grams to 55 grams, for 1% of the mass in the higher mode, to just 18 grams for 10% of the mass in the higher mode.

5.6. Victoria

5.6.1. Introduction

Victoria is a USNRC code, developed originally by Sandia National Labs. and later also in collaboration with AEA Technology, to model the release, transport, deposition and resuspension of fission products during a severe reactor accident [23]. It models chemistry in the vapour and condensed phases, assuming instantaneous chemical equilibrium.

Concerning aerosol transport, it models aerosol formation, agglomeration due to gravity, Brownian motion and turbulence, and deposition by gravitational settling,

Brownian diffusion, turbulence (diffusion and impaction), thermophoresis and impaction in bends.

The aerosol resuspension model is a time-decaying equation based on the results of the Paress experiments [20]. It is similar to the Paress equation used in Art, but includes a dependence of the resuspension rate on the mass of deposited aerosols, which does not exist in the original Paress model.

5.6.2. KINS

The KINS submission was performed with version 92-01 of Victoria, without any specific changes for this problem [35].

5.6.2.1. ISP calculation

The calculation was run on a Sun Center 2000 workstation and took more than 28 hours to run the resuspension phase, which is almost 15,000 times more than the reference *linpackd* code.

The test pipe was divided into 5 almost identical computational cells and the maximum time step used was 0.01 seconds.

The chemistry module in Victoria was excluded in the calculation, since it was not relevant for this case and would increase the run times significantly.

It is not possible in Victoria to specify an initial deposit and run a resuspension-only calculation. A full calculation, with deposition and resuspension phases, had to be done. Since the calculated total deposition at the end of the resuspension phase was 231 grams instead of the 162 grams measured in the experiment, the results were corrected by a factor of about 0.7. In terms of particle size distribution, the released data were not used, and the particle size at resuspension was assumed to be the same as when they deposited, without considering agglomeration or fragmentation in the deposit.

The results submitted for the particle size distribution at the outlet are actually those for the last computational cell. It was assumed that there was no significant change in the last cell itself.

Since Victoria's database does not include nitrogen, the carrier gas was replaced with a mixture of argon and helium containing equivalent mass and number of moles.

The initial conditions and the results obtained are summarised in Tab. 15 and Fig. 113. The Victoria model for resuspension calculates the mass remaining in the deposit as an exponentially decaying function of time, multiplied by the mass deposited at the beginning of each time step. Since almost 98% of the deposit is resuspended in the first step, the remaining deposited mass is very small and resuspension becomes almost negligible in the following steps. The effect of the diminishing initial deposit can be seen in Fig. 114, which shows that the rate of decrease of the initial deposit in each velocity step decreases with increasing carrier gas velocity.

Tab. 15 - Summary of results for resuspension phase (KINS)

Step	Mass remaining (g)	Particles exiting the test pipe	
		Geometric mean diameter (μm)	Geometric standard deviation
Start	162	0.20	1.69
1	4	0.28	1.41
2	3	0.23	1.35
3	3	0.22	1.07
4	3	0.21	1.08
5	3	0.16	1.22
6	3	0.11	1.44

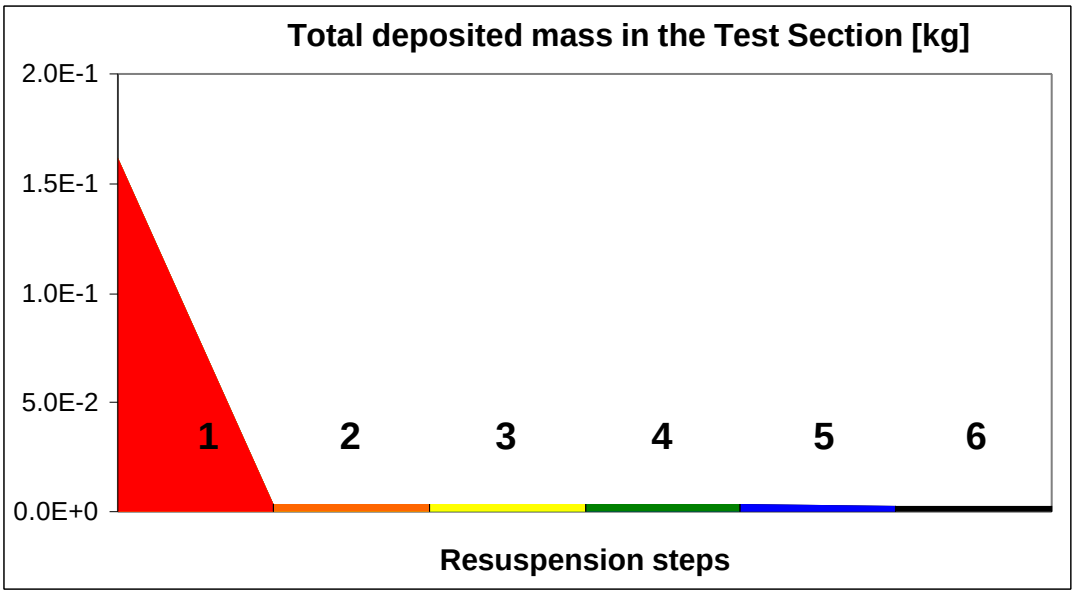

Fig. 113 - Mass remaining in the test pipe (KINS)

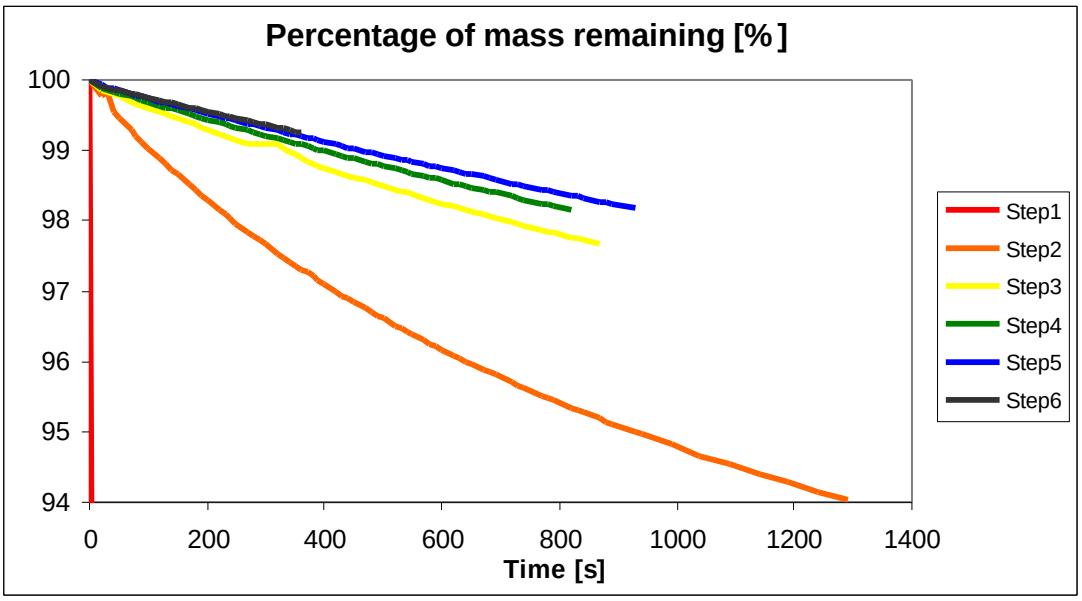

Fig. 114 - Resuspension rate in each velocity step (KINS)

Since practically all the deposited aerosols are resuspended in the first velocity step, the spatial profile of resuspension is almost exactly the same as the deposition profile calculated in the deposition exercise of ISP40 (Fig. 115).

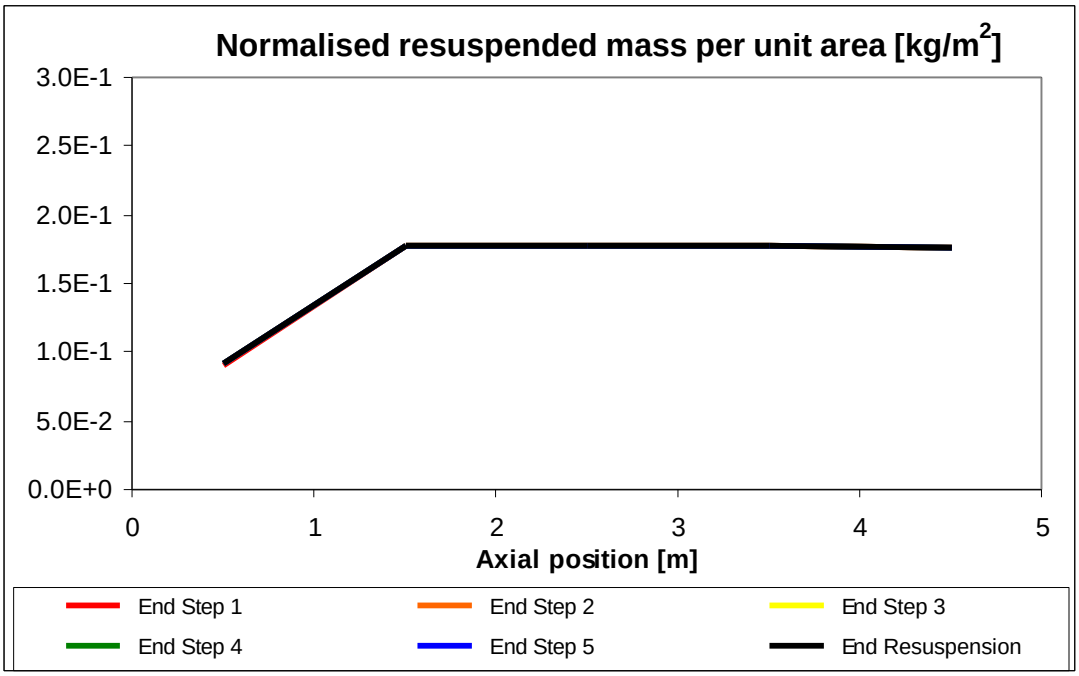

Fig. 115 - Spatial distribution of resuspension (KINS)

The results submitted by KINS show a decreasing mean particle size for successive velocity steps (Fig. 116). The geometric standard deviation decreases initially and then increases for the final steps. However, the quantity of aerosols being resuspended in all except the first velocity step is so small that associating a log-normal distribution to the resuspended particles is not very meaningful.

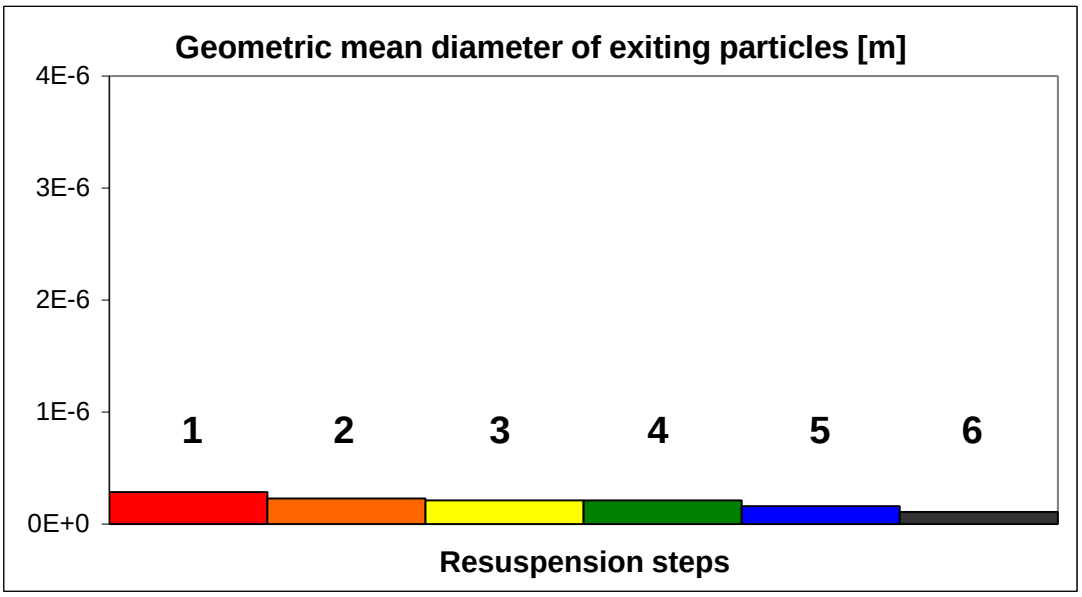

Fig. 116 - Mean particle size at the outlet of the test pipe (KINS)

5.6.3. VEIKI

The calculation submitted by VEIKI was performed with version 92 of Victoria, without any specific changes for this problem [40].

5.6.3.1. ISP calculation

The calculation was run in an IBM Risc 6000 workstation and took just under 4.5 hours to run the resuspension phase, which is about 3200 times more than the reference *linpackd* code.

The test pipe was divided into twelve identical control volumes and the time step used in the resuspension phase was 0.05 seconds.

The aerosol size distribution was discretised into 12 bins.

Since gaseous nitrogen is not included in the Victoria database, the carrier gas was simulated with a mixture of oxygen and helium calculated to get the same density.

A joint deposition-resuspension calculation had to be done, since it is not possible to start from a defined deposit and run only the resuspension phase. The wall temperature was changed in the deposition phase, in order to obtain the correct initial conditions for deposition.

The initial conditions and the results obtained for the resuspension calculations are summarised in Tab. 16 and Fig. 117. The resuspension rate in Victoria is a function of the carrier gas velocity and of the mass deposited. Since for each successive velocity step the carrier gas velocity increases but the deposited mass decreases, the effective resuspension rates oscillate and do not show a clear trend (Fig. 118). Resuspension is stronger in the first step (because of the large deposited mass) and in the last step (because of the high carrier gas velocity) and is weaker in the intermediate steps.

Tab. 16 - Summary of results for resuspension phase (VEIKI)

Step	Mass remaining (g)	Particles exiting the test pipe	
		Geometric mean diameter (μm)	Geometric standard deviation
Start	173		
1	59	0.20	1.64
2	44	0.11	1.61
3	26	0.09	1.85
4	13	0.09	1.66
5	6	0.09	1.48
6	3	0.09	1.50

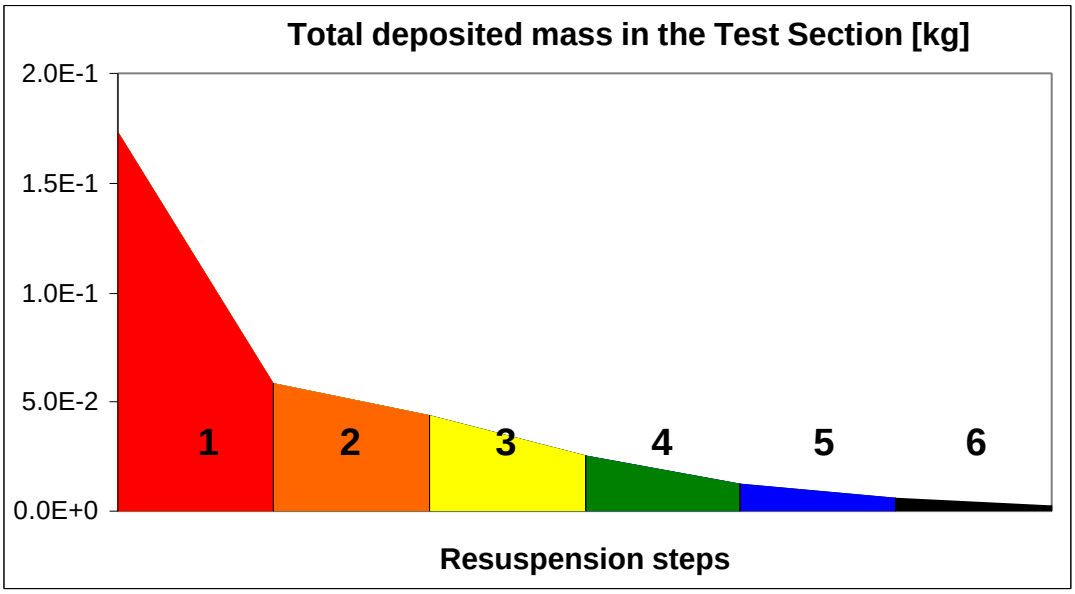

Fig. 117 - Mass remaining in the test pipe (VEIKI)

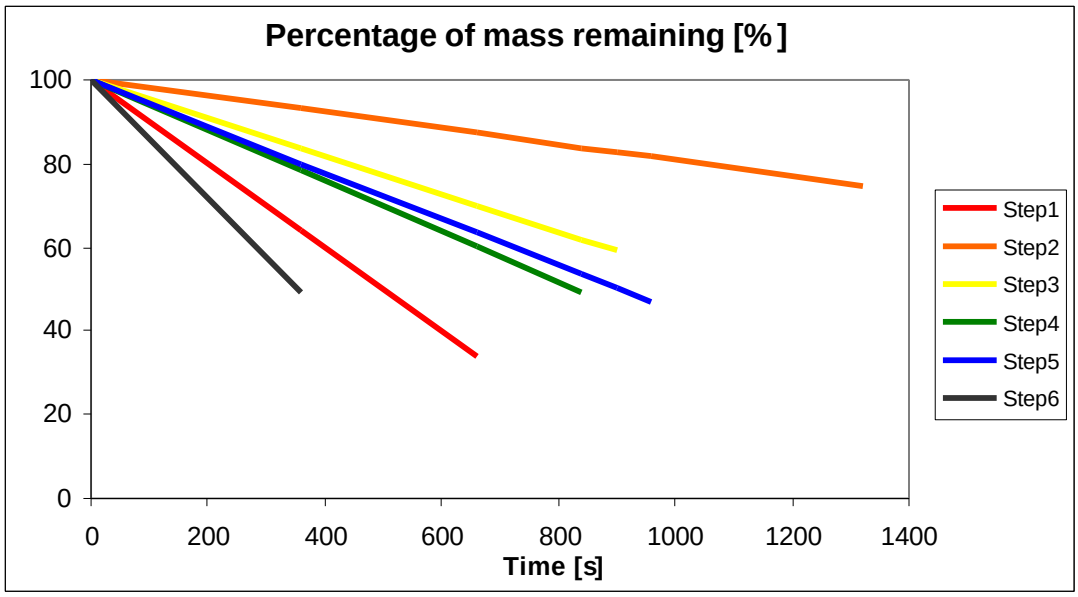

Fig. 118 - Resuspension rate in each velocity step (VEIKI)

The spatial distribution of resuspension follows closely the spatial distribution of deposition calculated by VEIKI in the deposition exercise, with one exception (Fig. 119). In the deposition calculations VEIKI predicted much less deposition by inertial effects - eddy impaction and gravitational settling - in the first computational cell than in the others. Consequently, the particles deposited in the first cell are smaller than those deposited elsewhere in the test pipe and hence less prone to resuspension at low gas velocities. At higher gas velocities the largest particles have already been removed and the characteristics of the deposit are more uniform along the test pipe.

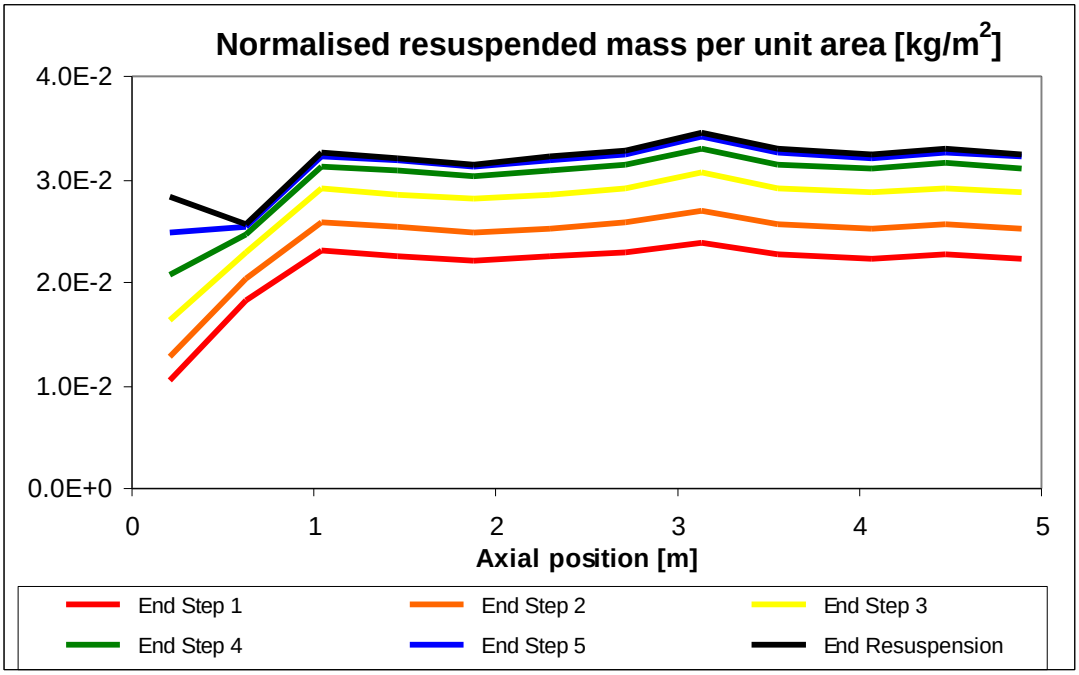

Fig. 119 - Spatial distribution of resuspension (VEIKI)

As for the deposition exercise, the initial mean particle size used by VEIKI is given as two times larger than the specified size for the deposition phase. Even so, the resuspended particles are calculated to be extremely small, with the geometric mean diameter decreasing as the carrier gas velocity increases (Fig. 120).

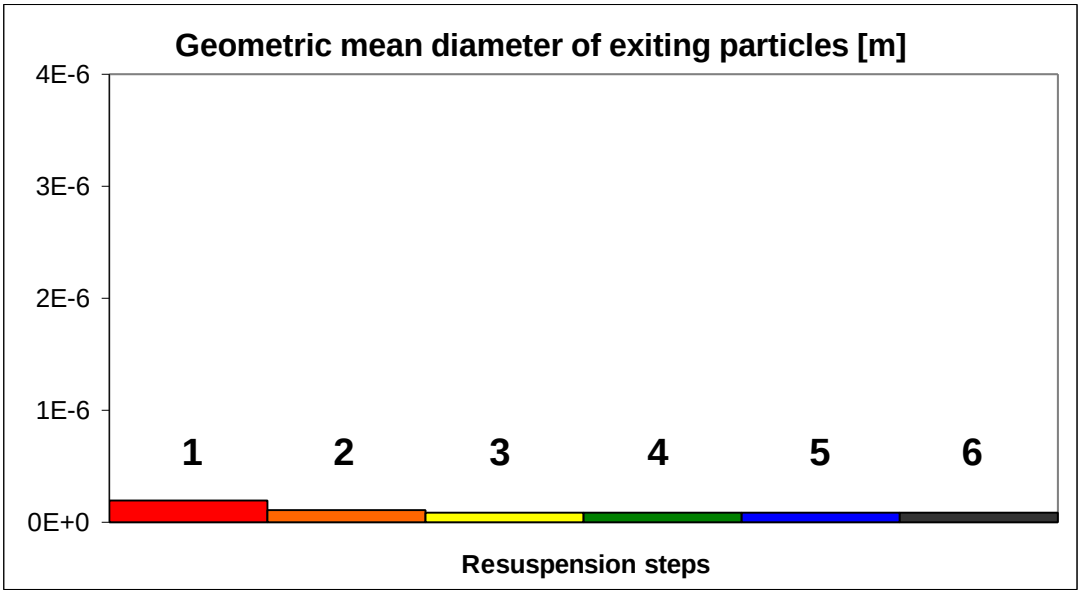

Fig. 120 - Mean particle size at the outlet of the test pipe (VEIKI)

5.7. Comparison

5.7.1. Computer codes used

Ten different submissions were received from eleven different organisations - two of the submissions were from work groups representing more than one organisation - and in two cases additional sensitivity analysis was also done to evaluate the importance of the initial particle size considered in the resuspension calculation.

Six computer codes were used, with one or two submissions per code. In terms of models used, this variety is reduced to four different models, since the version of Art that was used had its original resuspension model replaced with the one in Victoria, and Ecart and Sophaeros use what is basically the same resuspension model.

The resuspension model in Victoria and the modified Paress model used in the Art calculation use a time decaying law in which the parameters were calculated to fit the Paress experiments. The model in Ecart and Sophaeros calculates a balance of forces acting on a particle and, for the size bins for which the aerodynamic forces exceed the adhesive forces, calculates a resuspension rate with an equation also derived from fitting to experimental measurements (ORNL, ART, Paress and Winfrith). Although also using an equation for probability of resuspension obtained by fitting the Paress results, the model under development at ETH introduces the bed porosity as an additional factor conditioning the resuspension rates, to account for resuspension from multi-layer deposits. Finally, the Cæsar model, which at this phase is strictly a mono-layer resuspension model, uses particle tracking in the laminar sub-layer of the turbulent boundary layer to follow the movement of each single particle in the vicinity

of the pipe wall, until it detaches from the wall or, if it remains "on the wall", for a specified time.

One major problem that most participants faced was the impossibility of specifying a given initial deposit and solving only the resuspension phase. This forced them to run a deposition phase to generate the adequate initial conditions, and happened with all codes except Cæsar. This difficulty seems to have been under-estimated by most participants who had to spend a considerable amount of time fine-tuning the deposition calculations to obtain what they thought was a reasonable initial state. Even though most participants dedicated a large effort to this fine-tuning, the results obtained were not very satisfactory in terms of particle size distribution, always yielding particles considerably smaller than those observed in the experiment. And, as the sensitivity analysis performed by two of the participants shows, the particle dimension is an important parameter in the determination of the aerosol resuspension.

The way in which the models treat the particle size distribution is also considerably different. While in the case of Cæsar the initial particle size distribution in the deposit is specified by the user, with the inherent difficulty of guessing the correct distribution, the ETH model calculates the particle size by allowing the release of either individual particles, which retain the dimension they had when deposited, or agglomerates, which can be much larger. The Ecart model memorises the dimension of the deposited particles and assumes that there is no agglomeration or fragmentation in the deposit. Finally, the Victoria model is a bit over-simplistic, assuming that the size distribution of the resuspended aerosols is identical to the size distribution of the gasborne particles that reside in each computational cell at the time of resuspension.

5.7.2. Computational effort

The majority of the ISP participants used Unix workstations to perform their calculations. The exceptions were the ETH calculation, which was run on a personal computer, and the CIEMAT-JRC-CSN and JRC-CSN calculations, which were run on a Cray.

The comparison of run times was done for the resuspension calculations only. In the case of JAERI, however, only the total time was given, without distinction between the deposition and the resuspension phases. For the ETH calculation, the time given is the sum of the time used to calculate resuspension and the time used to do the topological analysis of the deposit - definition of the "resuspendable" agglomerates. However, if additional calculations are needed for the same deposit, this topological analysis is not repeated and the resuspension calculation takes only a fraction (3%) of the time indicated.

The calculations performed with Sophaeros were clearly faster than all others, calculating the whole resuspension exercise in less than 2 minutes against the times in the order of hours or days needed by the other codes. While the resuspension model in Sophaeros and the one in Ecart are similar, the fact that mostly implicit solutions are used for the transport equations avoids the need to use very small time steps and drastically reduces the CPU time needed for the calculation. This is particularly true for this resuspension problem, in which the high velocities of the carrier gas imposes strict limitations to the explicit calculations.

The different run times needed by Victoria (6 times more in the calculation by KINS than in the one by VEIKI), while due in part to the faster computer used by VEIKI,

remains difficult to explain. The main difference between the two calculations is in the way the nitrogen flow was simulated - argon/helium in the KINS calculation and oxygen/helium for VEIKI. This led not only to significantly different CPU times but also to different results for the two calculations, as discussed in the next section.

Tab. 17 - Computational effort (resuspension exercise)

Organisation	Code	Computer	linpackd (s)	ISP-40
CEA/IPSN/DRS	Sophaeros	Sun Sparc 10	8.0	109 sec
CIEMAT-JRC-CSN	Cæsar	Cray	4.08	50 days
ETH	ETH	Intel Pentium 200	3.24	4.6 hrs
ENEL	Ecart	IBM 486	14.44	
GRS	Sophaeros	IBM workstation	0.6	110 sec
JAERI	Art	AS7000	3.0	60 hrs
KINS	Victoria	Sun Center 2000	7.0	29 hrs
Univ. Pisa	Ecart	IBM Risc 6000/250	1.672	4.6 hrs
VEIKI	Victoria	IBM Risc 6000	5.0	4.5 hrs
JRC-CSN	Cæsar	Cray	4.08	59 hrs

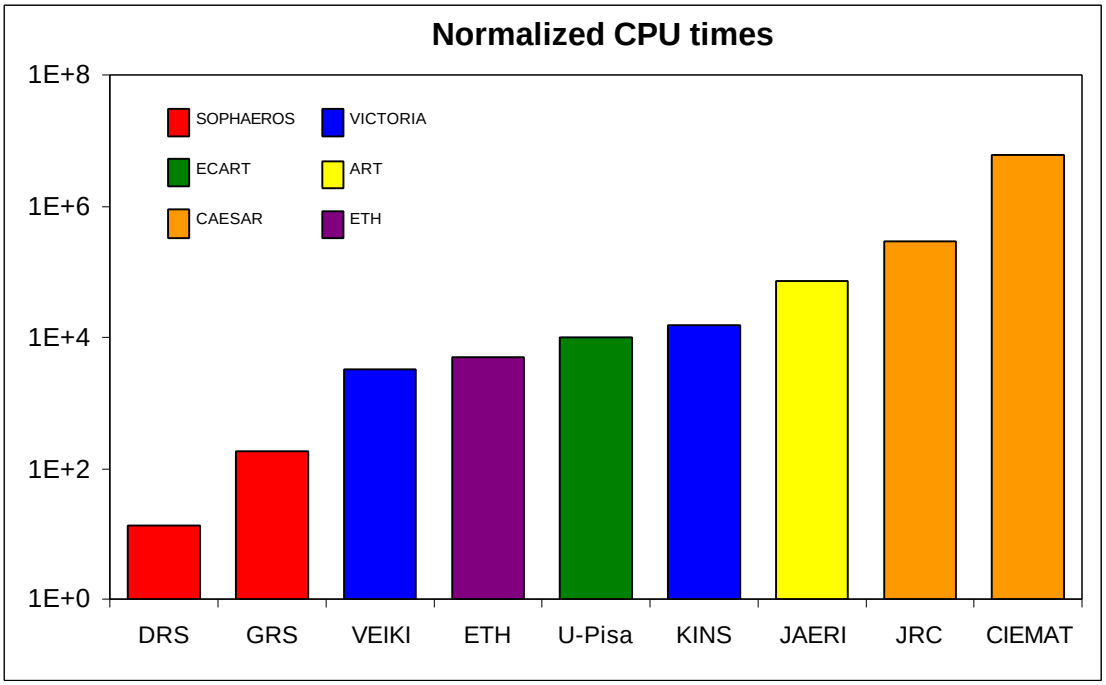

Fig. 121 - Normalised CPU times (resuspension exercise)

5.7.3. Aerosol resuspension

The difficulty faced by most participants in establishing the initial conditions for the resuspension calculations led to late submissions in several cases and, more important, severely limited the time available for analysis and interpretation of the results obtained by each participant. The comments submitted with each calculation were in most cases very brief, without an attempt to explain the results obtained, and, in some cases, missing completely. Any analysis of the results obtained is therefore conditioned by the lack of information about some of the calculations.

The results presented in Fig. 122 are normalised for the initial deposited mass. For the calculations which used an initial deposited mass different from the one specified, the mass remaining after each step was multiplied by a normalising factor.

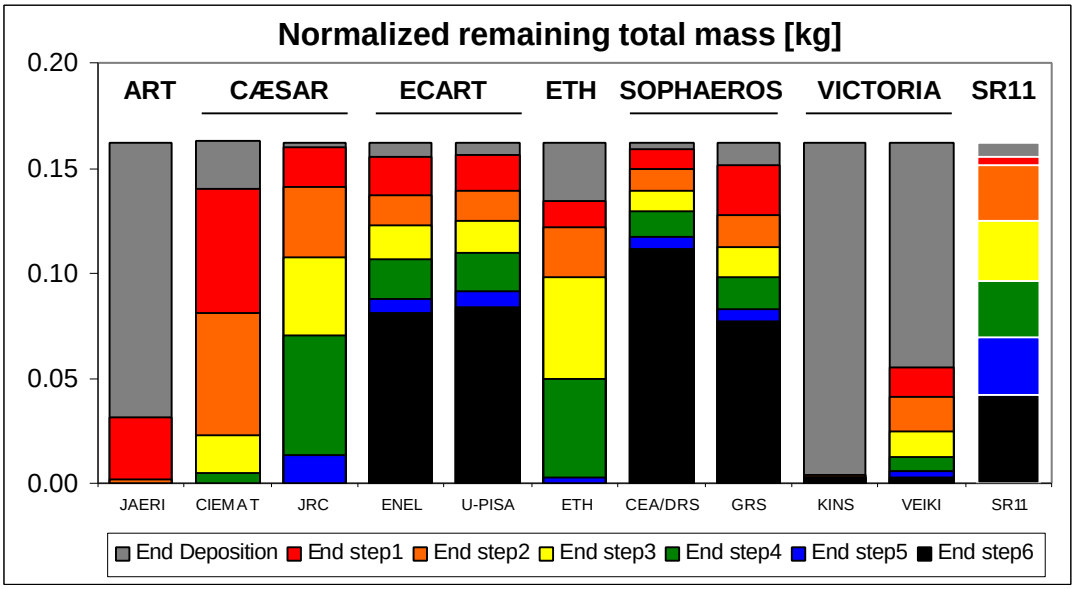

Fig. 122 - Aerosol mass remaining in the deposit

The results submitted can be separated into three groups. The Ecart and Sophaeros calculations, which predict a slow resuspension that leaves a significant mass in the deposit at the end of the 6th velocity step in the test; the Victoria and Art calculations which predict very fast and practically complete resuspension, though slightly slower in the VEIKI calculation; and the Cæsar and ETH calculations which predict slower deposition - more similar to the Ecart and Sophaeros predictions - in the first velocity steps, but increasing gradually towards the end and finally leading to almost complete resuspension in the 6th step.

There are important differences between the CIEMAT-JRC-CSN and the JRC-CSN calculations, both done with Cæsar. In addition to the different number of particles tracked, in the JRC-CSN calculations the tracking started, in each step, with the largest particles, progressing down towards the smallest ones. When a large enough number of particles had not resuspended, the calculation was stopped and it was assumed that any particles smaller than that would not resuspend either. In the CIEMAT-JRC-CSN calculation, the particle tracking was done for the whole range of particle sizes, leading to higher resuspension and to a distribution of resuspended particle sizes characterised by a smaller mean and a larger deviation due to the

presence of not only the large particles calculated by JRC-CSN but also some smaller particles.

Since in the experiment practically all the resuspension observed in each velocity step occurred in the first few minutes of the step, each step can practically be seen as an independent resuspension test with different carrier gas velocity. The results can then be compared by calculating the percentage of the deposited mass at the beginning of the step that is resuspended during that step (Fig. 123). While the same three groups are still identifiable, there are important differences in the way the Victoria and Art codes were run that lead to a significantly different behaviour, even if the end result is similar. The deposited mass is calculated by Victoria - and by the modified version of Art used by JAERI - to decay exponentially with time. The initial time used in the calculations is therefore significant in terms of the results obtained. In Victoria, the initial time is the time in the calculation when the 2,300 limit for the Reynolds number is exceeded for the first time. In the KINS calculation, the sequence of velocity steps was calculated sequentially, and the reference time was always the beginning of the first velocity step, when the Reynolds number of the flow first exceeded 2,300. The small mass remaining in the tube after the first velocity step suffered very little resuspension in the following steps, even if the carrier gas velocity was much higher, because the time-dependent exponential in the equation became extremely small. In the other two calculations, by JAERI and VEIKI, the reference time was moved to the beginning of each velocity step. Since JAERI predicted much higher deposition than VEIKI, the mass resuspended in each step was calculated to be almost 100% of the initial mass for that step. In the VEIKI calculation, the percentage of mass resuspended first decreases sharply from the first to the second velocity steps, due to the strong reduction of the deposited mass, and then increases with the increased carrier gas velocity, since the variation of deposited mass was small.

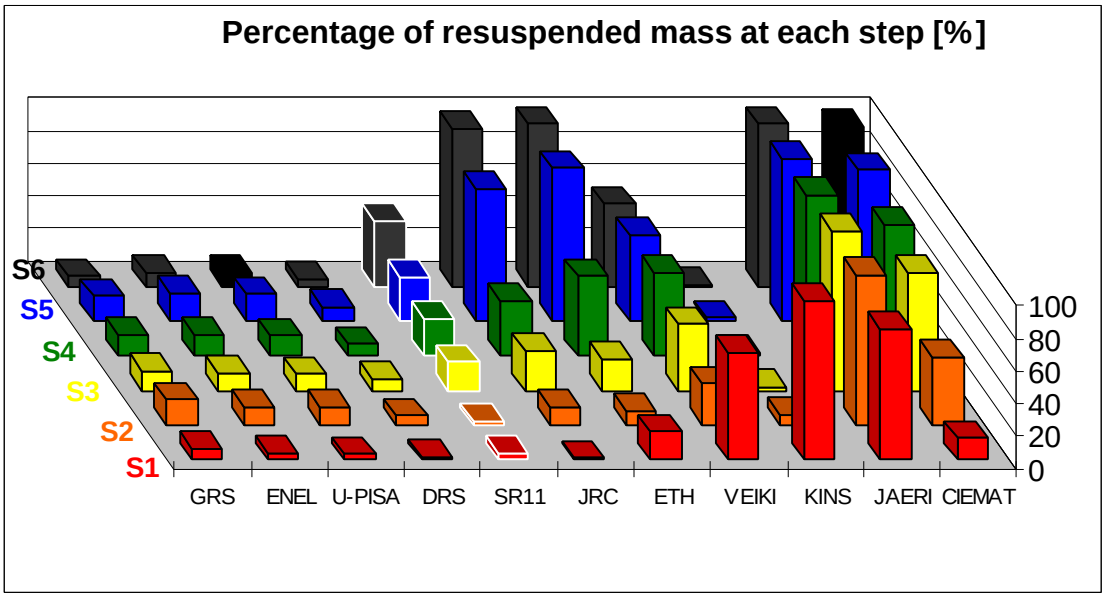

Fig. 123 - Resuspension in each velocity step

In the experimental results resuspension is very small in the first two steps and then increases for increasing carrier gas velocities. There is a small decrease from the first to the second step, but this is likely to be the result of resuspension of a small quantity

of loose material at the top of the deposit layer, which would probably have resuspended even at lower velocities.

A comparison of the calculated results with the experimental measurements shows that both Victoria and Art severely over-predicted resuspension mainly at the lower carrier gas velocities for which very little resuspension was observed in the experiment.

The small resuspension in the first step is well estimated by Ecart and Sophaeros which over-estimate slightly resuspension in the second step and then under-estimate it in all successive steps. There seems to be a threshold velocity for the initiation of resuspension which is lower than observed in the experiment, while the resuspension rates at high gas velocities are under-estimated. The results obtained with both Ecart and Sophaeros, however, depend on the duration of each velocity step. Since the resuspension rate is independent of time and relatively low, the resuspended mass is approximately proportional to the duration of the step. This effect is clear in the calculated resuspension for the last step, which was shorter than the previous ones and, to a certain extent, in the resuspension calculated for the second step, which was the longest. As mentioned before, in the experiment resuspension occurred in the first few minutes or even seconds of each step and was independent of the duration of the step.

While the ETH calculation over-estimates resuspension in the first velocity step, the calculated resuspension in the following steps shows a behaviour that is similar to the one calculated with Cæsar. Both codes over-predict resuspension slightly in the second, third and fourth steps and then more significantly in the last two steps, at higher carrier gas velocities.

In conclusion, while the Ecart and Sophaeros calculations obtain a better agreement with the final state of the test pipe after the six velocity steps, the calculations done with Cæsar (mainly the one by JRC-CSN) and the ETH code reproduce better the behaviour of the system in the first steps, diverging only for the higher velocities.

5.7.4. Particles exiting the test pipe

The aforementioned problems with the imposition of the adequate initial conditions for the resuspension calculation led most participants to concentrate their efforts in reproducing correctly the initial deposited mass, neglecting in some way, given the limited time available, the particle size distribution of the deposited particles. The exceptions were the CIEMAT-JRC-CSN and JRC-CSN submissions, in which the initial size distribution was imposed, and the CEA/IPSN/DRS calculation, in which an effort was done to obtain a reasonably good agreement with the particle size distribution at the outlet, even if that meant sacrificing the accuracy in terms of initial mass. The conditions used were considered the best possible compromise.

All the other calculations used particles that were considerably smaller than the ones observed in the experiment and that led to predictions of also much smaller particles at the outlet of the test pipe (Fig. 124). In the calculation by the JRC-CSN, the almost linear dependence observed between the minimum resuspendable aerosol and the carrier gas velocity, and also the sharp distinction between the particles that resuspend and those that do not lead to a very sharp decrease of the mean size of the resuspended particles when the carrier gas velocity increases.

A decrease of the particle sizes at the outlet with increasing gas velocity is also predicted by CEA/IPSN/DRS and, to a lesser extent, by all other participants, with the notable exception of JAERI, that predicts the opposite trend. Although this decreasing trend agrees in general with the measurements, it is not as clear in the experiment as in the CEA/IPSN/DRS calculations, and certainly not as clear as in the JRC-CSN calculations.

One final word about the particle sizes calculated in Victoria. In the released version of Victoria the size distribution of the resuspended particles is assumed to be the same as the size distribution of any gasborne particles residing in the same control volume at the time of resuspension. This imposes the inclusion of a negligible aerosol inlet rate even during the resuspension calculation, with a particle size distribution that actually defines the distribution of the resuspended particles. Since the organisations that used Victoria to calculate the resuspension exercise do not mention any specific changes to the code but also do not make any mention of the imposed aerosol flow at the inlet, it is not clear how the calculations were done and also why the particle size distribution at the outlet does not reflect exactly the supplied one, since in practice it could be imposed.

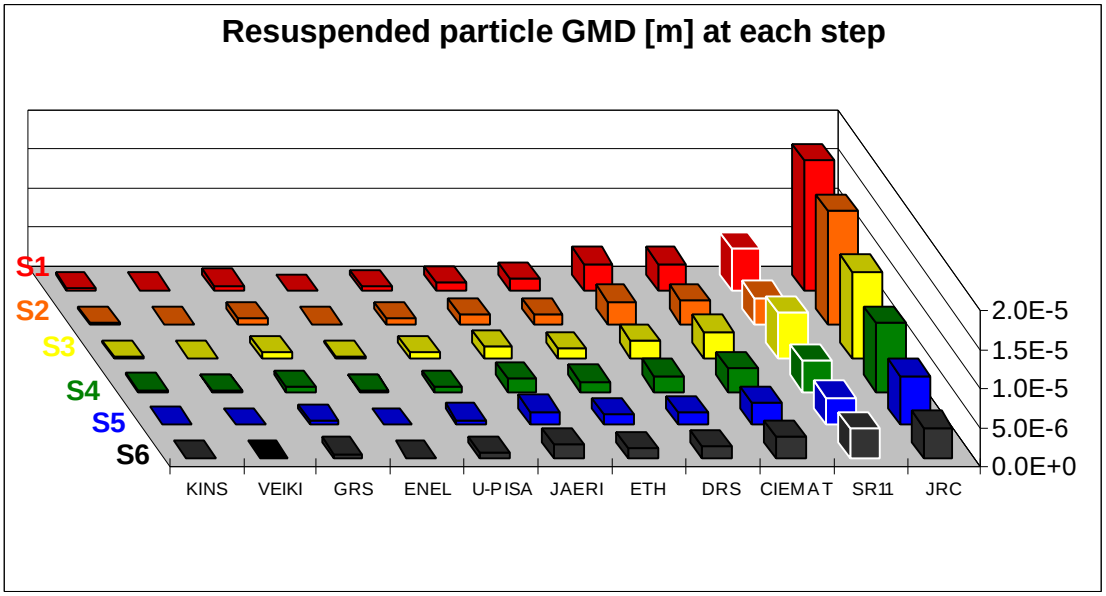

Fig. 124 - Geometric mean diameter of the particles at the outlet of the test pipe

6. Open calculations - Resuspension

6.1. Introduction

In the second ISP-40 workshop the participants were informed that an error in the specified geometric mean diameters of the resuspended particles had been detected and that the actual values should be one half of those specified.

This correction of the experimental data had limited consequences on the calculations performed due to the fact that the actual particle size distribution of the deposited particles is not known, and most of the submitted results were calculated without taking into account the particle size distribution of the resuspended aerosols (see the section on the ISP-40 calculations of resuspension). Consequently, only one of the participants submitted new results calculated using the corrected mean particle sizes.

This section is divided into two sub-sections, describing:

- new calculations using the corrected geometric mean diameter of the resuspended particles
- new sensitivity analysis on different parameters or initial conditions

6.2. New calculations with correct particle sizes

6.2.1. JAERI

The new calculation using the corrected geometric mean diameters was performed with Art mod. 2 [26], using the same nodalisation and time step as in the previous blind calculation.

As in the previous blind calculation, the experimentally measured distribution of particle sizes at the outlet of the test pipe (resuspended particles) was used, due to the lack of any better information, to characterise the size distribution of the deposited particles. The reduction by a factor of two of the geometric mean diameters in each of the six velocity steps consequently led to a reduction of the calculated mean particle sizes at the outlet of the test section.

The effect of the smaller particles on the amount of aerosols resuspended from the test section, however, is almost negligible (Fig. 125). A large fraction of the deposited aerosols are still resuspended in the first step (83% instead of 81% in the previous calculation) and only a very small fraction remains deposited after the second velocity step (1% in the revised calculation against 1.4% in the previous one).

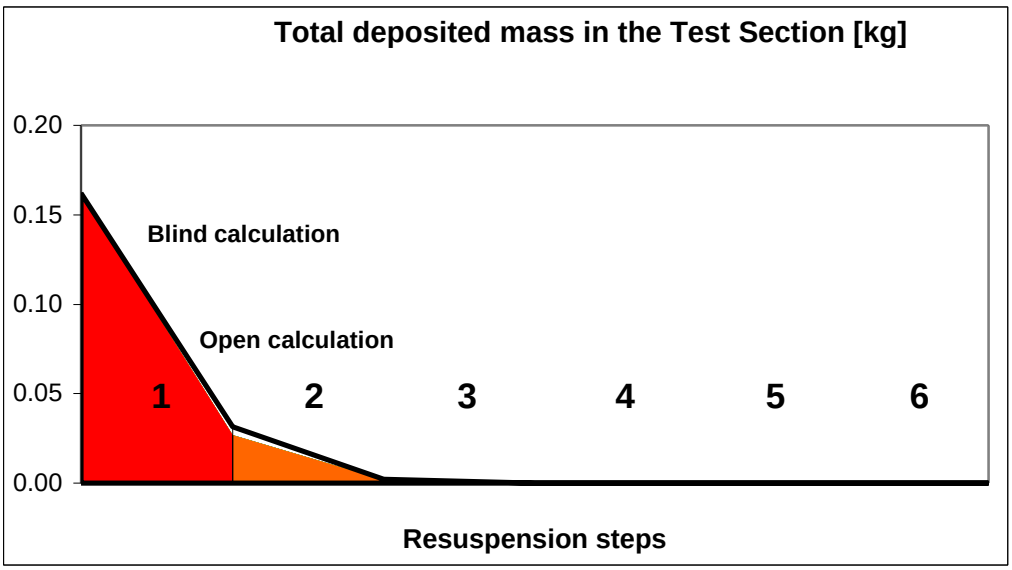

Fig. 125 - Mass remaining in the test pipe (JAERI)

Both the time dependence of the resuspension and its spatial distribution remain practically unchanged.

6.2.2. KINS

The new calculation using the corrected size distribution was performed with Victoria 92-01 [34], using the same nodalisation and time step as in the previous blind calculation.

As in the previous blind calculation, the experimentally measured distribution of particle sizes at the outlet of the test pipe (resuspended particles) was used, due to the lack of any better information, to characterise the size distribution of the deposited particles. The reduction by a factor of two of the geometric mean diameters in each of the six velocity steps consequently led to a reduction of the calculated mean particle sizes at the outlet of the test section.

This difference in particle sizes has no consequences in the amount of resuspension predicted by the code. While in the previous blind calculation 97.8% of the deposit was resuspended in the first velocity step, with very little resuspension afterwards, that amount is slightly smaller in the new calculation (95.8%). The calculation was re-started at the beginning of each time step, resetting the resuspension time to zero. This led to an increase of the resuspension in the latter velocity steps and complete resuspension is reached in the 5^{th} step, while in the blind calculation almost 2% of the initial mass remained in the deposit at the end of the test (Fig. 126).

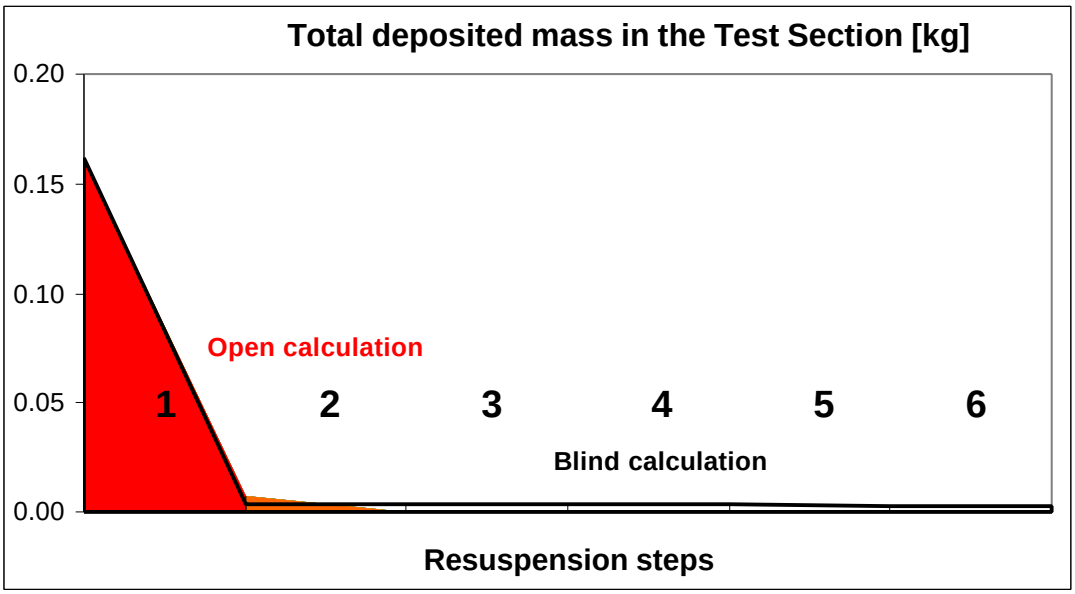

Fig. 126 - Mass remaining in the test pipe (KINS)

6.3. New sensitivity calculations

6.3.1. CSN-CIEMAT-JRC

A joint submission by CIEMAT, the CSN and the JRC studied the effect of the surface roughness of the pipe walls on the amount of resuspension calculated with Cæsar [30].

The original algorithm for generation of the single particle diameters from a given statistical distribution was replaced with a more correct one, and the correct geometric mean diameters of the resuspended materials were used. As in the two separate calculations submitted originally for this International Standard Problem, two separate sets of calculations were performed. The first calculation was done starting from the experimental particle size distribution in the first velocity step and allowing it to evolve for the next steps (identified as CSN in Fig. 127) while in the other (identified as CIEMAT) the experimental size distribution was imposed at the beginning of each velocity step.

The results obtained show a strong dependence on the value of the surface roughness used in the calculations, with a value of 1 μm leading to a much better agreement with the experimental results. Additionally, the results also highlight the importance of the particle size used in the calculations. Comparing the CIEMAT curves with the CSN ones, for either value of the surface roughness, the percentage of mass remaining in the deposit becomes considerably different mainly from the 3rd velocity step onwards. This is due to the fact that in the CSN calculation the larger particles have already been resuspended in the first velocity steps and the mean particle size becomes lower than the one used in the CIEMAT calculation.

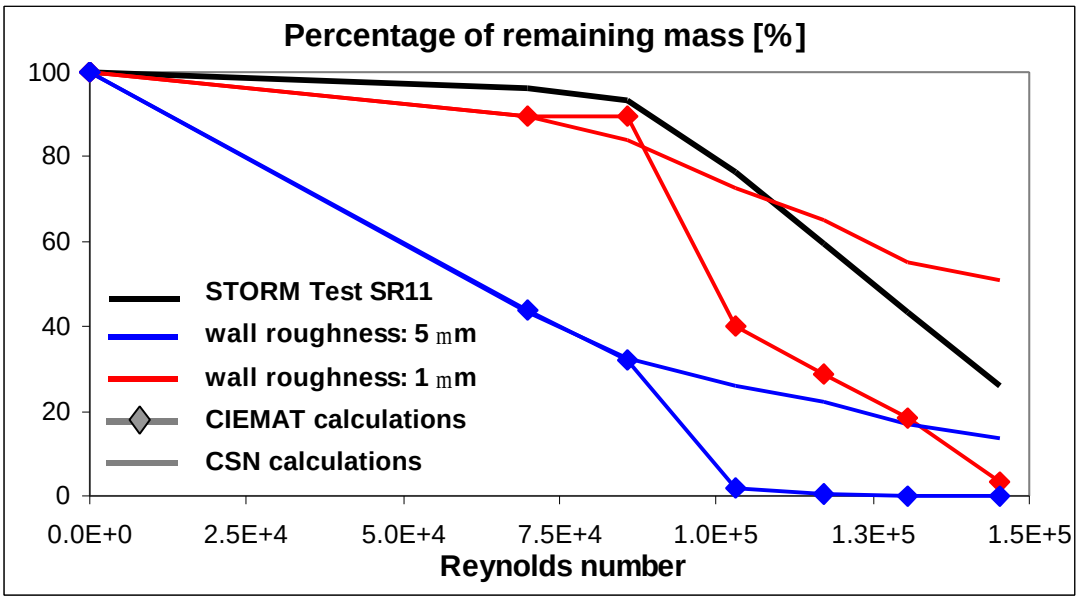

Fig. 127 - Sensitivity to wall surface roughness (CSN- CIEMAT-JRC)

6.3.2. GRS

As described for the blind calculation performed for ISP-40 by GRS, it is not possible with Sophaeros to specify an initial deposit and calculate only the resuspension phase. Therefore, having re-calculated the deposition phase to take into account the correction of the steam flow rate and, consequently, of the thermal-hydraulic conditions, GRS extended the new calculations to cover also the resuspension phase of the exercise [64].

The time step, nodalisation and discretisation of the particle size distribution were the same used previously for the blind calculations.

Two different calculations were run, the first allowing for particle re-deposition without restriction, the second with deposition inhibition due to a particle size dependent force criterion. Although the total amount of resuspension increased, in both cases, relatively to the previous blind calculation, the results are qualitatively similar (Fig. 128), with a very slight over-prediction of resuspension in the first velocity steps, stronger over-prediction in the third step, and under-prediction for the higher carrier gas velocities. Although the agreement with the final retained aerosol mass is very good, the resuspension rate remains practically constant in each velocity step, which differs considerably from the experimental results.

The sensitivity calculations described for the open deposition calculations performed by GRS were also extended to the resuspension phase. The conclusion drawn for the deposition calculation that the value of the adhesion coefficient did not affect the results of the calculation as long as it stayed below 10^{-6} N/m is also valid for the resuspension calculations.

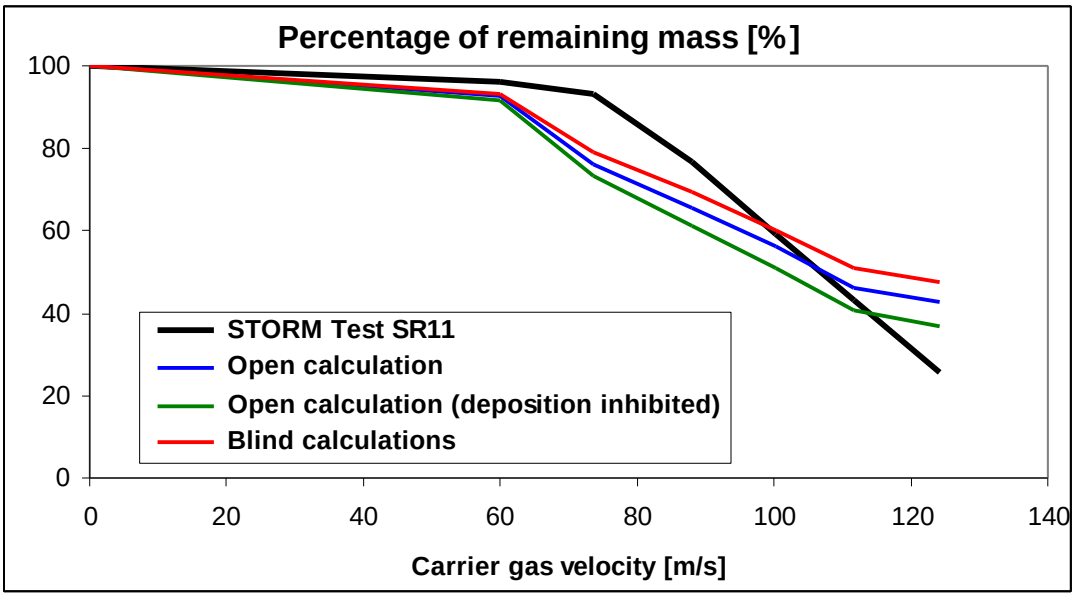

Fig. 128 - Percentage of mass remaining in the deposit (GRS)

Concerning the surface roughness, however, and due to the considerably higher velocity of the carrier gas during the six steps of the resuspension phase, the effect on the resuspension rates is significant, and a variation of the surface roughness from 10 µm to 1 mm leads to an increase of resuspension by about 90%.

6.3.3. University of Pisa

As mentioned in the description of the blind ISP-40 calculations, it is not possible in Ecart to specify an initial deposit and calculate only the resuspension phase of the exercise. A considerable effort was dedicated to finding an acceptable initial condition by running the deposition phase with different parameters. The blind calculations submitted by the University of Pisa were based on a deposition calculation in which the collisional shape factor had been modified from the default value of 1.0 to 2.2 [55].

When an error was detected in the experimental value of the steam flow rate and consequently in the supplied thermal-hydraulic conditions, the University of Pisa revised the previous deposition calculation and concluded that, to obtain a good agreement with the experimental value for total deposition in the test section, the increase in the collisional shape factor needed was actually much lower. The full deposition + resuspension calculation was therefore repeated using a collisional shape factor of 1.23. Additionally, one other calculation was run with the correct thermal-hydraulic conditions during the deposition phase but using the default value (1.0) of the collisional shape factor.

The results obtained for the new calculations are shown, together with the result of the original blind calculation and the experimental data, in Fig. 129. The calculation referenced as "open calculation 1" is the one with the default value of the collisional shape factor, while "open calculation 2" is the calculation with this value increased to 1.23.

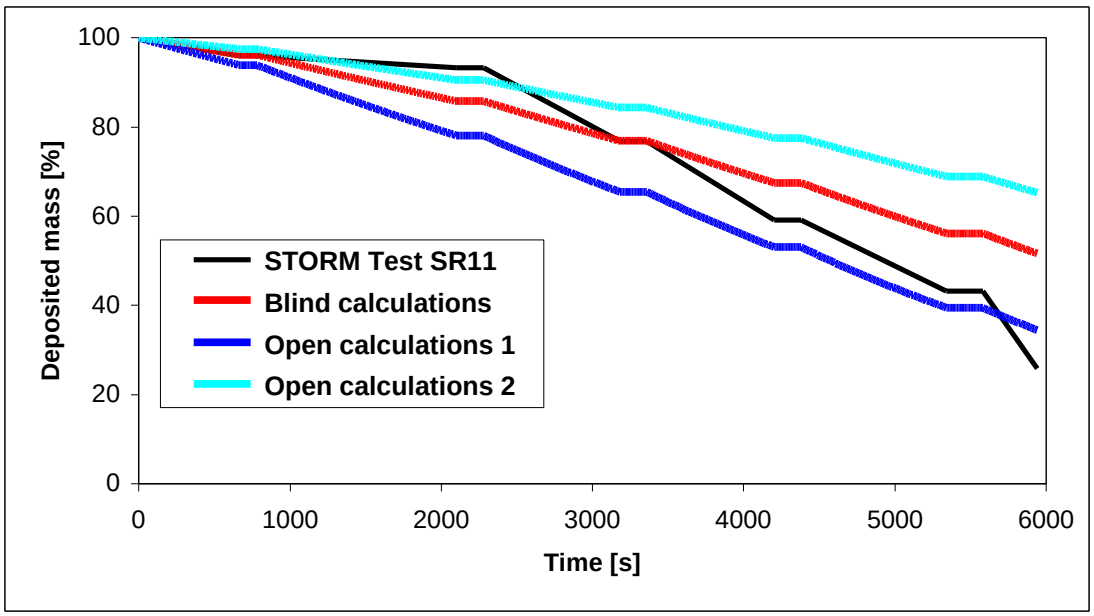

Fig. 129 - Percentage of mass remaining in the deposit (U. Pisa)

As for the previous calculations, it should be noted that the actual resuspension rate in the experiment decays very quickly after the first seconds in each velocity step. In the Ecart calculation, the resuspension rate is practically constant for the whole duration of each step. Having said that, the results obtained show that, while the agreement with the total amount of resuspension in the whole experiment is better for the case with the default value of the collisional shape factor, this is due to an over-estimation of resuspension in the lower-velocity steps and an under-estimation at higher carrier gas velocity. The calculation that used the value of 1.23 for the collisional shape factor shows a better agreement at lower velocities, while severely under-predicting resuspension at the higher velocities.

6.3.4. VEIKI

During the second ISP-40 workshop, the question of numerical convergence of the results obtained with Victoria had been raised, in relation with the fact that several of the participants - using different codes - had violated the Courant limits normally accepted in their submitted calculations, and in some cases had performed sensitivity analysis on the time steps used that showed this violation to have no effect on the results.

The new calculations performed by VEIKI [39] had the objective of evaluating the effect on the results of modifying the time step used in the Victoria resuspension calculations. While the Courant limit for the first velocity step of the resuspension phase and for the nodalisation used in the calculation (12 identical computational cells) is just above 0.007 seconds, the range of time steps used varied from 0.0001 seconds to 1 second. The calculations were run for only the first 10 seconds of the first velocity step, and the remaining masses in the deposit at the end of these 10 seconds were compared. The surprising results show a sharp increase of the resuspended mass for a decreasing time step (Fig. 130).

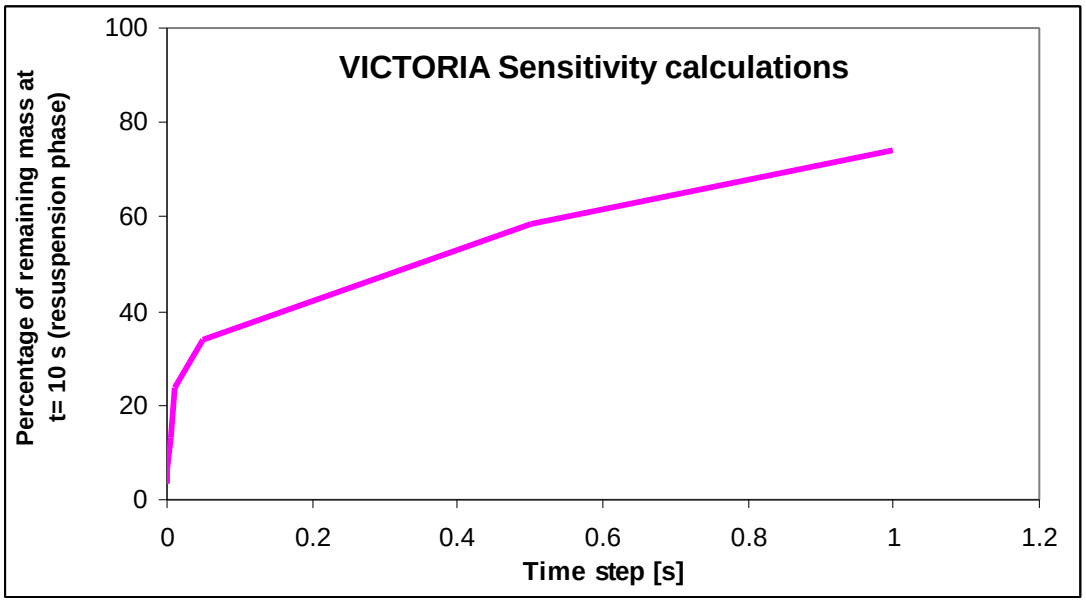

Fig. 130 - Dependence of resuspended mass on the time step (VEIKI)

From the description of the resuspension model in Victoria, this seems to be caused by an incorrect implementation of the model. Apparently, the instantaneous resuspension rate at the end of each time step, which decreases sharply with time, is being used to calculate the fraction of aerosols resuspended during that time step. Hence, for the same flow conditions, and since the resuspension rate decreases monotonically with time, the fraction of mass resuspended in the first time step is much higher for a small time step than for a large one.

6.4. Conclusions

Given the impossibility, with most codes, of specifying the initial size distribution of the deposited particles, the error committed in the specification of the geometric mean diameters did not have any significant effects on the results obtained in this International Standard Problem.

The sensitivity analysis performed by CSN-CIEMAT-JRC, GRS and the University of Pisa stressed even more the importance of a correct characterisation of the effective roughness of the pipe walls and of the particles present in the deposit. This is related not only to the chemical and physical properties of the deposited aerosols, but also to the mechanisms by which they deposited and, probably, to the history of the deposit in terms, for instance, of temperature variations between deposition and resuspension. For multi-layer deposits, the characterisation of the deposit poses major problems, since it is practically impossible to determine, in a visual examination of a deposit sample on a microscope, the limits of each agglomerate.

Finally, the new calculations by VEIKI identified a problem with the resuspension model in Victoria that deserves attention from the code developers.

7. Conclusions and recommendations

The main objective of any International Standard Problem has to be a contribution towards the improvement of the computer codes used in safety calculations of nuclear reactors. More than a demonstration of the capabilities of each code, it should assist in the identification of weak points in the modelling, and suggesting ways to improve it.

The quality of the computer models used is of fundamental importance in nuclear safety, since it is impossible to analyse experimentally all possible conditions found in a reactor and the safety assessment of nuclear power plants has to be based on the use of codes. This ISP, however, cannot be seen separately from all other activities of code development and validation, but only as an additional contribution to that work.

The International Standard Problem no. 40, being based on a STORM experiment on aerosol deposition and resuspension, had two clearly different parts for which different conclusions can be reached. While aerosol deposition models have gone through a long period of development and were expected to perform reasonably well under any conditions, resuspension models are a recent development in nuclear safety codes, but also in aerosol transport codes in general. They could, therefore, be expected to have much more difficulty in reproducing the experimental behaviour. At the same time, this is also the area in which more progress is expected.

Concerning the deposition phase of the exercise, the major differences relative to previous exercises concern, on one hand, the appearance of particle tracking codes, and on the other, the inclusion of resuspension models in the calculation of aerosol deposition. A few conclusions can be drawn from this exercise and from the discussion that followed the analysis:

Modelling of thermophoretic deposition is adequate. The Talbot equation [75] is used in the codes developed more recently and has been verified in a large number of separate effects experiments. In the STORM test SR11 all participants agreed that thermophoresis was by far the dominant deposition mechanism and there was acceptable agreement between the code predictions and the experimental results.

There are problems with the modelling of deposition due to turbulent flows. Although there is some consensus on the use of the Liu-Agarwal correlation [42] for calculating deposition due to eddy impaction and of the Davies equation [7] to calculate diffusion in turbulent flows, Melcor, due to the fact that it is based on the Maeros aerosol package, which was developed for containment aerosols, does not include a model for eddy impaction. It is, however, used in circuit (or full-plant) calculations, in some situations in which eddy impaction might play a significant role.

Aerosol deposition and resuspension need to be treated together. The conditions that favour turbulent deposition also favour resuspension, and there is physical evidence of resuspension and particle rebound during the deposition phase of the STORM tests.

Aerosol retention depends strongly on the thermal-hydraulic conditions. Even with perfectly accurate models for aerosol physics, a good prediction of the aerosol retention in the reactor coolant system depends on a correct characterisation of the thermal-hydraulic conditions.

One-dimensional, bulk parameter modelling is generally adequate to calculate aerosol retention in fully developed flow in straight pipes. Although there is no

conclusive evidence from this ISP, it is thought that a more detailed modelling of the flow in the vicinity of geometric discontinuities (bends and changes of the pipe cross-section) may be needed to obtain the correct local thermal-hydraulics and hence the correct aerosol retention.

The particle tracking codes used in this ISP are still in a preliminary phase of their development and, while having a stronger physical basis, generally require the knowledge of parameters which are not generally known. One major difficulty faced by both users of particle tracking codes in the deposition phase of this ISP was the definition of the particle concentration profile at the inlet of the test section.

In terms of the results obtained, there was a tendency of almost all codes to over-predict aerosol deposition in the test pipe. Given the uncertainties generally associated with reactor calculations this over-estimation is probably within an acceptable range. It is, however, a non-conservative tendency in terms of radioactive releases and hence deserves further thought. Apart from some of the calculations that included a resuspension module, the notable exception to this tendency is again Melcor, which tended to under-predict aerosol deposition.

Two other subjects were raised during the discussions, although not directly resultant from this International Standard Problem. In the first place, although surface roughness is generally not considered in the deposition models, it can significantly affect the "capture efficiency" and therefore aerosol deposition. Secondly, it is generally recognised that the linear superposition of physical phenomena is not correct. While ignoring the interaction between different mechanisms probably leads to conservative results for the source term, this might not always be true and should be examined more closely.

Aerosol resuspension can significantly affect the source term in the case of dry aerosol deposits in turbulent flows. The effect of liquid aerosols needs to be investigated.

Experimental data is needed for resuspension of aerosol mixtures with different liquid fractions. While the STORM experimental programme has produced a good set of results for deposition and resuspension of dry aerosols, similar results with different liquid fractions are needed to examine the possibility of existence of a minimum liquid fraction in the deposit above which resuspension is inhibited or severely limited.

Present aerosol resuspension models are inadequate. The general agreement that exists concerning aerosol deposition in straight pipes disappears when the subject is aerosol resuspension. The existing models are based on different concepts and there is disagreement even on which are the important parameters that affect resuspension. Qualitatively, the more mechanistic models used in this ISP produced a better agreement with the experimental results, although that was not always the case quantitatively, but they tended to over-predict resuspension at high carrier gas velocity and depend on unknown parameters. The simpler empirical or semi-empirical models, which can, under certain conditions, reproduce reasonably well at least some features of the process, suffer from the lack of a large database of experimental results, obtained under different test conditions, for different materials. The empirical coefficients used in those models were obtained by fitting a small number of experiments in a limited range of test conditions which are usually quite different from any reactor conditions. While the results of the STORM experiments are a

welcome addition to this knowledge base, much more data is needed before these models can obtain the degree of reliability of the similar models used for deposition calculations. In addition to this, some of these simpler models are also affected by errors in their implementation, which need to be corrected. The question of the need for better resuspension models cannot be addressed in the frame of an ISP and should be the object of a wider discussion.

The potential for resuspension depends strongly on the characteristics of the deposit. The capability of the codes to reproduce the experimental results for aerosol resuspension was severely hindered by the lack of knowledge of physical characteristics of the deposit, namely the sizes of the resuspendable agglomerates and the porosity of the bed.

Deposition models should give an indication of the state of the deposit, not only of the mass deposited. The results obtained in different STORM tests show that the physical characteristics of the deposit depend on the mechanism by which the aerosols deposited. It is generally accepted that they will also depend on the chemical and physical processes occurring after deposition - e.g. chemisorption with the pipe walls or sintering.

Separate effects tests are needed to relate the characteristics of the deposit to their chemical composition and to the mechanisms by which the deposit was formed. This can only be done in small, well controlled experiments, which are a necessary complement to the larger scale experiments of the kind done in the STORM facility.

Mono-layer resuspension models are only a step towards the development of multi-layer models. Ignoring the trapping of larger particles below smaller ones in the deposit, the mono-layer models would not be able to reproduce the size distribution of the resuspended particles, even if the physical characteristics of the deposit were completely known. The size of the resuspended particles, however, is crucial in determining whether they will re-deposit downstream or be carried into the containment or into the environment.

One more general conclusion can be drawn from this exercise, concerning the qualification procedures for the computer codes used in nuclear safety. While some of the participants in the ISP were simultaneously code users and code developers, others were only users, in some cases of poorly documented codes. This raises the question of user qualification, in addition to the usual procedures of code qualification. Nuclear safety codes, and mainly integrated system codes, include a huge number of individual models, each with its own input parameters. In some cases, the user must select among different models for the same mechanism, and they might not be equally adequate in all situations. If this is added to poor or out-dated documentation, it can create serious difficulties to new users. This was highlighted in this ISP by the doubts that were raised about the inclusion of different models in the calculations or about the possibility of specifying certain parameters with certain codes.

Training in the use of nuclear safety codes should not be an objective of the International Standard Problems, although this frequently happens. The creation of specific exercises for this purpose, e.g. based on a "code validation matrix", could help focussing the International Standard Problems on code assessment. For the more widely used codes, this training is sometimes possible in the framework of the respective users' group, but this is not always the case.

8. References

[1] J. Areia Capitão
ISP-40: RAFT calculation
Presented at the 2nd ISP-40 Workshop. Ispra (Italy), March 1998

[2] J. Areia Capitão
ISP-40: Open calculation with RAFT
Presented at the 3rd ISP-40 Workshop. Ispra (Italy), June 1998

[3] J.R. Brock
On the Theory of Thermal Forces on Aerosol Particles
Journal of Colloidal Science 17, p. 768. 1962

[4] J.E. Brockmann
Range of Possible Dynamic and Collision Shape Factors
Report SAND84-0410, Vol. 2, Appendix F. Sandia National Laboratories (USA), February 1985

[5] P. Cherukat and J.B. McLaughlin
The Inertial Lift on a Rigid Sphere in a Linear Shear Flow Field near a Flat Wall
Journal of Fluid Mechanics 263, pp. 561 - 591. 1994

[6] M. Cranga, J.L. Cheissoux and M. Missirlian
ATHLET-CD Mod 0.2-Cycle E, SOPHAEROS V1.0 Documentation
GRS-P-3, Volume 4. GRS (Germany), May 1997

[7] C.N. Davies
Aerosol Science
Academic Press. 1966

[8] A. de los Reyes, R. Hummel and J. Areia Capitão
ISP-40: STORM Facility Data Book
Technical Note I.97.61. JRC-Ispra (Italy), April 1997

[9] A. de los Reyes
Estudio de los Mecanismos de Transporte de Aerosoles en el Sistema Primario de Centrales Nucleares de Agua Ligera en Caso de Accidente Grave
Ph.D. Thesis. Universidad Politécnica de Madrid, Madrid (Spain), July 1997

[10] A. de los Reyes et al.
The CAESAR Model for Particle Resuspension in Turbulent Flows
Journal of Aerosol Science, Vol. 28, pp. S327-S328. 1997

[11] A. de los Reyes, E. Hontañón and J. Areia Capitão
OECD/CSNI/ISP 40: CAESAR Calculations for Resuspension
Presented at the 2nd ISP-40 Workshop. Ispra (Italy), March 1998

[12] F. De Rosa and R. Mari
Document about ISP-40 Results Submission
Presented at the 2nd ISP-40 Workshop. Ispra (Italy), March 1998

[13] P. Dilara, A. Krasenbrink and R. Hummel
STORM Test SR11-ISP40 Quick Look Report
Technical Note. JRC-Ispra (Italy), March 1998

[14] P. Dumaz et al.
Fission Product Deposition and Revaporization Phenomena in Scenarios of Large Temperature Differences
ANS Proceedings - 1993 National Heat Transfer Conference. Atlanta (USA), 1993

[15] A. Fallot
ISP-40: Deposition test calculated with AEROSOL-B2 (CIRCUIT)
Presented at the 2nd ISP-40 Workshop. Ispra (Italy), March 1998

[16] H.-G. Friederichs and B.M. Schmitz
ISP-40 Recalculation: Parameter Study
Presented at the 3rd ISP-40 Workshop. Ispra (Italy), June 1998

[17] S.K. Friedlander and H.F. Johnstone
Deposition of Suspended Particles from Turbulent Gas Streams
Industrial and Engineering Chemistry 49, pp. 1151-1156. 1957

[18] H. Friess
Solution to ISP Nr. 40 (Resuspension Part)
Presented at the 2nd ISP-40 Workshop. Ispra (Italy), March 1998

[19] H. Friess and G. Yadigaroglu
Inclusion of Structural Parameters in the Modelling of Aerosol Resuspension
Proceedings of the Third OECD Specialist Meeting on Nuclear Aerosols. Cologne (Germany), June 1998

[20] A. Fromentin
Particle Resuspension from a Multi-Layer Deposit by Turbulent Flow
PSI-Bericht Nr.38 (LACE Report TR-083). Paul Sherrer Institut, Würenlingen (Switzerland), 1989

[21] N.A. Fuchs
The Mechanics of Aerosols
Pergamon Press. 1964

[22] J. Gauvain and G. Lhiaubet
ESCADRE mod1.0 - AEROSOLS-B2 - Release 3.3: Aerosol Behaviour in Piping Systems or Containments - Reference Document
Technical Note SEMAR 95/81. IPSN (France)

[23] T. J. Heames et al.
VICTORIA: A Mechanistic Model of Radionuclide Behavior in the Reactor Coolant System Under Severe Accident Conditions -Rev. 1-
NUREG/CR-5545, SAND90-0756. Sandia National Laboratories (USA), December 1992

[24] A. Hidaka, T. Yoshino and J. Sugimoto
Analysis of Aerosol Deposition and Resuspension in STORM Experiment (ISP-40) with ART Code
To be published as JAERI-Tech report

[25] A. Hidaka
ISP 40: New Deposition Calculation
E-Mail to A. de los Reyes. May 1998

[26] A. Hidaka
ISP-40: New Resuspension Calculation
E-Mail to A. de los Reyes. May 1998

[27] W.C. Hinds
Aerosol Technology
John Wiley and sons. New York (USA), 1982

[28] E. Hontañón and R. Arias
OECD-CSNI ISP-40: Analysis with VICTORIA 92 of Aerosol Deposition Phase
Report DFN/SN-09/II-98. CIEMAT Spain, 1998

[29] E. Hontañón et al.
Assessment of Aerosols Deposition Models against STORM Experiments
Proceedings of the Third OECD Specialist Meeting on Nuclear Aerosols. Cologne (Germany), June 1998

[30] E. Hontañón, A. de los Reyes and J. Areia Capitão
Effect of Roughness on Particle Adhesion to Surfaces
Proceedings of the Third OECD Specialist Meeting on Nuclear Aerosols. Cologne (Germany), June 1998

[31] K.H. Im, R.K. Ahluwalia and H.C. Lin
The RAFT Computer Code for Calculating Aerosol Formation and Transport in Severe LWR Accidents
NP-5287-CCM, Research Project 2802-3. Argonne National Laboratory (USA), July 1987

[32] M. Kajimoto et al.
ART Mod2 for the Analysis of Radionuclide Transport; Model Description and User's Manual
To be published as JAERI-Code report

[33] H.-C. Kim
ISP-40: Final Report Corrections (KINS Deposition)
E-Mail to A. de los Reyes. July 1998

[34] H.-C. Kim
ISP-40: Final Report Corrections (KINS Resuspension)
E-Mail to A. de los Reyes. June 1998

[35] H.-C. Kim and J.-S. Choi
ISP-40 Deposition and Resuspension Calculation Using MELCOR and VICTORIA
Presented at the 2nd ISP-40 Workshop. Ispra (Italy), March 1998

[36] C. Kroeger
Particle Tracking Code DeNIRO: Lagrangeian Random Walk Simulation
Presented at the 2nd ISP-40 Workshop. Ispra (Italy), March 1998

[37] C. Kroeger and Y. Drossinos
A Numerical Simulation of Particle Deposition in a Heated Turbulent Boundary Layer
Submitted to Int. J. Multiphase Flow, 1998

[38] C. Kroeger and Y. Drossinos
A Monte Carlo Simulation of Particle Deposition in a Two-Dimensional Turbulent Boundary Layer
Presented at the Third OECD Specialist Meeting on Nuclear Aerosols. Cologne (Germany), June 1998

[39] G. Lajtha
ISP-40: Time Step Sensitivity
E-Mail to A. de los Reyes. April 1998

[40] G. Lajtha and L.G. Horváth
Results of VICTORIA and MELCOR Code
Presented at the 2nd ISP-40 Workshop. Ispra (Italy), March 1998

[41] G. Lerchl and H. Austregesilo
ATHLET Mod1.1-Cycle C, User's Manual
GRS-P-1, Volume 1. GRS (Germany), October 1995

[42] B.Y. Liu and S.K. Agarwal
Experimental Observation of Aerosol in Turbulent Flow
Journal of Aerosol Science, 5, p 145-155. 1974

[43] D. Magnus and M. Auglaire
Summary report of the TRACTEBEL contribution to OECD ISP40
Note CONFINE/4NT/22. Tractebel (Belgium), September 1997

[44] J.C. Micaelli et al.
CATHARE: Best Estimate Thermohydraulics Code for Reactor Safety Studies
Paper presented at the International Conference on Thermal Reactor Safety. Avignon (France), 1989

[45] M. Missirlian
OECD/CSNI ISP40: STORM Test SD11/SR11
Presented at the 3rd ISP-40 Workshop. Ispra (Italy), June 1998

[46] M. Missirlian and G. Lajtha
SOPHAEROS CODE V1.3 - Programmer's Manual
Technical Note SEMAR 96/100. IPSN (France), December 1996

[47] M. Missirlian and G. Lajtha
SOPHAEROS CODE V1.3 - Theoretical Manual
Technical Note SEMAR 96/97. IPSN (France), December 1996

[48] M. Missirlian and G. Lajtha
SOPHAEROS CODE V1.3 - User's Manual
Technical Note SEMAR 96/99. IPSN (France), December 1996

[49] M. Missirlian, M. Kissane and B.M. Schmitz
SOPHAEROS V2.0: IPSN In-vessel Reactor Coolant System Code for Fission Product and Aerosol Transport -Development and Validation Status-
Proceedings of the Third OECD Specialist Meeting on Nuclear Aerosols. Cologne (Germany), June 1998

[50] R. Monti
ISP-40 Calculations with Sophaeros
Presented at the 2nd ISP-40 Workshop. Ispra (Italy), March 1998

[51] R. Monti and J. Areia Capitão
ISP-40 Open Calculation with Sophaeros
Presented at the 3rd ISP-40 Workshop. Ispra (Italy), June 1998

[52] OECD/NEA
CSNI Standard Problem Procedures
CSNI Report No 17 (Revision 3). OECD/NEA, Paris (France), November 1998

[53] OECD/NEA
Summary Record of the Preparatory ISP-40 Workshop
NEA/SEN/SIN/WG4(97) 6. OECD/CSNI, Paris (France), May 1997

[54] OECD/NEA
Summary Record of the Preliminary Comparison and Interpretation Workshop on the International Standard Problem No. 40 Exercise
NEA/SEN/SIN/WG4(98) 6. OECD/CSNI, Paris (France), June 1998

[55] F. Oriolo and S. Paci
DCMN Calculations for the ISP-40 on STORM Test SR11 using the ECART Computer Code
DCMN 003 (98). Dipartimento di Costruzioni Meccaniche e Nucleari, Università di Pisa, Pisa (Italy), 1998

[56] F. Parozzi
Development of Computer Models on Chemical and Physical Behaviour of Fission Products and Aerosols in the Primary Coolant System of a LWR During a Severe Accident - Part II: Fission Products and Aerosol Transport
ENEL-DSR-CRTN, N6/91/06/MI, Contract No. 3558-88-12 EL ISP I -Final report-. ENEL (Italy), July 1991

[57] F. Parozzi
ECART Aerosol Models
Presented at the 2nd ISP-40 Workshop. Ispra (Italy), March 1998

[58] F. Parozzi et al.
ECART User Manual Part 1: User's Guidance
ENEL Nuclear Energy Division Report. ENEL (Italy), May 1997

[59] F. Parozzi et al.
ECART User Manual Part 2: Code Structure and Theory
ENEL Nuclear Energy Division Report. ENEL (Italy), May 1997

[60] N. Pohl, Th. Steinrötter and H. Unger
Simulation der Depositionsphase des Versuchs STORM SR11 mit dem Programmsystem MELCOR
Technical Note RUB E-203. Ruhr-Universität Bochum, Bochum (Germany), -in preparation-

[61] P.G. Saffman
The Lift on a Small Sphere in a Slow Shear Flow
Journal of Fluid Mechanics 22, pp. 385 - 400. 1965

[62] H.-J. Schmid
ISP-40 Calculations with Marie
Presented at the 2nd ISP-40 Workshop. Ispra (Italy), March 1998

[63] B.M. Schmitz
International Standard Problem no. 40 (ISP-40) STORM Test SR-11 on Mechanical Resuspension -Part 1: Deposition Exercise- Calculation with SOPHAEROS V1.4GRS
Technical notice TN-SMZ-97-3. GRS (Germany), September 1997

[64] B.M. Schmitz
International Standard Problem no. 40 (ISP-40) STORM Test SR-11 on Mechanical Resuspension -Part 2: Resuspension Exercise- Open Recalculation with SOPHAEROS V1.4
Technical Notice TN-SMZ-98-2. GRS (Germany), in preparation

[65] B.M. Schmitz
Further Development of ATHLET-CD. Aerosol Module SOPHAEROS. Mechanical Resuspension Model
Technical Notice TN-SMZ-96-1. GRS (Germany), March 1996

[66] B.M. Schmitz
Further Development of ATHLET-CD. Mechanical Resuspension Module for SOPHAEROS V1.3 -Implementation and Validation-
Technical Notice TN-SMZ-97-2. GRS (Germany), April 1997

[67] B.M. Schmitz
International Standard Problem no. 40 (ISP-40) STORM Test SR-11 on Mechanical Resuspension -Part 2: Resuspension Exercise- Blind Post-test Calculation with SOPHAEROS V1.4GRS
Technical Notice TN-SMZ-98-1. GRS (Germany), in preparation

[68] G.A. Sehmel
Particle Deposition from Turbulent Air Flow
Journal of Geophysical Research 75, pp. 1766 - 1781. 1970

[69] P. Slavyagin
ISP-40 Calculations with Melcor
Presented at the 2nd ISP-40 Workshop. Ispra (Italy), March 1998

[70] P. Slavyagin
ISP-40 Open Calculations with Melcor
Presented at the 3rd ISP-40 Workshop. Ispra (Italy), June 1998

[71] G.S. Springer
Thermal Force on Particles in the Transition Regime
Journal of Colloidal Science, 34, p 215-220. 1970

[72] Th. Steinrötter and H. Unger
Simulation der Depositionsphase des Versuchs STORM SR11 mit dem Programmsystem ATHLET-CD
Technical Report RUB E-202 of the Research Project BMBF 150 1037. Ruhr-Universität Bochum, Bochum (Germany), (in preparation)

[73] R.M. Summers et al.
MELCOR Computer Code Manuals (Vol. 1), Primer and User's Guides: Version 1.8.3
NUREG/CR-6119, SAND93-2185. Sandia National Laboratories (USA), September 1994

[74] R.M. Summers et al.
MELCOR Computer Code Manuals (Vol. 2), Reference Manuals: Version 1.8.3
NUREG/CR-6119, SAND93-2185. Sandia National Laboratories (USA), September 1994

[75] L. Talbot and al.
Thermophoresis of Particles in a Heated Boundary Layer.
Journal of Fluid Mechanics, 101, p 737-758. 1980

[76] K. Trambauer et al.
ATHLET-CD Mod.0.2-Cycle E, User's Manual
GRS-P-3, Volume 1. GRS (Germany), May 1997

[77] R.C. Weast
Handbook of Chemistry and Physics
R.C. Weast ed. 52nd Edition 1971-1972

[78] A.L. Wright et al.
Series-2 Aerosol Resuspension Test. Data Summary Report
Draft Report NRC FIN no. B0488. Oak Ridge National Laboratory (USA), 1986